12-1997

Experimental Investigation of Water Spray Cooling Characteristics of a Solid Heated Surface

Rainer F. Ponzel

EXPERIMENTAL INVESTIGATION OF WATER SPRAY COOLING CHARACTERISTICS OF A SOLID HEATED SURFACE

by

Rainer F. Ponzel

A Thesis
Submitted to the
Faculty of The Graduate College
in partial fulfillment of the
requirements for the
Degree of Master of Science
Department of Mechanical and
Aeronautical Engineering

Western Michigan University
Kalamazoo, Michigan
December 1997

ACKNOWLEDGMENTS

As always, many people have contributed valuable ideas and constructive criticism for this research paper. I would like to acknowledge the people who contributed to the completion of this thesis. First to the members of my committee, Dr. Chris S. K. Cho, Dr. Srinivas Garimella, and Dr. Jerry H. Hamelink, I extend my sincere appreciation for their guidance and support and more importantly for "not giving up on me."

My gratitude is extended to Western Michigan University. Financial support for this work by a research grant from the Graduate College is very much appreciated. I am especially grateful to Dr. Cho for his financial support, his valuable technical assistance, and for helping me with experiments in the Heat Transfer Laboratory.

Finally, I would like to thank my family, and friends for their enduring patience and support. In particular, my wife, Amy J. Ponzel, who was always there providing understanding, perspective, and love.

Rainer F. Ponzel

EXPERIMENTAL INVESTIGATION OF WATER SPRAY COOLING CHARACTERISTICS OF A SOLID HEATED SURFACE

Rainer F. Ponzel, M.S.

Western Michigan University, 1997

Water spray cooling characteristics of a solid heated surface were investigated to better understand the physical phenomenon of nucleate boiling heat transfer for full cone sprays. An experimental test loop was developed to conduct the spray cooling experiments. A uniform heat flux condition was assumed, and the liquid flow rate and nozzle orifice diameter were selected as the main variables. Two water temperatures were chosen to perform the study. Saturated water spray was utilized to measure the wall superheat temperature. Subcooled water spray was applied to investigate the effect of water spray in the single-phase regime.

Experiments conducted using the saturated water spray revealed the heat transfer rate as a function of Weber number and the superheat temperature. The surface temperature was related to the characteristic velocity. The subcooled water spray tests indicated that liquid flow rate and nozzle orifice diameter were insignificant in the single-phase regime. Furthermore, a correlation was developed in terms of Reynolds number and Prandtl number. Test results also indicated a better cooling effect during the evaporation of the liquid film above saturation temperature.

TABLE OF CONTENTS

Table of Contents—Continued

LIST OF TABLES

LIST OF FIGURES

NOMENCLATURE

A	test object cross-sectional area, (m^2)
c_p	liquid specific heat at constant pressure, (kJ/kg °C)
d_0	nozzle orifice diameter, (m)
d_{32}	Sauter mean diameter, (SMD), (μm)
h	heat transfer coefficient, ($q'' / \Delta T$), (W/m^2 °C)
h_{fg}	latent heat of vaporization, (kJ/kg)
k	thermal conductivity, (W/m °C)
L	test surface diameter, (m)
Nu	Nusselt number, ($h\ d_0 / k_f$), (dimensionless)
Pr	Prandtl number, ($c_f\ \mu_f / k_f$), (dimensionless)
Δp	pressure drop across spray nozzle, (psig)
q''	heat flux, (W/m^2)
Q	spray volumetric flow rate, (m^3/s)
Q''	volumetric spray flux, ($m^3/s\ m^2$)
Re_{do}	Reynolds number, ($\rho_f (2\Delta p / \rho_f)^{0.5}\ d_0 / \mu_f$), (dimensionless)
T	temperature, (°C)
T_f	spray liquid inlet temperature, (°C)
T_w	test surface temperature, (°C)

ΔT_{sat}	temperature difference, (T_w - T_{sat}), (°C)
ΔT_w	temperature difference, (T_w - T_f), (°C)
We_{SMD}	spray Weber number, (ρ_f ($2\Delta p$ / ρ_f) d_{32} / σ), (dimensionless)
We_{do}	Weber number, (ρ_a ($2\Delta p$ / ρ_f) d_0 / σ), (dimensionless)
x	nozzle-to-surface distance, (mm)

Greek Symbols

θ	spray cone angle, (degrees)
σ	surface tension, (N/m)
ρ	density, (kg/m^3)
μ	viscosity, (kg/m s)

Subscripts

a	ambient (air or vapor)
f	liquid
g	vapor
sat	saturation
sub	subcooling
w	test surface

INTRODUCTION

High heat transfer coefficients associated with boiling have made the application of spray cooling increasingly attractive in the removal of high heat fluxes from devices that have high heat dissipation rates. Applications of this type include the use of boiling heat transfer to cool supercomputer electronics, avionics, x-ray medical devices, and lasers. The experimental approach of water spray cooling of a solid heated surface was intended to investigate this relatively new cooling technique and to achieve a superior cooling effect of a highly heated surface.

The experiments described in this paper were designed to analyze the surface cooling rates for subcooled water and saturated water spray, with the heat source surface temperature raised well above the saturation temperature of 100 °C. Usually, film boiling conditions are observed for the above settings. Some of these conditions were studied by Hodgson and Sutherland (1968).

A major problem employing spray cooling is the immense concentration of heat removal within the impingement zone, causing large temperature gradients within the cooled surface, which can result in catastrophic failure of temperature sensitive devices. Sprays are more difficult to characterize than other boiling systems. Sprays utilize the momentum of liquid entering the spray nozzle to cause breakup into fine drops, which impinge individually upon the heated surface.

The spray consists of a breakup of the liquid flow to fine drops. A dispersion

of drops is formed by forcing the liquid through a small orifice at relatively high pressures. Liquid breakup results in dramatic increase of the surface area to volume ratio of the liquid, and it also helps to produce a more uniform spatial distribution of heat removal, both in the single-phase and nucleate boiling regimes, as reported by Estes and Mudawar (1995). Another important feature of spray cooling is a delay of liquid separation from the surface during vigorous boiling, resulting in the liquid film being attached to the entire surface. Figure 1 is a schematic representation of the evaporation from the liquid film surface and the nucleate boiling in the liquid film for full cone sprays.

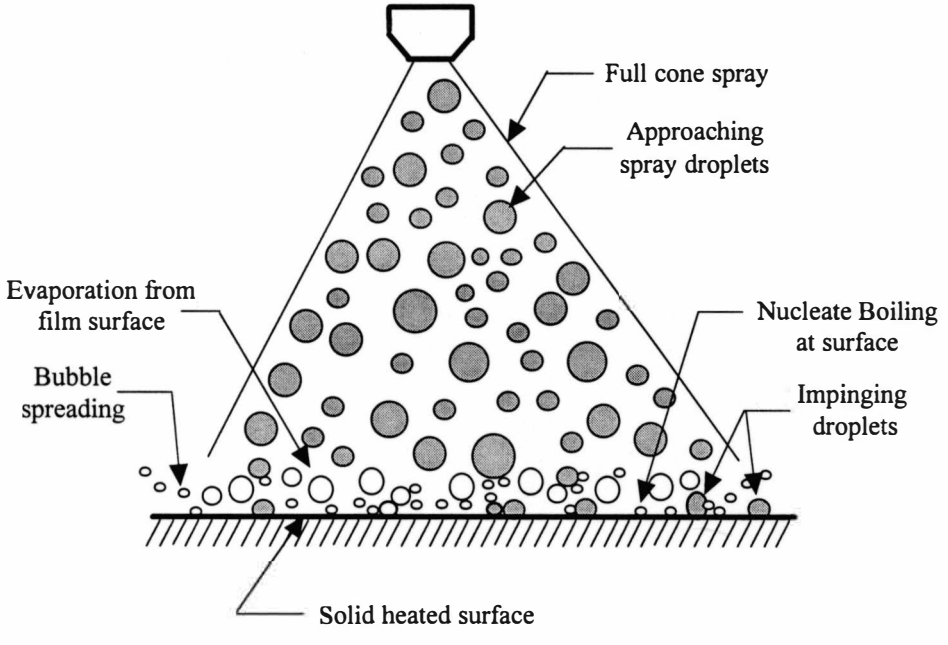

Figure 1. Spray Cooling Mechanisms.

The combination of small particle sizes and relatively large impact speeds are key characteristics of spray cooling techniques and significantly increase the cooling effectiveness per flow rate in comparison to other cooling techniques. Cavities on the heater surface provide a source for vapor/gas nuclei required for nucleate boiling, as defined by Rohsenow (1985). The bubbles, generated within the thin liquid film, burst upon reaching the liquid surface, and the upper surface of the bubble disintegrates thereby forming small droplets which fall back onto the flooded surface. The heat transfer coefficient depends on the presence of nucleate boiling. The increase of bubble frequency results in a substantial increase of the heat transfer coefficient.

The spray cooling method employing phase change heat transfer is accompanied by very high heat fluxes for low temperature differentials between the cooled surface and the heat transfer fluid. The high heat flux cooling techniques which use the phase change include: jet impingement cooling, forced convection boiling and spray cooling. The spray cooling method is one of the most effective techniques to remove very large fluxes at very low superheats.

However, a comprehensive review of the studies undertaken for spray cooling reveals a general lack of understanding of many of the underlying heat transfer mechanisms of sprays. Typical spray cooling applications, such as the heat treatment of metals and alloys, involve very high surface temperatures beyond the Leidenfrost temperature. At such high temperatures the liquid cannot wet the surface. Higher heat fluxes are observed compared to direct immersion in the liquid. This

phenomenon is due to the high droplet momentum which enables the droplets to get close to the heated surface. The Leidenfrost regime is not of interest in electronic cooling because the electronic device typically has to be maintained below 85 °C.

The present study is concerned with spray boiling from a circular heater module almost entirely impacted by the liquid spray. This experimental approach will focus on the spray cooling of a solid surface by applying a constant high heat flux and cooling the surface by a liquid spray impinging on it, thus removing the heat flux. The objective is to identify the key parameters influencing the heat transfer mechanism and to obtain a proper correlation in terms of Reynolds number and Prandtl number.

LITERATURE REVIEW

Jet Impingement Cooling

In order to remove a high heat flux from a heated surface and to provide a high heat transfer coefficient, various cooling techniques have been proposed. Experimental results of the jet impingement cooling technique that dissipates heat by forced convection cooling and by phase change have been reported by several authors.

Martin (1977) provided a comprehensive survey of the heat and mass transfer between the impinging jets and the solid surface. Katto (1978) developed a generalized correlation for the burnout heat flux in jet impingement cooling. Holman (1978) investigated jet impingement cooling for the maximum heat flux level of 72.4 W/cm^2 and developed two general correlations. He reported that nucleate boiling heat flux was solely dependent on the excess saturation temperature and that film boiling is independent of the jet nozzle diameter.

Bergles (1983, 1986) reported the results of a liquid jet impingement cooling method using saturated and subcooled Freon 113. Goodling and Jager (1987) investigated the wafer scale cooling technique and reported results of the jet impingement boiling heat transfer using Freon 12. Both sides of a wafer were utilized for their jet impingement cooling approach and the superheat temperature was controlled within 10 °C for the power setting of 430 W. The jet impingement cooling

technique using a single jet and multiple jets was investigated by Trabold and Obot (1991). The parametric study included the effect of the jet Reynolds number and the standoff spacing as well as nozzle-to-surface diameter ratio. An integral analysis was presented for each of the convective regions by Liu and Lienhard (1991). The radial variation of the Nusselt number was interpreted in terms of the development of the thermal boundary layer.

Spray Cooling

The evaporation and ignition of liquid droplets impinging on a hot surface are of interest in a number of areas related to combustion engines, cooling of electronic equipment, and heat exchanger design. Toda (1974) reported that the liquid film thickness was the main parameter for classifying the thermal region. Comini (1979) investigated the dropwise evaporation phenomenon and obtained a heat transfer coefficient of h = 80 kW/m^2 °C at the heat flux level of 1600 kW/m^2 using water coolant.

Brimacombe *et al.* (1980) presented a comprehensive review of the studies concerning spray cooling as it applies to steel making. His analysis revealed that the volumetric spray flux, Q", has the greatest effect on the heat transfer coefficient. Grissom (1981) grouped spray cooling into three modes: the flooded mode, the dry wall mode, and the Leidenfrost mode. He established that the surface temperature was a linear function of the incident liquid mass flux. Ubanovich *et al.* (1981) and Reiners *et al.* (1985) discovered that the practice of positioning the spray nozzle

closer to the heated surface, in order to increase the heat transfer coefficient, often resulted in severe spatial non-uniformity in the cooling rate. This lead to the assumption that the spatial variation of spray hydrodynamic parameters within the spray field is another factor complicating the prediction of the heat transfer coefficient in spray cooling.

Yanosy (1985) studied water spray cooling in a vacuum and concluded that a reduction in the heat transfer in a vacuum was caused by changes in the thermal and transport properties of water. He noted that the vacuum conditions influenced the spray characteristics. However, he did not clearly indicate which properties were mainly affected by the vacuum conditions. The rate of evaporation of water from a horizontal surface into a turbulent stream of hot air was investigated by Haji and Chow (1988). Their experiment confirmed the existence of an inversion temperature below which the water evaporation rate was higher in air than in steam.

A number of studies focus on the use of spray cooling to cool high heat flux electronic devices. In these cases direct contact with the coolant necessitates the use of dielectric liquids. Cho *et al.*, Wu, and Sharma (1987, 1988) conducted an experimental investigation of the characteristics of spray cooling and jet impingement methods. Freon 113 was used as the coolant in both approaches, and the burnout heat flux was correlated with the Weber number. The results of their burnout heat flux data showed that greater heat transfer rates were accomplished with the spray cooling method. The effect of droplet size on CHF was not found to be significant in the studies conducted with pressure atomized spray by Cho and Wu (1988). It should be

noted that droplet size variation was not very large in these studies because single liquids were used in a limited pressure range. However, Cho and Wu (1988) presented CHF as a strong function of the spray velocity for pressurized atomized sprays.

Mudawar and Valentine (1989) developed dimensionless design correlations for the transition boiling, nucleate boiling, and single-phase cooling regimes. Like Monde (1980) and Toda (1972), they found that volumetric flux, Q", in water sprays is the dominant spray parameter influencing cooling performance. Mudawar and Valentine also demonstrated that the heat transfer coefficient was only a function of the surface temperature in the nucleate boiling regime. The heat transfer coefficient was unaffected by variations of the spray hydrodynamic parameters in the nucleate boiling regime. The Sauter mean diameter, d_{32}, was significant in the single-phase regime, and the mean droplet velocity, U_m, was important in the transition boiling regime.

The evaporation of small liquid droplets impinging on a hot stainless steel plate was investigated by Xiong and Yuen (1991). Ghodbane and Holman (1991) obtained a correlation for Freon 113 spray cooling which indicated that the heat flux was proportional to $We^{0.6}$. The correlation represented a correlation of the pressure drop and mass flow rate with the heat flux.

Estes and Mudawar (1995) reported the spray cooling test results in terms of volume flux and Sauter mean diameter. By definition, the Sauter mean diameter represents a ratio of all droplet's volume to all droplet's surface area. Estes and

Mudawar concluded that CHF increases with increasing flow rate and increasing subcooling. Also, CHF was greater for nozzles which generate smaller drops. Furthermore, they found that SMD for full cone sprays is dependent upon orifice diameter and the Weber and Reynolds numbers based on the orifice flow conditions prior to liquid breakup. In addition, they developed a dimensionless correlation which gives good predictions for fluids with vastly different surface tensions.

Estes and Mudawar also developed a correlation which accurately predicts CHF for water, FC-72, and FC-87 for different full cone nozzles over a wide range of flow rate and subcoolings. The CHF data were correlated with respect to the local volumetric flux, Q", and Sauter mean diameter (SMD), d_{32}, as shown in Equation 1. Where $q"_m$ is defined as the heater power at CHF divided by the heater surface area.

$$\frac{q"_m}{\rho_g Q" h_{fg}} = f\left\{\frac{\rho_f}{\rho_g}, \frac{\rho_f Q"^2 d_{32}}{\sigma}, \frac{\rho_f c_{p,f} \Delta T_{sub}}{\rho_g h_{fg}}\right\} \quad (1)$$

Spray parameters which actually influence CHF include the following thermophysical properties (ρ_f, ρ_g, σ, h_{fg}, c_p), flow parameters (ΔT_{sub}, Δp, Q), orifice parameters (d_0, θ), and heater diameter (L). The nozzle-to-surface distance (H) is a function of both heater size and spray cone angle.

A comprehensive review of the spray cooling literature revealed that most studies were primarily conducted with Fluorinerts FC-72 and FC-87, and coolants such as Freon 113. However, correlations need to be developed for water spray

cooling to identify the key parameters for full cone sprays using saturated and subcooled water spray. The emphasis of the present study was to investigate the cooling performance of a highly heated circular heater module impacted by saturated and subcooled water spray. The specific objectives of this primarily experimental investigation are as follows:

1. Design and fabricate a flow loop to conduct water spray cooling experiments for full cone sprays, using saturated and subcooled water spray.

2. Investigate the spray cooling characteristics of a solid heated surface for various liquid flow rates and nozzle orifice diameters.

3. Develop a better understanding of nucleate boiling heat transfer for full cone sprays, and also understand which spray parameters affect cooling performance.

4. Develop correlations for saturated and subcooled water spray to identify the key parameters influencing the spray cooling mechanism.

In this paper, spray parameters such as nozzle size, nozzle-to-surface distance, droplet size, and flow rate will be analyzed and evaluated as a function of surface heat flux. The premise is to maximize heat removal and to find the best combination of the spray parameters influencing the heat transfer phenomenon.

EXPERIMENTAL PROCEDURES

Experimental Apparatus

The spray cooling experiments were conducted in an environmental chamber. The dimensions of the chamber were 1250 mm × 800 mm × 600 mm. The environmental chamber was equipped with a Plexiglas observation window and a blower for ventilation. The test chamber was located inside the environmental chamber and consisted of the heater module and spray nozzle assembly. A water spray cooling test loop was fabricated to investigate the spray cooling characteristics of a solid heated surface. A schematic of the flow loop is shown in Figure 2. The test loop consisted of several heating sections to maintain the desired liquid spray temperature at the nozzle outlet. Control valves mounted into a by-pass loop and a needle valve facilitated precise conditioning of the fluid flow rate.

Municipal water passed through a multistage filtration loop to generate very high distilled-quality water. A five micron cartridge filter removed sediments and particles from the incoming water supply through the process of mechanical removal. A deminealizer provided additional treatment for removal of dissolved solids. The nuclear grade resin (expressed at $CaCO_3$) consisted of a strong base anion exchanger and a strong acid sulfonated polystyrene cation exchanger. The mixed bed exchange resin was supplied by Cole-Parmer Instrument Company. The ion exchange water

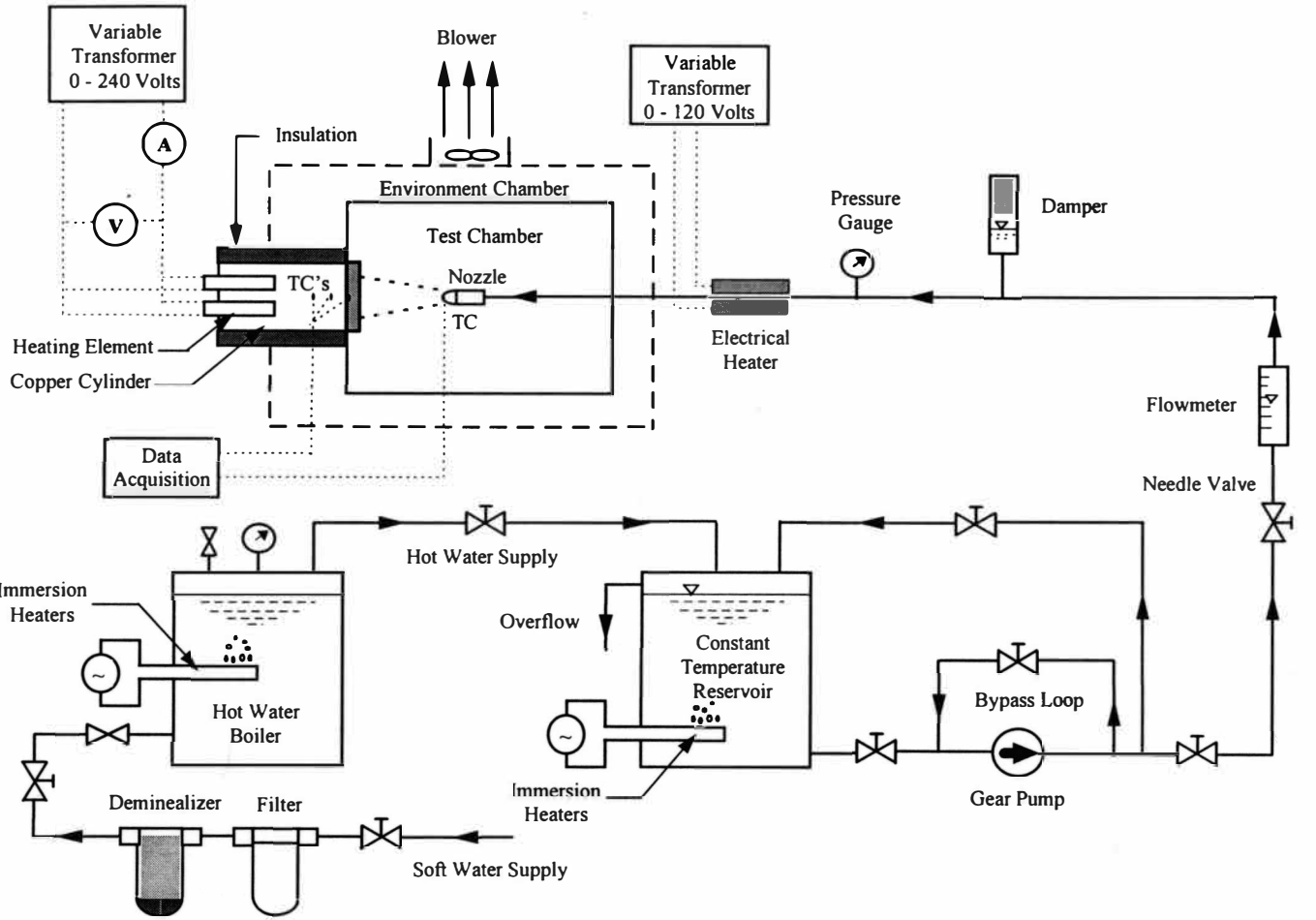

Figure 2. Schematic of Flow Loop.

purification unit produced high quality deionized water with a resistivity as high as 15 – 18 MΩ-cm.

The water was treated to obtain a resistivity similar to those of dielectric liquids generally used for direct immersion cooling of microelectronics components. The treated water was preheated to 72 °C inside a hot water boiler and pumped to a constant temperature stainless steel reservoir. The maximum capacity of the reservoir was 0.0335 m^3. The constant temperature water bath consisted of three tubular electrical heating elements that generated a total heat rate of 8 kW. The water temperature was controlled within 0.5 °C from the set point by a temperature controller and a magnetic switch; this allowed fine tuning of the spray temperature.

A ½ hp close-coupled gear pump circulated the saturated water from the constant temperature reservoir through the loop to the spray nozzle. The body and gears of the positive displacement gear pump were made of high-grade bronze. The gear pump generated a total pumping pressure of 100 psig with a maximum flow rate of 4.4 gpm at 0 psig. The loop was mainly fabricated of insulated copper tubing. A flexible rubber hose was used to connect the pump to the main test loop, in order to prevent transmittal of vibrations. A bypass line was installed around the gear pump to regulate the water flow rate and to bypass the balanced flow to the reservoir. Damping tubes were placed downstream of the gear pump to absorb and reduce large pressure fluctuations. Water passed through a carefully calibrated ball-type flow meter that had an accuracy of two percent of the full scale. The flow rate calibration curve was compared against the flow rate calculations for each test run.

The nozzle inlet pressure was determined by a dial pressure gauge which had a measurement range of 0 - 100 psig. The pressure gauge was situated just upstream of the spray nozzle. An in-line electrical heater was placed close to the spray nozzle pipe section to compensate for heat loss and to reheat the fluid to the saturation temperature.

The test object was machined from a pure oxygen-free copper cylinder 50 mm in diameter and 178 mm in length. Copper was selected as the test object material because the high thermal conductivity of copper provided uniform temperature distribution in radial direction. One end of the copper specimen was highly polished to obtain a smooth test surface. The surface condition is important in spray cooling. Pais et al. (1992) and Sehmbey et al. (1992) showed that the heat transfer coefficient increased tremendously for very smooth surfaces under spray cooling with air atomized water. However, for pressure atomized liquids, the opposite is true. The test surface had a cross-sectional area of 1.9635×10^{-3} m^2. A schematic of the test object is shown in Figure 3.

Three holes, 12.8 mm in diameter, were machined into the bottom surface of the copper cylinder. Three Watlow cartridge heaters (Cat. No. J3A112) were inserted into the drilled holes. Each cartridge heating element generated a total power dissipation rate of 750 Watts at 240 Volts. A variable transformer provided the power to the heating elements. The power level was varied from zero to 1150 kW/m^2. The three cartridge heaters were wired in parallel connection. The copper cylinder was heated gradually by increasing the power level of the variable transformer. The power

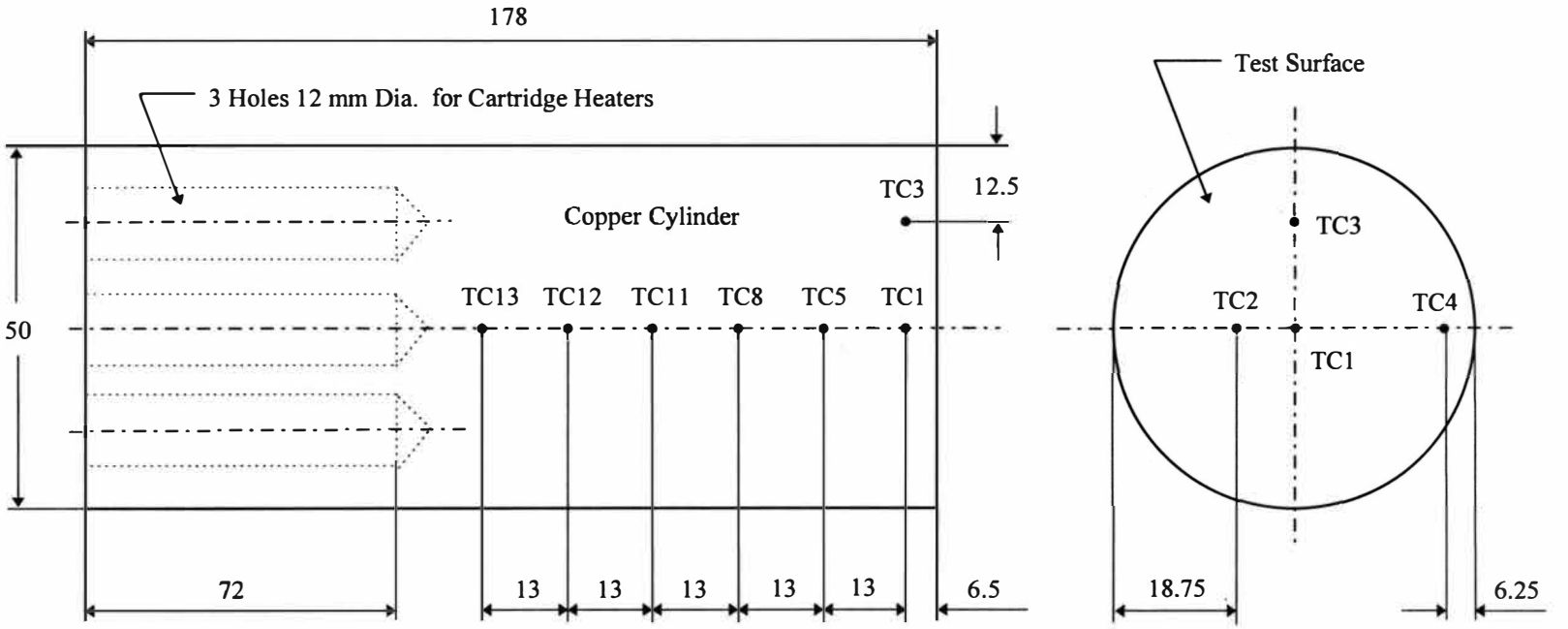

Not drawn to scale.

All Dimensions in Millimeters

• k Type Thermocouples

Note: TC6, TC7, TC9, and TC10 not drawn in this view

Figure 3. Schematic of Test Object.

output was monitored by two digital multimeters with true-rms performance. The AC current and voltage readings were used to calculate the power requirements.

The spray nozzle was oriented normally to the cylindrical test surface, and the nozzle tips were changed to vary the nozzle orifice diameter. The spray nozzle was precisely centered along the axial direction of the heater module. A schematic of the Nozzle-to-Heater configuration is shown in Figure 4. The distance between the nozzle and the test surface was slightly adjusted throughout the experiments, to enable the test surface to be fully covered by the liquid spray. The average distance between the nozzle tip and the test surface was 40 mm for all tests. The distance was measured with a digital micrometer.

Thirteen holes, 1.0668 mm in diameter, were precisely drilled into the copper cylinder to provide accurate positioning for the thermocouples. The positions of the thermocouples measured from the test surface were 6.5 mm, 19.5 mm, 32.5 mm, 45.5 mm, 58.5 mm, and 71.5 mm, respectively. Thirteen type K–Inconel 600 sheathed thermocouples were carefully inserted into the copper cylinder to monitor the axial as well as the radial temperature distribution. However, the test surface temperature was measured indirectly by six type K thermocouples located along the axial direction of the copper cylinder. The surface temperature was extrapolated from the thermocouples embedded beneath the test surface. One dimensional heat conduction was assumed for the extrapolation procedure. The thermocouples were inserted carefully to prevent distortion of the thermocouple bead and to position the thermocouple junction at the correct radial locations. K type thermocouples were also

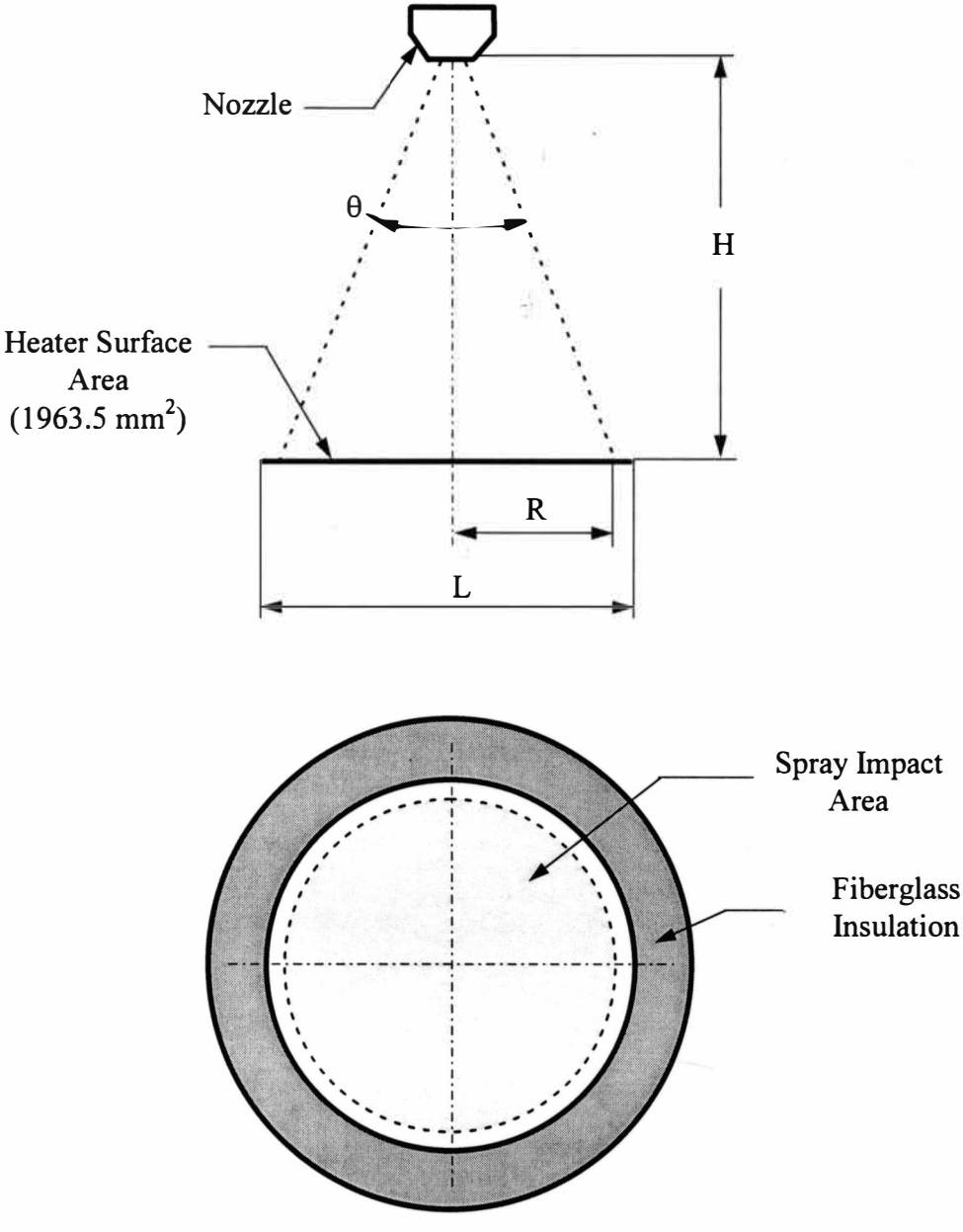

Figure 4. Schematic of Nozzle-to-Heater Configuration.

used to monitor the water temperature in the reservoir and at the nozzle outlet, as well as the ambient air temperature inside the environmental chamber.

The copper cylinder was mounted through a cylindrical opening of a 20 mm thick Teflon plate. A schematic of the test chamber is shown in Figure 5. A high temperature mechanical seal made of Viton was used to prevent water leakage. The copper cylinder was supported by structural members to eliminate deflection of the Teflon plate. A drainage tube was installed in close proximity to the test surface to prevent flooding of the test area during continuous operation. The drain could also be used to recover the unevaporated portion of the liquid.

Temperature readings were made by an A/D data acquisition system which was calibrated to a resolution of 0.2 °C with a Leeds & Northrup Instruments calibrator. Labtech Notebook ® Version 9 was selected as the data acquisition and control software. The software package was programmed to record all thermocouple temperatures.

The outside surface area of the copper cylinder was insulated with fiberglass insulation. The thermal conductivity of the fiberglass insulation is 0.05 W/m K. The radial thickness of the ceramic insulation was 30 mm. Two thermocouples were embedded radially at 10 mm and 20 mm from the surface of the copper cylinder to measure the temperature gradient across the insulation. The heat loss through the insulation was determined from the temperature gradient and was less than one percent. A sample heat loss calculation is presented in Appendix C.

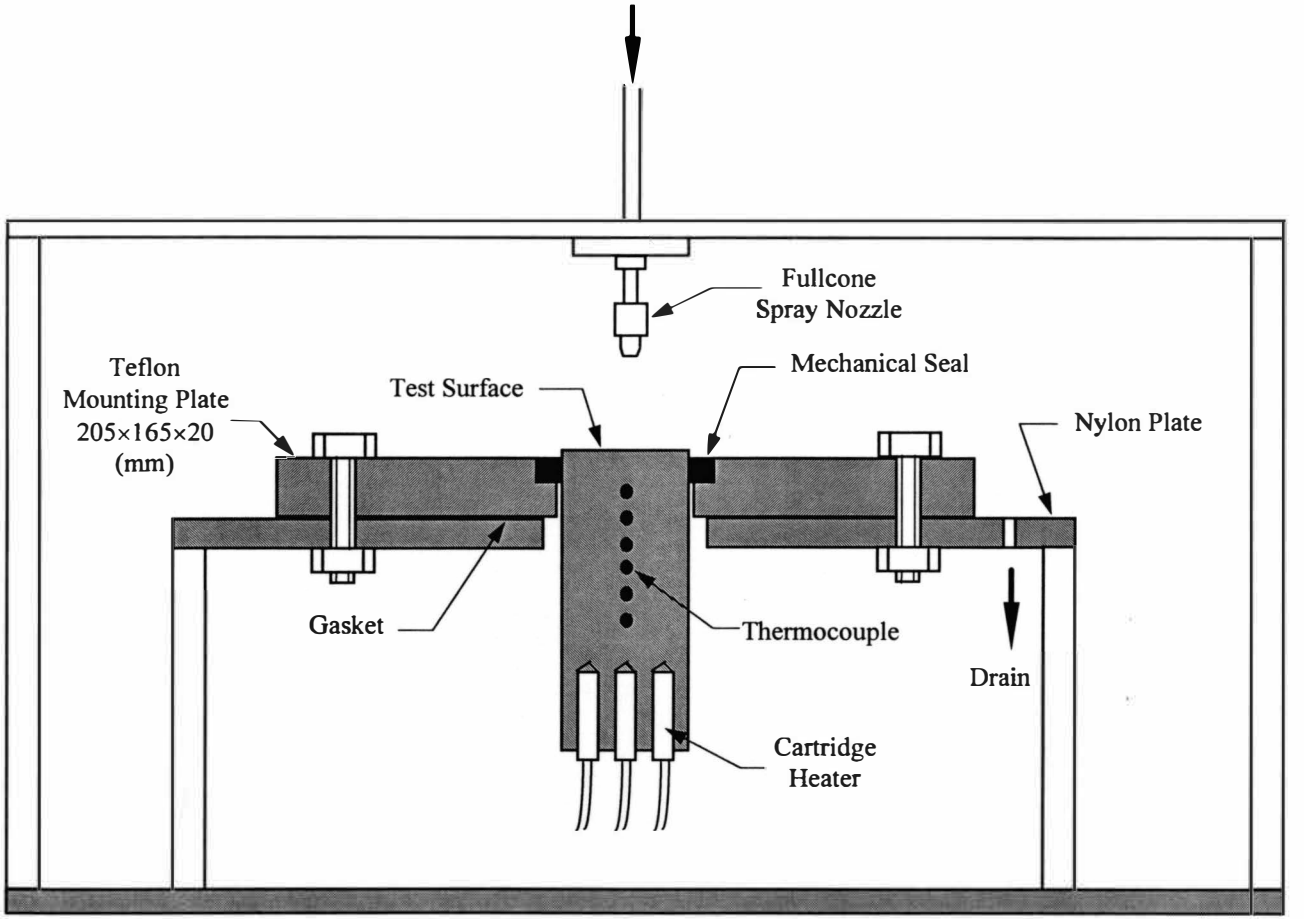

Figure 5. Schematic of Test Chamber.

Experimental Methods

The spray cooling experiments were conducted for saturated water spray and subcooled water spray conditions. Three nozzle orifice diameters and three liquid flow rates were selected to investigate and understand the water spray cooling mechanism. Table 1 represents the resulting water spray cooling cases.

Table 1

Spray Cooling Cases

Flow Rate	Saturated Water Spray			Flow Rate	Subcooled Water Spray		
$Q \times 10^{-6}$ m^3/sec	Nozzle TG 0.9	Nozzle TG 0.5	Nozzle TG 0.3	$Q \times 10^{-6}$ m^3/sec	Nozzle TG 0.9	Nozzle TG 0.5	Nozzle TG 0.3
8.7	Test 1	Test 4	Test 7	7.7	Test 10	Test 13	Test 16
5.4	Test 2	Test 5	Test 8	5.4	Test 11	Test 14	Test 17
3.7	Test 3	Test 6	Test 9	3.7	Test 12	Test 15	Test 18

Spray pattern and liquid droplet size are primarily a function of the nozzle orifice diameter and the liquid pressure. Full-cone spray nozzles (Spray Systems Co. TG 0.9, TG 0.5, and TG 0.3) were selected and the corresponding nozzle orifice diameters were 0.51 mm, 0.61 mm, and 0.76 mm, respectively. As a result of the instability, the fluid swirls and disintegrates to a fine liquid spray inside the full-cone spray nozzle. The three water flow rates of 8.7×10^{-6} m^3/sec, 5.4×10^{-6} m^3/sec and

3.7×10^{-6} m^3/sec were carefully measured for each individual test run and verified against the flow meter calibration curves. The flow rate, Q, was calculated by measuring the difference of the water volume in the reservoir and dividing it by the actual run time for each test run.

Prior to each test, the highly polished heater surface was carefully cleaned with acetone and alcohol to remove any residue on the surface. Also, the flow loop was cleared of any air left in the system. Boiling curves were obtained by increasing the voltage in small increments across the heating elements inserted into the bottom of the test object. Data collection was initiated only after the heater module and the system reached steady state temperature conditions. The power increments were reduced to less than 50 kW/m^2 to ensure accurate measurements of nucleate boiling temperatures and in order to prevent burnout of the heater surface.

The test surface temperature was obtained by extrapolating the temperatures along the axis of the copper cylinder. Curve fitting of the collected data indicated that the temperature profile along the axial direction was linear, as expected. A slope and an interception was obtained using the extrapolation technique. The interception represented the surface temperature where the distance is zero with respect to the test surface. The slope was used to calculate the surface heat flux applying Fourier's law of one-dimensional heat conduction in rectangular coordinates. The magnitude of the rate of heat flow per unit area is given by Equation 2.

$$q'' = -k \frac{dT}{dx} \tag{2}$$

The value for the thermal conductivity of copper was estimated at the average temperature between the test surface temperature and the highest temperature reading near the heating elements. The calculated heat flux based on the slope was compared with the heat flux obtained using temperature readings at two selected thermocouple locations. The distances of the two thermocouple locations from the test surface along the axial direction were known. Therefore, heat flux at the selected locations was calculated assuming one-dimensional heat conduction. The difference in heat flux calculation was less than one percent, which confirms the overall accuracy of the temperature measurements.

Observations were made during each test run to better understand the spray cooling mechanism. When the copper cylinder was not heated, the test surface was fully covered by a liquid film and flooding of the liquid occurred. The impinged liquid droplets were flattened on the test surface and formed a thin liquid film as observed by Toda (1974). The surface heat flux was gradually increased, which resulted in the evaporation of the liquid film with a reduction of the liquid film thickness. Eventually the nucleate boiling site became visible around the outer circumferential area of the test surface. Additional increase of the heat flux enlarged the nucleate boiling site towards the center and resulted in an increase of the noise level of the impinging spray. To analyze the effect of the impinging liquid temperature, spray cooling tests were conducted for saturated water spray and subcooled water spray.

RESULTS

Three full cone spray nozzles, designated as nozzles TG 0.9, TG 0.5, and TG 0.3, were used to obtain the water spray cooling data. Table 2 illustrates the significant spray nozzle parameters.

Table 2

Spray Nozzle Parameters

Nozzle TG	Orifice Diameter $d_0 \times 10^{-6}$ m	Spray Angle θ Degrees	Volumetric Spray Flux $Q'' \times 10^{-3}$ $m^3\ s^{-1}/m^2$	SMD $d_{32} \times 10^{-6}$ m
0.9	760	48.6	4.4 - 1.8	148 - 261
0.5	610	38.2	3.9 - 1.9	104 - 168
0.3	510	41.0	2.7 - 1.8	90 - 114

Spray Cooling by Saturated Water Spray

Boiling curves for saturated water spray, with respect to the varying flow rate, are presented in Figure 6, Figure 7, and Figure 8, respectively. Boiling curves for saturated water spray, with respect to the varying nozzle size, are shown in Figure 9, Figure 10, and Figure 11, respectively. The effect of the wall superheat temperature

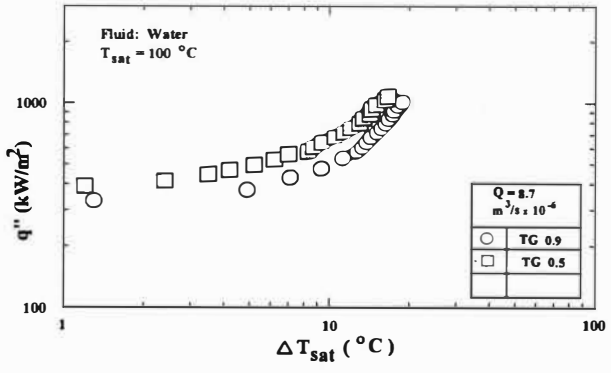

Figure 6. Boiling Curves for Saturated Spray, Q = 8.7 $m^3/s \times 10^{-6}$.

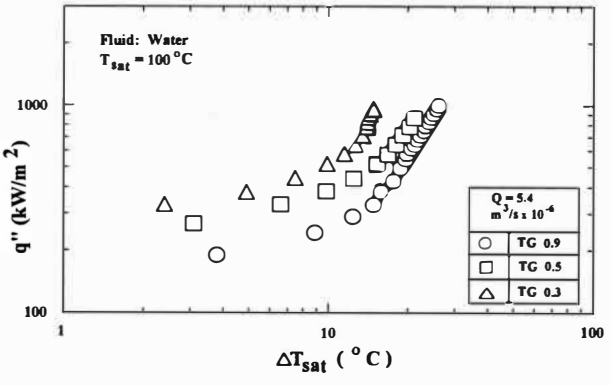

Figure 7. Boiling Curves for Saturated Spray, Q = 5.4 $m^3/s \times 10^{-6}$.

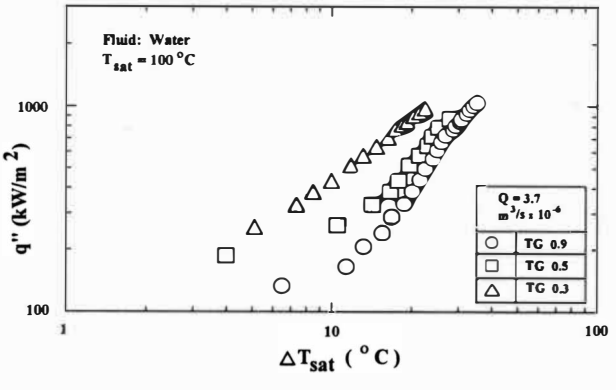

Figure 8. Boiling Curves for Saturated Spray, Q = 3.7 $m^3/s \times 10^{-6}$.

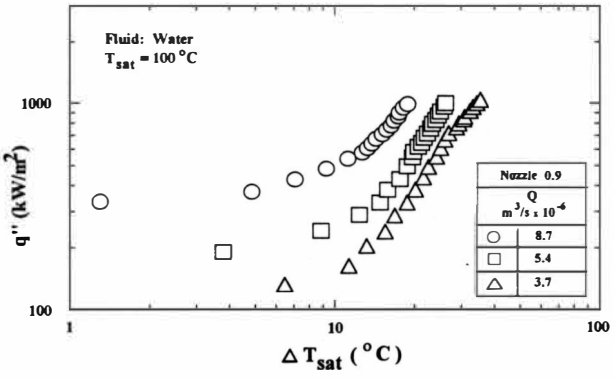

Figure 9. Boiling Curves for Saturated Spray, Nozzle TG 0.9.

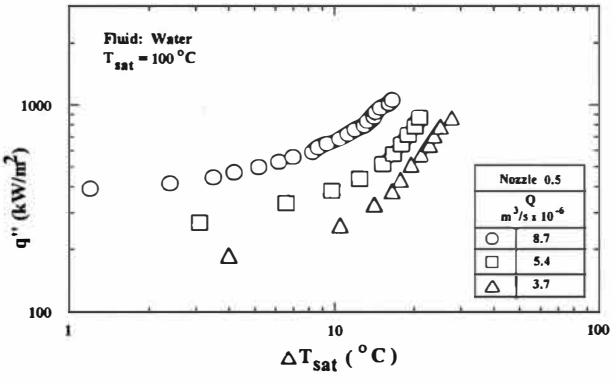

Figure 10. Boiling Curves for Saturated Spray, Nozzle TG 0.5.

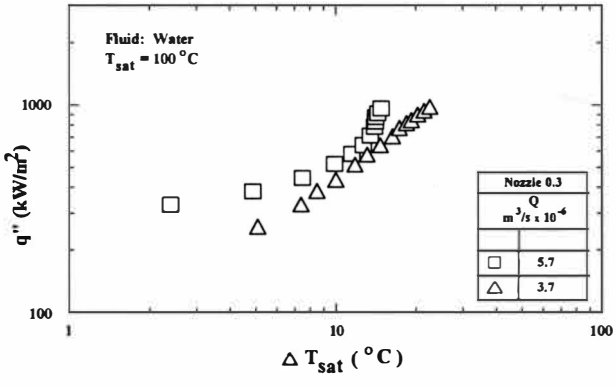

Figure 11. Boiling Curves for Saturated Spray, Nozzle TG 0.3.

on the water spray cooling phenomenon was determined for three liquid flow rates of 8.7×10^{-6} m^3/sec, 5.4×10^{-6} m^3/sec, and 3.7×10^{-6} m^3/sec. The corresponding water flow rates per surface area, Q", are 4.43×10^{-3} $m^3/s\ m^2$, 2.75×10^{-3} $m^3/s\ m^2$, and 1.88×10^{-3} $m^3/s\ m^2$. Figures 6, 7, and 8 represent the wall superheat temperatures as a function of the nozzle orifice diameter. The three tested nozzle orifice diameters were 0.76 mm (nozzle TG 0.9), 0.61 mm (nozzle TG 0.5), and 0.51 mm (nozzle TG 0.3), respectively. Figure 6 outlines the measured wall superheat temperature for the various nozzle orifice diameters, and a flow rate, Q, of 8.7×10^{-6} m^3/sec. The test results for the remaining flow rate of 5.4×10^{-6} m^3/sec, and 3.7×10^{-6} m^3/sec are shown in Figure 7 and Figure 8. Comparison of these test results clearly indicates the effect of the nozzle orifice diameter on the wall superheat temperature. Decreasing the nozzle orifice diameter resulted in a lower wall superheat temperature. For example, the lowest wall superheat temperature, and the highest heat flux were obtained with the smallest nozzle orifice diameter of 0.51 mm and the largest flow rate of 8.7×10^{-6} m^3/sec. The highest wall superheat temperature, and the lowest heat flux were achieved with the largest nozzle orifice diameter of 0.71 mm and the lowest flow rate of 3.7×10^{-6} m^3/sec.

The trend of decreasing wall superheat temperature as a direct result of decreasing the nozzle orifice diameter, is repeatedly seen throughout Figures 6, 7, and 8, respectively. This spray cooling phenomenon is caused by the large number of smaller liquid droplets associated with small nozzle orifice diameters. Droplet size

distribution is an important factor, and the nozzle orifice diameter controls these spray characteristics.

The fine mist flow enhances the surface cooling due to the intensification of the liquid film evaporation. Hence, small nozzles are more effective in terms of maximum cooling efficiency. As a result, supercooling of the heated test surface is achieved. Figure 9, Figure 10, and Figure 11 present the influence of the liquid flow rate on the wall superheat temperature. The nozzle orifice diameter was held constant in each figure, while the liquid flow rate was varied. The resulting boiling curves with respect to the varying flow rate indicate that a higher flow rate produces a lower wall superheat temperature. The above observations show that the water flow rate significantly affects the spray cooling behavior of a heated surface.

Spray Cooling by Subcooled Water Spray

In the first part of this study, the spray cooling technique was investigated for saturated water spray. The results were almost entirely presented in the region of the nucleate boiling regime. However, numerous industrial processes, for instance, the spray quenching of metallic surfaces, necessitate the use of spray cooling in the single-phase region. The subcooling effect of the liquid spray was investigated in the second part of this study. Water was supplied at a spray inlet temperature, T_f, of 23 °C. The effect of liquid subcooling is similar to that observed in the first part of this study. The heat flux increased gradually with the increasing temperature gradient between the surface temperature and the subcooled water spray. The impingement of

fine liquid droplet generated a thin liquid film that migrated outward in radial direction.

The jet impingement cooling method was not investigated in this study. Trabold and Obot (1991), and Liu and Lienhard (1991) reported that a similar type of thin liquid film can be created by the jet impingement cooling technique. The fluid column impinges at the center of a heated surface and moves outward in a radial direction. At the time of the radial motion the fluid is gradually heated causing the fluid temperature to rise as a function of the radial location. The primary difference between jet impingement cooling and spray cooling is an altered liquid supply technique.

During spray cooling, fluid is continuously added to the entire area of the moving liquid film. The surface may be maintained at a uniform temperature level if a proper spray pattern is provided. Also, the Weber number, which is the ratio of inertia force and surface tension force, can be a significant variable in spray cooling.

Test surface wall temperatures for subcooled water spray, with respect to the varying flow rate, are presented in Figure 12, Figure 13, and Figure 14, respectively. Test surface wall temperatures for subcooled water spray, with respect to the varying nozzle size, are shown in Figure 15, Figure 16, and Figure 17, respectively. For the second part of this study, test conditions were selected similar to the cases of saturated water spray. The variance was the liquid spray temperature, which was provided at 23 °C. The experiments were conducted for three nozzle orifice diameters and three varying liquid flow rates.

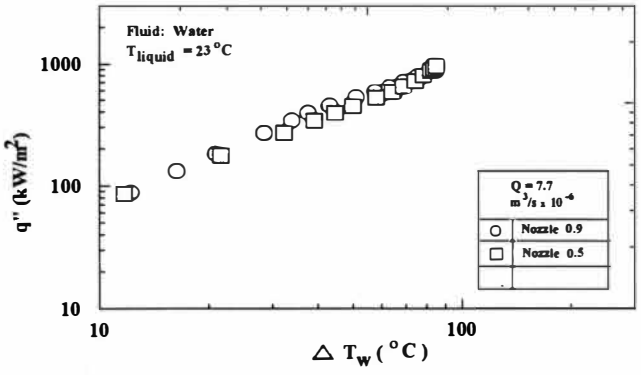

Figure 12. Boiling Curves for Subcooled Spray, Q = 7.7 $m^3/s \times 10^{-6}$.

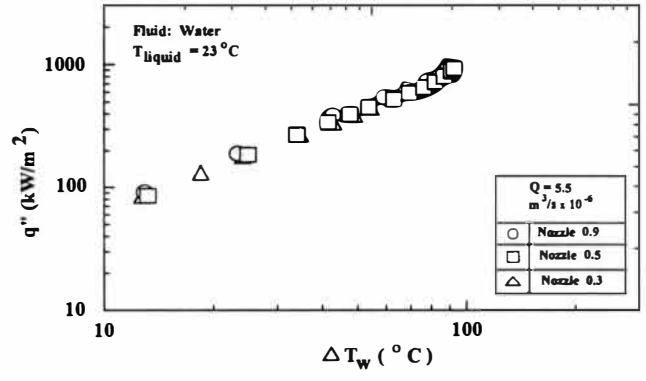

Figure 13. Boiling Curves for Subcooled Spray, Q = 5.5 $m^3/s \times 10^{-6}$.

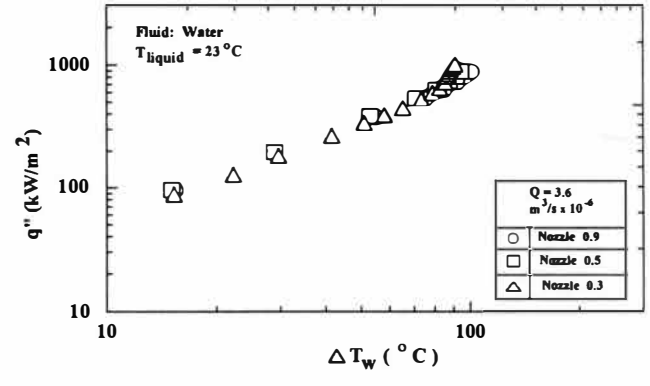

Figure 14. Boiling Curves for Subcooled Spray, Q = 3.6 $m^3/s \times 10^{-6}$.

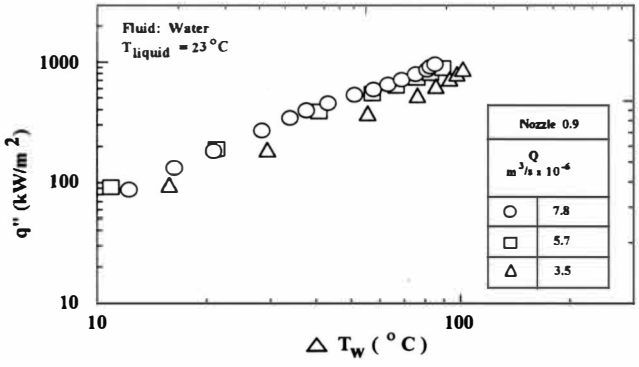

Figure 15. Boiling Curves for Subcooled Spray, Nozzle TG 0.9.

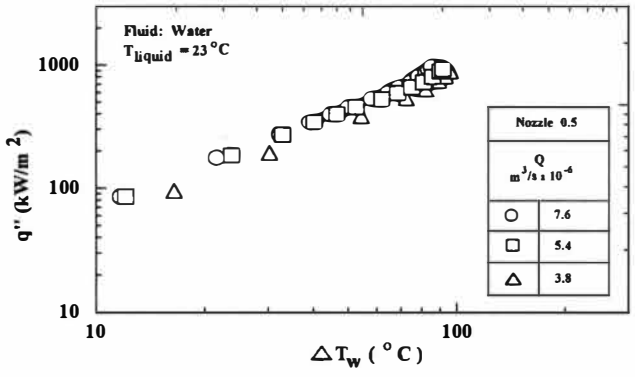

Figure 16. Boiling Curves for Subcooled Spray, Nozzle TG 0.5.

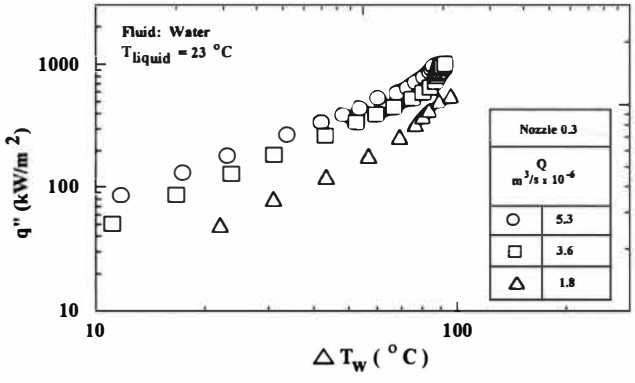

Figure 17. Boiling Curves for Subcooled Spray, Nozzle TG 0.3.

The dependence of the wall temperature difference, ΔT_{wall}, on the nozzle orifice diameter is shown in Figures 12, 13, and 14. The liquid flow rate was controlled at a steady and uniform level for every experimental test run. The plotted data reveal that the nozzle orifice diameter is insignificant for subcooled water spray in the single-phase region. The results suggest that the droplet diameter may not be an important parameter in the single-phase region because the droplets do not evaporate. The characteristic liquid film velocity becomes a significant parameter in the single-phase region since a movement of the thin liquid film occurs. The droplet size becomes an important parameter only when evaporation of a thin liquid film occurs.

Figures 15, 16, and 17, present the effect of the liquid flow rate in terms of the wall temperature difference, ΔT_{wall}, and the surface heat flux, while the nozzle orifice diameter was held constant during each test. It should be noted that the case with flow rate 1.8×10^{-6} m^3/sec in Figure 17 is only shown to depict the trend for decreasing flow rates. Flow rate 7.7×10^{-6} m^3/sec could not be achieved with the smallest nozzle TG 0.3 due to the small nozzle orifice diameter. Therefore, the case with flow rate 1.8×10^{-6} m^3/sec verifies the trend which is slightly seen in Figure 15 and Figure 16, respectively. The graphical analysis of the subcooled water spray cases indicates that q", and ΔT_{wall} are less susceptible to the change of water flow rates when compared to the results shown in Figures 9, 10, and 11. Boiling curves for the subcooled water spray cases reveal an almost uniform slope for all cases with subcooled water spray. The heat flux is increasing with increasing ΔT_w.

The above observations for subcooled water spray show that the nozzle orifice diameter and the water flow rate do not significantly affect the spray cooling behavior of a heated surface in the single-phase regime.

Correlation for Spray Cooling With Saturated Water Spray

The surface cooling rate is directly affected by the droplet diameter. Time consuming and costly optical drop sizing is necessary to predict the heat transfer performance of a given spray. For the final analysis of the extrapolated surface temperature and the corresponding heat flux data, the Sauter mean diameter (SMD) is used to obtain a correlation for water spray cooling with saturated water spray. The SMD is calculated from the empirical relationship proposed by Mudawar (1995). The SMD correlation was developed for full cone spray nozzles and two fluids: FC 72 and water. The spray droplets were characterized by a Phase Doppler Particle Analyzer.

The resulting SMD correlation is presented in Equation 3. The Weber number, We, in Equation 3 is defined based on the nozzle orifice diameter, d_0, and is shown in Equation 4, while Equation 5 is a common expression for the Reynolds number, Re, based on the nozzle orifice conditions.

$$\frac{d_{32}}{d_0} = 3.67 \left[We_{d_0}^{0.5} \, \mathrm{Re}_{d_0} \right]^{-0.259} \tag{3}$$

$$We_{d_0} = \frac{\rho_a \left(2\Delta p / \rho_f \right) d_0}{\sigma} \tag{4}$$

$$\mathbf{Re}_{d_0} = \frac{\rho_f \left(2\Delta p / \rho_f\right)^{0.5} d_0}{\mu_f} \tag{5}$$

where: d_{32} is the Sauter mean diameter, d_0 is the nozzle orifice diameter, Δp is the pressure drop across the spray nozzle in psig, and σ is the surface tension. The value of the surface tension of liquid water against its vapor was calculated from the following interpolation equation given in the ASME steam tables — sixth edition:

$$\sigma = B\left[\frac{T_c - T}{T_c}\right]^{\mu}\left[1 + b\left[\frac{T_c - T}{T_c}\right]\right] \tag{6}$$

where the critical point, T_c, is assumed at T_c = 647.15 K, and the values of the constants are: B = 235.8 $\times$ 10^{-3} N/m, b = - 0.625, and μ = 1.256. The unit used for the surface tension, σ, in Equation 6 is N/m. The properties for the working fluid were obtained at the saturation temperature for liquid water. The density, ρ_a, of the ambient air inside the test chamber was obtained at the average chamber temperature measured throughout the experiments.

Table 3 presents a summary of the spray cooling data for saturated water spray during the course of the experiments. The data were obtained for various combinations of the flow rate and the nozzle orifice diameter. A non-dimensional equation was determined that best described the experimental data. The data were correlated by developing a non-linear curve fitting method for the model equation. The non-linear curve fitting method provided the best fit parameters for the final

correlation equation. As a result, the spray cooling heat flux with saturated water spray is correlated by

$$\frac{q'' x}{\mu_f h_{fg}} = 93.8 \left(We_{d_{32}}\right)^{0.43} \left(\frac{c_f \Delta T}{h_{fg}}\right)^{0.98} \tag{7}$$

where: x represents the nozzle-to-surface distance H, as shown in Figure 4, We_{32} is the Weber number defined in terms of Sauter mean diameter (SMD) rather than the nozzle orifice diameter (d_0) to investigate the influence of the droplet diameter, the superheat temperature (ΔT) is defined as $\Delta T = T_w - T_{sat}$, and c_f is the specific heat of the liquid. The correlated data for spray cooling with saturated water spray using Equation 7 are plotted in Figure 18.

The correlation in Equation 7 indicates that the heat transfer rate in the two-phase flow regime is a function of the droplet diameter, the characteristic velocity or liquid film flow rate, and the superheat temperature. The effect of nozzle-to-surface distance was not investigated in this study, and the distance x from the nozzle to the surface was held constant at H = 40.1 mm. It should be noted that the maximum surface heat flux during the experiments was not high enough to reach the critical heat flux. Hence, critical heat flux data could not be obtained. Mudawar (1995) reported that the data points merge to a single boiling curve as the heat flux increases. The highest critical heat flux would be obtained at the lowest liquid flow rate and the largest nozzle orifice diameter.

Table 3

Summary of Spray Cooling Data for Saturated Water Spray

Nozzle Orifice Diameter	Liquid Flow Rate	Pressure Drop	Heat Transfer Coefficient	Test Surface Temperature	Heat Flux	Reynolds Number	Weber Number	Weber Number
$d_0 \times 10^{-6}$	$Q \times 10^{-6}$	Δp	h	T_w	q"	Re	We_{do}	We_{SMD}
m	m^3/s	psig	$W/m^2\ °C$	°C	kW/m^2			
760	8.7	18.1	52511 - 257308	98.3 - 118.8	244.7 - 987.2	42129	3.98	3220
760	5.4	5.3	49763 - 38264	103.8 - 126.1	189.1 - 998.7	22797	1.17	943
760	3.7	2.0	20477 - 29374	106.5 - 135.3	133.1 - 1036.9	14004	0.44	356
610	8.6	42.0	328167 - 63615	99.3 - 116.6	350.2 - 1056.0	51509	7.41	5997
610	5.4	15.2	86290 - 41066	103.1 - 121.1	267.5 - 866.5	30987	2.68	2170
610	3.7	6.6	46675 - 31018	104.0 - 127.9	186.7 - 865.4	20419	1.16	942
510	5.5	49.2	137125 - 64500	86.7 - 114.8	133.0 - 954.6	46611	7.26	5874
510	3.7	19.6	50314 - 43311	93.2 - 122.5	129.8 - 974.5	29419	2.89	2340

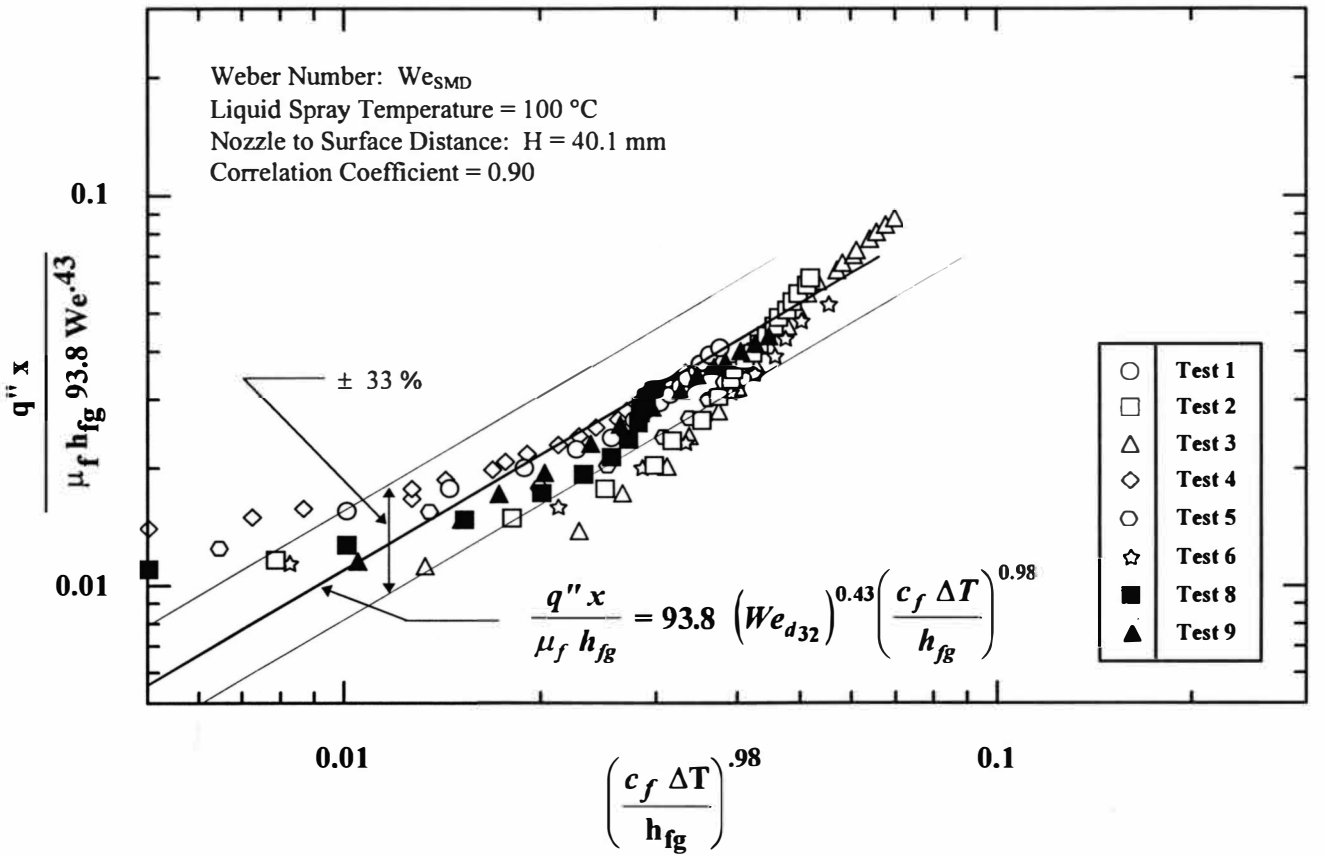

Figure 18. Correlation for Spray Cooling With Saturated Water Spray, $T_w > T_{sat}$.

Correlation for Spray Cooling With Subcooled Water Spray

The water spray cooling data in the single-phase region were correlated in terms of the Reynolds number, Nusselt number, and Prandtl number. The Reynolds number is defined by the volumetric spray flux of the liquid and the nozzle orifice diameter as shown in Equation 8. The Nusselt number is defined in terms of heat transfer coefficient and nozzle orifice diameter and was calculated using Equation 9.

$$\mathbf{Re} = \frac{Q'' \, d_0}{\nu_f} \tag{8}$$

$$Nu = \frac{h \, d_0}{k_f} \tag{9}$$

where: Q" = Q/A, or liquid flow rate divided by the test surface area. The volumetric spray flux, Q", which has a unit of velocity, represents the characteristic liquid film velocity on the test surface. The properties of the working fluid, Prandtl number, Pr, thermal conductivity, k_f, and the kinematic viscosity, ν_f, were evaluated at the film temperature using Equation 10. The film temperature was represented by the average of the test surface temperature and the supplied liquid spray temperature.

$$T_{film} = \frac{T_w + T_f}{2} \tag{10}$$

Table 4 presents a summary of the spray cooling data for subcooled water spray during the course of the experiments. The data were obtained for various combinations of the flow rate and the nozzle orifice diameter. Equation 11 is an expression of the final correlation for water spray cooling by subcooled water spray. The obtained correlation for a movement of the single-phase liquid film over a heated surface is shown in Equation 11. The correlated data for spray cooling with subcooled water spray using Equation 11 are plotted in Figure 19.

$$Nu = 2.53\ \mathrm{Re}^{0.67}\ \mathrm{Pr}^{0.31} \tag{11}$$

The above correlation for spray cooling of a high heat flux surface covered by a subcooled liquid film shows similar cooling characteristics with a single-phase forced convection cooling method.

The spray cooling technique is effective when a liquid film evaporates from a heated surface, as demonstrated in the obtained boiling curves for saturated and subcooled water spray. The liquid flow rate plays an important role in controlling the test surface temperature in both cases of liquid film with and without evaporation. The liquid flow rate is an especially significant parameter during the liquid film evaporation.

Table 4

Summary of Spray Cooling Data for Subcooled Water Spray

Nozzle Orifice Diameter	Liquid Flow Rate	Pressure Drop	Heat Transfer Coefficient	Test Surface Temperature	Heat Flux	Reynolds Number	Nusselt Number	Prandtl Number
$d_0 \times 10^{-6}$	$Q \times 10^{-6}$	Δp	h	T_w	q''	Re	Nu	Pr
m	m^3/s	psig	$W/m^2\ K$	°C	kW/m^2			
760	7.8	21.9	7081 - 11264	36.2 - 109.1	87.8 - 960.8	3.7 - 6.8	8.7 - 12.9	5.5 - 2.7
760	5.7	10.9	7278 - 9765	34.9 - 113.4	91.7 - 889.6	2.6 - 5.1	9.0 - 11.2	5.7 - 2.7
760	3.5	3.0	6327 - 8688	39.8 - 125.6	94.9 - 875.7	1.7 - 3.4	7.8 - 9.9	5.2 - 2.4
610	7.6	51.7	7246 - 11299	34.8 - 108.2	85.5 - 962.7	2.8 - 5.3	7.2 - 10.4	5.6 - 2.8
610	5.4	13.0	6226 - 9820	35.2 - 114.9	85.3 - 917.2	2.0 - 3.9	6.2 - 9.0	5.7 - 2.7
610	3.8	25.8	6392 - 9289	39.5 - 119.3	94.6 - 878.7	1.5 - 2.9	6.3 - 8.5	5.2 - 2.5
510	5.3	72.7	6832 - 11112	34.7 - 109.0	85.4 - 964.5	1.6 - 3.1	5.7 - 8.6	5.7 - 2.8
510	3.6	30.4	4743 - 10896	34.1 - 115.7	49.8 - 1003.5	1.1 - 2.2	3.9 - 8.4	5.6 - 2.6

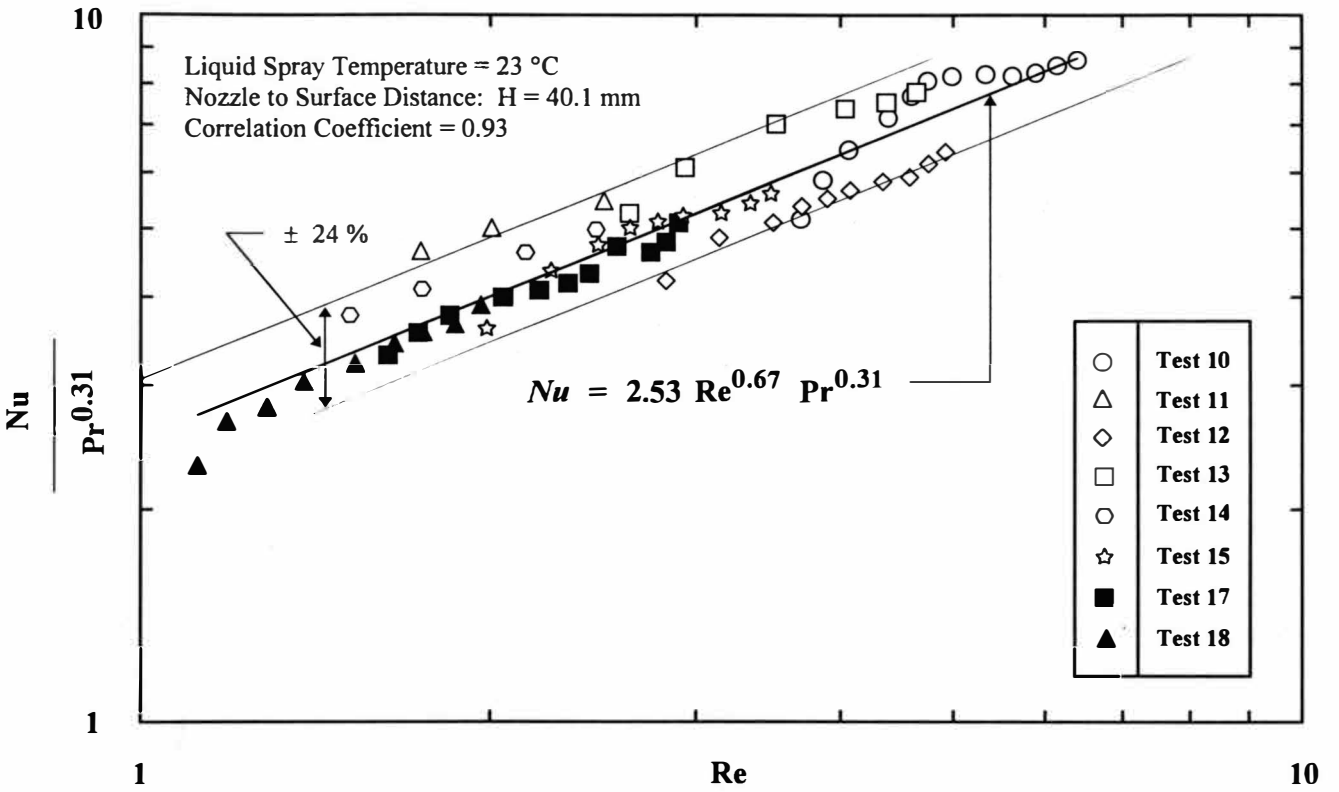

Figure 19. Correlation for Spray Cooling With Subcooled Water Spray, $T_w < T_{sat}$.

CONCLUSIONS

Water spray cooling of a solid heated copper surface was investigated experimentally. Saturated water spray and subcooled water spray were used to study the effect of water flow rate and nozzle orifice diameter on boiling heat transfer. Full cone spray nozzles were used to generate the uniform sprays. Since the entire heater surface was impacted by the liquid spray during all the experiments, the effect of nozzle-to-surface distance on the cooling performance of the heated surface was not considered in this study.

Based on the experimental data collected and the visual observations made in this investigation, the following conclusions were formulated:

1. Analysis of the wall temperature, and heat flux data for the saturated water spray, indicated a clear correlation between the characteristic velocity, the nozzle orifice diameter, and the superheat temperature.

2. Higher saturated water flow rate essentially contributed to reducing the surface temperature, and a smaller orifice diameter resulted in a decrease of the test surface temperature as well.

3. A nondimensional correlation equation was developed for saturated water spray cooling heat transfer. The correlation of the spray cooling data, with saturated water spray, indicates a strong effect of the Weber number on the overall heat transfer characteristics of water spray cooling.

4. The subcooled water spray presented only small fluctuations in the test surface temperature by changing the water flow rate.

5. The effect of nozzle orifice diameter on the surface temperature was insignificant in the single-phase region.

6. The results indicate that spray cooling by fine droplets can be effective during the evaporation phase of a thin liquid film.

The spray cooling experiments have demonstrated that nucleate boiling significantly influences the heat transfer process in water spray cooling. The study has also shown that spray cooling of a solid heated surface by saturated water spray is a very efficient high heat flux cooling technique.

Appendix A

Experimental Data

Analysis of Experimental Data

Flow rate calculation

$A_{Res.}$ cross-sectional area of reservoir (mm^2)

H_1 water level at start (mm)

H_2 water level at end (mm)

Q flow rate (ml/sec.)

t run time (sec.)

$$Q = \frac{(H_1 - H_2) \times A_{Res}}{t \times 1000} \quad \text{..... (Eq. 12)}$$

Power requirement calculation

A_{Cu} cross-sectional area of copper cylinder (m^2)

E voltage (V)

I amperage (A)

q'' heat flux in terms of electrical power input (kW/m^2)

R_{Hot} heater resistance at operation temperature (Ohms)

W wattage (W)

$$W = E \times I \quad \text{..... (Eq. 13)} \qquad R_{Hot} = \frac{E^2}{W} \quad \text{..... (Eq. 14)}$$

$$q'' = \frac{E^2}{R_{Hot} \times A_{Cu} \times 1000} \quad \text{..... (Eq. 15)}$$

Experimental Data for Test 1

Date: 4-12-97 File Name: Test1a.prn Nozzle 1 TG 0.9
Time: 14:32 - 17:20 Case: Saturated Water Spray Duration = 360 sec.
Test: Test 1

Run	Float Point	Water Level at Start mm	Water Level at End mm	Actual Run Time sec.	Calculated Flow Rate ml/sec.	Voltage Range	Actual Voltage V	Amps A	Watts W	Hot Resistance Ohms	Range KW/m^2	Actual KW/m^2	Proposed KW/m^2	Proposed Voltage	Pressure (+/- 1) psig	Twater Deg. C	Troom Deg. C
1	20	250	224	381	8.8	115	115.5	4.54	524.4	25.4	263.7	266.0	265.0	115.3	18.0	97.8	22.0
2	20	252	226	381	8.8	125	125.2	4.92	616.0	25.4	311.5	312.5	315.0	125.7	17.0	97.2	21.3
3	20	250	224	381	8.8	135	135.1	5.3	716.0	25.5	362.7	363.2	360.0	134.5	19.0	96.0	21.8
4	20	250	224	381	8.8	145	145.2	5.68	824.7	25.6	417.2	418.4	420.0	145.5	18.0	96.9	22.5
5	20	252	226	381	8.8	155	155.0	6.04	936.2	25.7	474.9	474.9	475.0	155.0	19.0	97.8	23.5
6	20	250	225	381	8.5	165	165.1	6.43	1061.6	25.7	537.9	538.5	540.0	165.3	18.0	97.2	22.9
7	20	251	226	381	8.5	175	175.0	6.78	1186.5	25.8	601.9	601.9	600.0	174.7	18.0	97.8	22.6
8	20	245	219	381	8.8	180	180.7	6.97	1259.5	25.9	633.9	638.9	640.0	180.9	18.0	98.0	22.1
9	20	251	225	381	8.8	185	185.6	7.13	1323.3	26.0	666.9	671.3	670.0	185.4	18.0	97.4	22.3
10	20	247	221	381	8.8	190	190.4	7.31	1391.8	26.0	703.1	706.0	710.0	190.9	18.0	97.3	23.2
11	20	251	226	381	8.5	195	195.6	7.53	1472.9	26.0	742.6	747.1	750.0	196.0	18.0	96.5	22.7
12	20	251	225	381	8.8	200	200.5	7.74	1551.9	25.9	783.3	787.2	790.0	200.9	18.0	96.6	20.6
13	20	249	224	381	8.5	205	205.7	7.96	1637.4	25.8	824.9	830.6	830.0	205.6	18.0	97.6	22.4
14	20	249	223	381	8.8	210	210.3	8.16	1716.0	25.8	868.0	870.5	870.0	210.2	18.0	97.7	22.1
15	20	250	224	381	8.8	215	215.6	8.38	1806.7	25.7	911.4	916.5	915.0	215.4	18.0	97.3	23.4
16	20	249	223	381	8.8	220	220.5	8.59	1894.1	25.7	956.5	960.8	960.0	220.4	18.0	96.9	22.8
17	20	246	220	381	8.8	225	225.4	8.79	1981.3	25.6	1001.5	1005.0	1005.0	225.4	18.0	96.4	23.1
18	20	242	217	381	8.5	230	230.6	9.01	2077.7	25.6	1048.5	1053.9	1050.0	230.2	18.0	94.6	23.8
19	20	211	186	381	8.5	235	235.8	9.22	2174.1	25.6	1095.4	1102.8	1100.0	235.5	18.0	96.5	23.7
Averg.	**20.0**	**247.2**	**221.6**	**381.0**	**8.7**					**25.7**					**18.1**	**97.0**	**22.6**

Notes:
Diameter of Copper Cylinder = 50.1 mm
Cross-sectional Area of Copper Cylinder: A_{copper} = 0.001971357 m^2
Length of Copper Cylinder = 178 mm

Reservoir Dimensions:
Diameter: D = 405 mm
Height at overflow: H = 260 mm
Volume at overflow: V = 33.5 L = 33494.5 ml
Cross-sectional Area: A = 128824.9338 mm^2

Observations:
No bubble formation at Max. Heat Flux.
Large evaporation at Max. Heat Flux.
Full Cone Spray is covering total heated surface area.

Nozzle TG 1.0			
psi	15	20	**18.1**
gpm	0.12	0.14	0.13
ml/sec	10.73	8.83	**8.36**

Estimated flow rate at 18.1 *psi* using Linear Interpolation technique.

1 Gal = 3785.411784 ml

Nozzle-to-Surface Distance = 40.1 mm

Note: Float Point and Pressure stable.

Experimental Data for Test 2

Date: 4-13-97 File Name: Test2a.prn Nozzle 1 TG 0.9
Time: 14:50 - 18:00 Case: Saturated Water Spray Duration = 360 sec.
Test: Test 2

Run	Float Point	Water Level at Start mm	Water Level at End mm	Actual Run Time sec.	Calculated Flow Rate ml/sec.	Voltage Range	Actual Voltage V	Amps A	Watts W	Hot Resistance Ohms	Range KW/m^2	Actual KW/m^2	Proposed KW/m^2	Proposed Voltage	Pressure (+/- .5) psig	Twater Deg. C	Troom Deg. C
1	12.5	251	234	381	5.7	100	100.1	3.96	396.4	25.3	200.7	201.1	200.0	99.8	5.5	98.1	22.7
2	12.5	253	236	381	5.7	115	115.5	4.56	526.7	25.3	264.9	267.2	265.0	115.0	5.0	97.6	22.9
3	12.5	251	235	381	5.4	125	125.3	4.93	617.7	25.4	311.9	313.4	315.0	125.6	5.0	97.7	22.4
4	12.5	252	237	381	5.1	135	135.1	5.31	717.4	25.4	363.4	363.9	365.0	135.3	5.0	97.7	23.1
5	12.5	250	233	381	5.7	145	145.0	5.69	825.1	25.5	418.5	418.5	420.0	145.3	5.0	97.8	23.5
6	12.5	251	236	381	5.1	155	155.0	6.07	940.9	25.5	477.3	477.3	475.0	154.6	5.0	97.9	22.9
7	12.5	251	236	381	5.1	165	165.6	6.46	1069.8	25.6	538.7	542.7	540.0	165.2	5.0	98.0	22.9
8	12.5	250	235	381	5.1	175	174.8	6.79	1186.9	25.7	603.4	602.1	600.0	174.5	5.0	97.2	22.9
9	12.5	252	235	381	5.7	180	180.4	6.98	1259.2	25.8	635.9	638.7	640.0	180.6	5.5	97.7	23.2
10	12.5	255	240	381	5.1	185	185.5	7.14	1324.5	26.0	668.2	671.9	670.0	185.2	5.0	97.6	23.3
11	12.5	255	239	381	5.4	190	190.5	7.33	1396.4	26.0	704.6	708.3	710.0	190.7	5.0	97.6	24.1
12	12.5	251	235	381	5.4	195	195.5	7.54	1474.1	25.9	743.9	747.7	745.0	195.1	5.0	97.6	23.8
13	12.5	252	236	381	5.4	200	200.7	7.76	1557.4	25.9	784.5	790.0	790.0	200.7	5.5	97.7	23.8
14	12.5	251	235	381	5.4	205	205.5	7.97	1637.8	25.8	826.8	830.8	830.0	205.4	5.5	97.7	23.8
15	12.5	251	235	381	5.4	210	210.5	8.19	1724.0	25.7	870.4	874.5	875.0	210.6	5.5	97.8	23.1
16	12.5	252	236	381	5.4	215	215.5	8.4	1810.2	25.7	914.0	918.3	915.0	215.1	5.5	97.8	24.4
17	12.5	251	236	381	5.1	220	220.4	8.6	1895.4	25.6	958.0	961.5	960.0	220.2	5.5	97.7	24.2
18	12.5	250	234	381	5.4	225	225.7	8.82	1990.7	25.6	1003.5	1009.8	1005.0	225.2	5.5	97.8	24.2
19	12.5	249	234	381	5.1	230	230.8	9.03	2084.1	25.6	1049.9	1057.2	1050.0	230.0	5.5	96.8	23.0
20	12.5	242	226	381	5.4	235	235.7	9.22	2173.2	25.6	1095.8	1102.4	1100.0	235.4	5.5	97.0	23.2
Averg.	**12.5**	**251.0**	**235.2**	**381.0**	**5.4**					**25.6**					**5.3**	**97.6**	**23.4**

Notes:
Diameter of Copper Cylinder = 50.1 mm
Cross-sectional Area of Copper Cylinder: A_{copper} = 0.001971357 m^2
Length of Copper Cylinder = 178 mm

Reservoir Dimensions:
Diameter: D = 405 mm
Height at overflow: H = 260 mm
Volume at overflow: V = 33.5 L = 33494.5 ml

Cross-sectional Area: A = 128824.9338 mm^2

Observations:
First bubble formation starting at 135 Volts (T1 = 120 Deg. C)
Nucleate Boiling increasing with Heat Flux.
Full Cone Spray is covering 1/2 of the total heated surface area.
Nice boiling observation along the circular edge of the copper surface.
Large droplet size. Very heavy splashing of droplets at Max. Heat Flux.

Nozzle TG 1.0			
psi	15	20	**5.3**
gpm	0.12	0.14	0.081
ml/sec	10.73	8.83	**5.12**

Estimated flow rate at 5.3 *psi* using Linear Interpolation technique.

1 Gal = 3785.411784 ml

Nozzle-to-Surface Distance = 30.1 mm

Note: Float Point and Pressure stable.

Experimental Data for Test 3

Date: 5-17-97 File Name: Test3a.prn Nozzle 1 TG 0.9
Time: 12:35 - 16:01 Case: Saturated Water Spray Duration = 360 sec.
Test: Test 3

Run	Float Point	Water Level at Start mm	Water Level at End mm	Actual Run Time sec.	Calculated Flow Rate ml/sec.	Voltage Range	Actual Voltage V	Amps A	Watts W	Hot Resistance Ohms	Range KW/m^2	Actual KW/m^2	Proposed KW/m^2	Proposed Voltage	Pressure psig	T_{water} Deg. C	T_{room} Deg. C
1	6.25	250	237	381	**4.4**	85	84.8	3.36	284.9	25.2	145.2	144.5	145.0	84.9	2.0	97.4	27.6
2	6.25	251	241	381	3.4	95	95.0	3.76	357.2	25.3	181.2	181.2	180.0	94.7	2.0	97.3	27.7
3	6.25	251	240	381	3.7	105	105.3	4.17	439.1	25.3	221.5	222.7	220.0	104.7	2.0	97.6	27.7
4	6.25	254	243	381	3.7	115	114.8	4.54	521.2	25.3	265.3	264.4	265.0	114.9	2.0	97.7	27.6
5	6.25	252	242	381	3.4	125	125.7	4.96	623.5	25.3	312.8	316.3	315.0	125.4	2.0	97.8	27.8
6	6.25	252	241	381	3.7	135	135.4	5.33	721.7	25.4	363.9	366.1	365.0	135.2	2.0	97.8	27.9
7	6.25	254	244	381	3.4	145	145.2	5.71	829.1	25.4	419.4	420.6	420.0	145.1	2.0	98.0	28.6
8	6.25	254	243	381	3.7	155	154.9	6.07	940.2	25.5	477.6	477.0	475.0	154.6	2.0	98.0	28.4
9	6.25	250	238	381	4.1	165	165.0	6.44	1062.6	25.6	539.0	539.0	540.0	165.1	2.0	97.0	28.3
10	6.25	252	241	381	3.7	175	175.8	6.84	1202.5	25.7	604.4	610.0	610.0	175.8	2.0	97.1	28.3
11	6.25	255	244	381	3.7	185	185.7	7.17	1331.5	25.9	670.3	675.4	675.0	185.6	2.0	97.4	28.6
12	6.25	250	239	381	3.7	195	194.9	7.53	1467.6	25.9	745.2	744.5	745.0	195.0	2.0	97.4	28.7
13	6.25	252	241	381	3.7	200	200.8	7.78	1562.2	25.8	786.2	792.5	790.0	200.5	2.0	97.6	28.6
14	6.25	248	236	381	4.1	205	205.4	7.99	1641.1	25.7	829.3	832.5	830.0	205.1	2.0	97.1	31.8
15	6.25	251	240	381	3.7	210	210.7	8.2	1727.7	25.7	870.6	876.4	875.0	210.5	2.0	97.4	31.4
16	6.25	254	243	381	3.7	215	215.1	8.38	1802.5	25.7	913.5	914.4	915.0	215.2	2.0	97.9	31.3
17	6.25	246	235	381	3.7	220	220.6	8.6	1897.2	25.7	957.1	962.4	960.0	220.3	2.0	97.1	31.5
18	6.25	244	233	381	3.7	225	225.8	8.82	1991.6	25.6	1003.1	1010.2	1010.0	225.8	2.0	97.1	31.6
19	6.25	230	220	381	3.4	230	230.8	9.02	2081.8	25.6	1048.7	1056.0	1055.0	230.7	2.0	96.5	31.9
20	6.25	217	206	381	3.7	235	235.9	9.23	2177.4	25.6	1096.1	1104.5	1100.0	235.4	2.0	97.3	31.7
21	6.25	202	191	381	3.7	240	240.6	9.42	2266.5	25.5	1144.0	1149.7	1150.0	240.6	2.0	97.3	31.6
Averg.	**6.3**	**246.1**	**235.1**	**381.0**	**3.7**					**25.6**					**2.0**	**97.4**	**29.5**

Notes:
Diameter of Copper Cylinder = 50.1 mm
Cross-sectional Area of Copper Cylinder: A_{copper} = 0.001971357 m^2
Length of Copper Cylinder = 178 mm

Reservoir Dimensions:
Diameter: D = 405 mm
Hight at overflow: H = 260 mm
Volume at overflow: V = 33.5 L = 33494.5 ml
Cross-sectional Area: A = 128824.9338 mm^2

Observations:
First boiling observation at 115 V.
Very small spray angle due to low flow rate.
Heavy nucleate boiling at Max. Heat Flux.
Nucleate boiling regime is covering total surface area.
High noise level.

Nozzle TG 1.0			
psi	15	20	2
gpm	0.12	0.14	0.068
ml/sec	10.73	8.83	**4.29**

Estimated flow rate at 5.3 *psi* using Linear Interpolation technique.

1 Gal = 3785.411784 ml

Nozzle-to-Surface Distance = 30.1 mm

Note: Float Point and Pressure stable.

Experimental Data for Test 4

Date: 5-18-97 File Name: Test4a.prn Nozzle 2 TG 0.5
Time: 13:40 - 17:05 Case: Saturated Water Spray Duration = 360 sec.
Test: Test 4

Run	Float Point	Water Level at Start mm	Water Level at End mm	Actual Run Time sec.	Calculated Flow Rate ml/sec.	Voltage Range	Actual Voltage V	Amps A	Watts W	Hot Resistance Ohms	Range KW/m^2	Actual KW/m^2	Proposed KW/m^2	Proposed Voltage	Pressure (+/- 1) psig	Twater Deg. C	Troom Deg. C
1	20	243	217	381	8.8	135	136.6	5.38	734.9	25.4	364.1	372.8	365.0	135.2	43.0	97.1	29.6
2	20	250	225	381	8.5	140	140.3	5.52	774.5	25.4	391.2	392.9	390.0	139.8	37.0	97.4	28.2
3	20	250	225	381	8.5	145	146.0	5.73	836.6	25.5	418.6	424.4	420.0	145.2	39.0	97.3	29.6
4	20	249	223	381	8.8	150	150.9	5.91	891.8	25.5	447.0	452.4	450.0	150.5	40.0	97.0	29.3
5	20	250	225	381	8.5	155	156.1	6.11	953.8	25.5	477.0	483.8	480.0	155.5	42.0	97.1	29.6
6	20	249	224	381	8.5	160	160.0	6.25	1000.0	25.6	507.3	507.3	510.0	160.4	45.0	97.1	28.8
7	20	247	222	381	8.5	165	165.1	6.44	1063.2	25.6	538.7	539.3	540.0	165.2	40.0	97.7	29.7
8	20	249	223	381	8.8	170	170.0	6.63	1127.1	25.6	571.7	571.7	575.0	170.5	44.0	97.3	29.9
9	20	251	225	381	8.8	175	175.3	6.82	1195.5	25.7	604.4	606.5	610.0	175.8	41.0	97.2	28.6
10	20	247	221	381	8.8	180	181.2	7.02	1272.0	25.8	636.7	645.3	640.0	180.5	43.0	97.6	30.4
11	20	249	224	381	8.5	185	185.4	7.16	1327.5	25.9	670.5	673.4	675.0	185.6	42.0	97.6	29.9
12	20	249	224	381	8.5	190	190.3	7.32	1393.0	26.0	704.4	706.6	710.0	190.8	42.0	97.6	30.1
13	20	249	223	381	8.8	195	195.6	7.53	1472.9	26.0	742.6	747.1	745.0	195.3	42.0	97.4	28.8
14	20	250	225	381	8.5	200	200.4	7.74	1551.1	25.9	783.7	786.8	785.0	200.2	43.0	97.7	30.6
15	20	249	224	381	8.5	205	205.5	7.97	1637.8	25.8	826.8	830.8	830.0	205.4	43.0	97.4	30.1
16	20	249	224	381	8.5	210	210.3	8.17	1718.2	25.7	869.1	871.6	870.0	210.1	42.0	97.4	30.2
17	20	246	221	381	8.5	215	215.3	8.38	1804.2	25.7	912.7	915.2	915.0	215.3	40.0	97.8	30.7
18	20	251	226	381	8.5	220	220.8	8.61	1901.1	25.6	957.4	964.4	965.0	220.9	42.0	97.4	31.1
19	20	236	210	381	8.8	225	225.6	8.83	1992.0	25.5	1005.1	1010.5	1010.0	225.5	44.0	96.8	30.6
20	20	223	197	381	8.8	230	230.8	9.06	2091.0	25.5	1053.4	1060.7	1060.0	230.7	46.0	96.4	31.9
21	20	221	196	381	8.5	235	236.6	9.28	2195.6	25.5	1098.8	1113.8	1105.0	235.7	42.0	95.7	32.7
22	20	204	178	381	8.8	240	242.2	9.50	2300.9	25.5	1146.1	1167.2	1165.0	242.0	42.0	96.9	33.7
Averg.	**20.0**	**243.7**	**218.3**	**381.0**	**8.6**					**25.7**					**42.0**	**97.2**	**30.2**

Notes:
Diameter of Copper Cylinder = 50.1 mm
Cross-sectional Area of Copper Cylinder: A_{copper} = 0.001971357 m^2
Length of Copper Cylinder = 178 mm

Reservoir Dimensions:
Diameter: D = 405 mm
Hight at overflow: H = 260 mm
Volume at overflow: V = 33.5 L = 33494.5 ml
Cross-sectional Area: A = 128824.9338 mm^2

Observations:
No bubble formation at Max. Heat Flux.
Large evaporation at Max. Heat Flux.
Full Cone Spray is covering total heated surface area.

Nozzle 2 TG 0.5			
psi	40	60	**42**
gpm	0.1	0.12	0.102
ml/sec	6.31	7.57	**8.6**

Estimated flow rate at 42.0 *psi* using Linear Interpolation technique.

1 Gal = 3785.411784 ml
Nozzle to Surface Distance = 40.1 mm

Note: Float Point and Pressure stable.

Experimental Data for Test 5

Date: 3-18-97 File Name: Test5.prn Nozzle: 2 TG 0.5
Time: 19:27 - 21:20 Case: Saturated Water Spray Duration = 360 sec.
Test: Test 5

Run	Float Point	Water Level at Start mm	Water Level at End mm	Actual Run Time sec.	Calculated Flow Rate ml/sec.	Voltage Range	Actual Voltage V	Amps A	Watts W	Hot Resistance Ohms	Range KW/m^2	Actual KW/m^2	Proposed KW/m^2	Proposed Voltage	Pressure psig	Twater Deg. C	Troom Deg. C
1	12.50	254	239	381	5.1	120	120.2	4.7	564.9	25.6	285.6	286.6	290.0	120.9	16.0	96.2	24.2
2	12.50	256	242	381	4.7	135	135.1	5.27	712.0	25.6	360.6	361.2	360.0	134.9	15.0	94.3	24.8
3	12.50	258	243	381	5.1	145	145.4	5.67	824.4	25.6	415.9	418.2	415.0	144.8	15.0	96.4	25.1
4	12.50	255	239	381	5.4	155	155.5	6.05	940.8	25.7	474.2	477.2	475.0	155.1	15.5	96.4	25.4
5	12.50	250	231	381	6.4	170	170.8	6.6	1127.3	25.9	566.5	571.8	565.0	169.8	15.0	96.1	25.4
6	12.50	255	239	381	5.4	180	180.2	6.92	1247.0	26.0	631.1	632.6	630.0	179.8	15.0	96.6	25.8
7	12.50	257	241	381	5.4	190	191.4	7.35	1406.8	26.0	703.2	713.6	700.0	189.6	15.0	96.8	25.3
8	12.50	250	234	381	5.4	200	201.0	7.75	1557.8	25.9	782.3	790.2	785.0	200.3	15.0	95.8	26.8
9	12.50	249	232	381	5.7	210	210.2	8.14	1711.0	25.8	866.3	867.9	870.0	210.4	15.0	95.9	25.9
10	12.50	255	240	381	5.1	220	220.1	8.54	1879.7	25.8	952.6	953.5	955.0	220.3	15.0	95.8	26.0
Averg.	**12.5**	**253.9**	**238.0**	**381.0**	**5.4**					**25.8**					**15.2**	**96.0**	**25.5**

Notes:
Diameter of Copper Cylinder = 50.1 mm
Cross-sectional Area of Copper Cylinder: Acopper = 0.001971357 m^2
Length of Copper Cylinder = 178 mm

Reservoir Dimensions:
Diameter: D = 405 mm
Height at overflow: H = 260 mm
Volume at overflow: V = 33.5 L = 33494.5 ml
Cross-sectional Area: A = 128824.9338 mm^2

Observations:
No Bubble formation.
No Nucleate Boiling.
Relatively large vapor generation due to large flow rate.

	Nozzle TG 0.5		
psi	20	30	15
gpm	0.071	0.087	0.061
ml/sec	4.48	5.49	2.8

Estimated flow rate at 15 *psi* using Linear Interpolation technique.

1 Gal = 3785.411784 ml

Note: Float Point and Pressure stable.

Experimental Data for Test 6

Date: 3-17-97 File Name: Test6.prn Nozzle: 2 TG 0.5
Time: 20:04 - 22:10 Case: Saturated Water Spray Duration = 360 sec.
Test: Test 6

Run	Float Point	Water Level at Start mm	Water Level at End mm	Actual Run Time sec.	Calculated Flow Rate ml/sec.	Voltage Range	Actual Voltage V	Amps A	Watts W	Hot Resistance Ohms	Range KW/m^2	Actual KW/m^2	Proposed KW/m^2	Proposed Voltage	Pressure psig	T_{water} Deg. C	T_{room} Deg. C
1	6.25	249	237	381	4.1	100	100.2	3.93	393.8	25.5	199.0	199.8	200.0	100.3	6.6	96.8	24.2
2	6.25	254	244	381	3.4	120	120.0	4.69	562.8	25.6	285.5	285.5	290.0	120.9	6.6	97.3	24.1
3	6.25	245	235	381	3.4	135	134.6	5.25	706.7	25.6	360.6	358.5	360.0	134.9	6.6	96.7	24.6
4	6.25	250	239	381	3.7	145	145.2	5.65	820.4	25.7	415.0	416.1	415.0	145.0	6.6	96.1	24.3
5	6.25	252	240	381	4.1	155	155.2	6.02	934.3	25.8	472.7	473.9	475.0	155.4	6.6	96.1	24.4
6	6.25	248	238	381	3.4	170	170.1	6.56	1115.9	25.9	565.4	566.0	565.0	169.9	6.6	96.4	24.4
7	6.25	246	232	381	4.7	180	180.0	6.89	1240.2	26.1	629.1	629.1	630.0	180.1	6.6	96.7	24.9
8	6.25	244	234	381	3.4	190	190.1	7.3	1387.7	26.0	703.2	703.9	700.0	189.6	6.6	96.8	24.3
9	6.25	247	237	381	3.4	200	199.6	7.71	1538.9	25.9	783.8	780.6	785.0	200.2	6.6	96.2	24.6
10	6.25	251	240	381	3.7	210	210.8	8.17	1722.2	25.8	867.0	873.6	870.0	210.4	6.6	96.1	24.2
11	6.25	255	244	381	3.7	220	220.0	8.55	1881.0	25.7	954.2	954.2	955.0	220.1	6.6	96.0	25.6
Averg.	**6.3**	**249.2**	**238.2**	**381.0**	**3.7**					**25.8**					**6.6**	**96.5**	**24.5**

Notes:
Diameter of Copper Cylinder = 50.1 mm
Cross-sectional Area of Copper Cylinder: Acopper = 0.001971357 m^2
Length of Copper Cylinder = 178 mm

Reservoir Dimensions:
Diameter: D = 405 mm
Height at overflow: H = 260 mm
Volume at overflow: V = 33.5 L = 33494.5 ml
Cross-sectional Area: A = 128824.9338 mm^2

Observations:
Bubble formation beginning at 155 Volts.
Nucleate Boiling increasing with Heat Flux.
Relatively little vapor generation due to low flow rate.
Nice boiling observation along the circular edge of the copper surface.

	Nozzle TG 0.5		
psi	20	30	**6.6**
gpm	0.071	0.087	0.044
ml/sec	4.48	5.49	**2.8**

Estimated flow rate at 6.6 *psi* using Linear Interpolation technique.

1 Gal = 3785.411784 ml

Note: Float Point and Pressure stable.

Experimental Data for Test 8

Date: 3-25-97 File Name: Test8.prn Nozzle: 3 TG 0.3
Time: 19:42 - 22:10 Case: Saturated Water Spray Duration = 360 sec.
Test: Test 8

Run	Float Point	Water Level at Start mm	Water Level at End mm	Actual Run Time sec.	Calculated Flow Rate ml/sec.	Voltage Range	Actual Voltage V	Amps A	Watts W	Hot Resistance Ohms	Range KW/m^2	Actual KW/m^2	Proposed KW/m^2	Proposed Voltage	Pressure psig	T_{water} Deg. C	T_{room} Deg. C
1	12.5	246	230	381	5.4	85	85.8	3.38	290.0	25.4	144.4	147.1	150.0	86.6	48.0	98.2	23.8
2	12.5	251	235	381	5.4	100	100.4	3.96	397.6	25.4	200.1	201.7	200.0	100.0	48.0	97.6	24.1
3	12.5	252	235	381	5.7	120	120.2	4.73	568.5	25.4	287.4	288.4	300.0	122.6	48.0	98.0	23.9
4	12.5	247	231	381	5.4	135	135.4	5.31	719.0	25.5	362.6	364.7	360.0	134.5	47.0	97.8	24.2
5	12.5	250	234	381	5.4	145	145.3	5.7	828.2	25.5	418.4	420.1	420.0	145.3	48.0	96.7	24.3
6	12.5	246	230	381	5.4	155	155.4	6.08	944.8	25.6	476.8	479.3	475.0	154.7	50.0	97.6	24.1
7	12.5	253	237	381	5.4	170	170.5	6.65	1133.8	25.6	571.8	575.1	570.0	169.7	50.0	97.6	24.2
8	12.5	251	234	381	5.7	180	180.8	7.00	1265.6	25.8	636.3	642.0	635.0	179.8	50.0	97.5	24.1
9	12.5	252	236	381	5.4	190	191.2	7.36	1407.2	26.0	704.9	713.8	700.0	189.3	50.0	96.9	24.5
10	12.5	251	235	381	5.4	200	200.3	7.74	1550.3	25.9	784.1	786.4	785.0	200.1	49.0	96.8	24.7
11	12.5	256	240	381	5.4	210	210.1	8.15	1712.3	25.8	867.8	868.6	870.0	210.3	49.0	97.6	25.3
12	12.5	248	232	381	5.4	215	216.2	8.4	1816.1	25.7	911.0	921.2	915.0	215.5	50.0	97.3	25.2
13	12.5	247	231	381	5.4	220	220.6	8.58	1892.7	25.7	954.9	960.1	950.0	219.4	50.5	96.9	24.7
14	12.5	227	211	381	5.4	225	226.1	8.81	1991.9	25.7	1000.6	1010.4	1000.0	224.9	50.0	97.5	25.9
15	12.5	206	190	381	5.4	230	232.2	9.06	2103.7	25.6	1047.0	1067.1	1050.0	230.3	50.0	97.7	24.8
Averg.	12.5	245.5	229.4	381	5.5					25.6					49.2	97.4	24.5

Notes:
Diameter of Copper Cylinder = 50.1 mm
Cross-sectional Area of Copper Cylinder: A_{copper} = 0.001971357 m^2
Length of Copper Cylinder = 178 mm

Reservoir Dimensions:
Diameter: D = 405 mm
Height at overflow: H = 260 mm
Volume at overflow: V = 33.5 L 33494.5 ml
Cross-sectional Area: A = 128824.9338 mm^2

Observations:
No bubble formation at Max. Heat Flux and therefore no Nucleate Boiling.
Large evaporation at Max. Heat Flux.
Very small (fine) droplet size. Nozzle TG 0.3 generates mist.
Note Full Cone Spray generated by Nozzle TG 0.3.

Nozzle TG 0.3			
psi	40	60	49.2
gpm	0.06	0.073	0.066
ml/sec	3.79	4.61	4.16

Estimated flow rate at 49.2 *psi* using Linear Interpolation technique.

1 Gal = 3785.411784 ml

Nozzle to Surface Distance = 30.1 mm

Note: Float Point and Pressure stable.

Experimental Data for Test 9

Date: 3-24-97 File Name: Test9.prn Nozzle: 3 TG 0.3
Time: 19:45 - 22:30 Case: Saturated Water Spray Duration = 360 sec.
Test: Test 9

Run	Float Point	Water Level at Start mm	Water Level at End mm	Actual Run Time sec.	Calculated Flow Rate ml/sec.	Voltage Range	Actual Voltage V	Amps A	Watts W	Hot Resistance Ohms	Range KW/m^2	Actual KW/m^2	Proposed KW/m^2	Proposed Voltage	Pressure psig	T_{water} Deg. C	T_{room} Deg. C
1	6.25	244	232	381	4.1	85	85.0	3.34	283.9	25.4	144.0	144.0	150.0	86.7	19.0	97.3	26.6
2	6.25	251	240	381	3.7	100	100.6	3.97	399.4	25.3	200.2	202.6	200.0	100.0	18.0	97.2	26.7
3	6.25	252	241	381	3.7	120	120.5	4.73	570.0	25.5	286.7	289.1	300.0	122.7	19.0	97.6	26.8
4	6.25	250	239	381	3.7	135	135.5	5.31	719.5	25.5	362.3	365.0	360.0	134.6	19.0	97.4	26.9
5	6.25	250	239	381	3.7	145	145.5	5.69	827.9	25.6	417.1	420.0	420.0	145.5	19.0	97.5	26.5
6	6.25	251	239	381	4.1	155	155.0	6.05	937.8	25.6	475.7	475.7	475.0	154.9	19.5	97.4	26.7
7	6.25	250	240	381	3.4	170	170.0	6.61	1123.7	25.7	570.0	570.0	570.0	170.0	19.0	97.4	26.6
8	6.25	250	238	381	4.1	180	180.4	6.98	1259.2	25.8	635.9	638.7	635.0	179.9	19.0	97.6	26.8
9	6.25	248	237	381	3.7	190	190.7	7.34	1399.7	26.0	704.8	710.0	700.0	189.3	20.0	97.2	27.1
10	6.25	250	240	381	3.4	200	200.5	7.73	1549.9	25.9	782.3	786.2	785.0	200.3	19.0	98.2	26.8
11	6.25	250	239	381	3.7	210	209.6	8.12	1702.0	25.8	866.6	863.3	870.0	210.4	20.0	97.8	26.2
12	6.25	251	240	381	3.7	215	215.5	8.37	1803.7	25.7	910.7	915.0	915.0	215.5	21.0	97.7	27.4
13	6.25	246	235	381	3.7	220	221.3	8.60	1903.2	25.7	954.1	965.4	950.0	219.5	21.0	97.4	27.7
14	6.25	232	221	381	3.7	225	226.0	8.80	1988.8	25.7	999.9	1008.8	1000.0	225.0	20.5	98.1	28.2
15	6.25	219	208	381	3.7	230	230.9	9.01	2080.4	25.6	1047.1	1055.3	1050.0	230.3	20.0	97.5	29.4
16	6.25	206	195	381	3.7	235	236.2	9.23	2180.1	25.6	1094.7	1105.9	1100.0	235.6	20.5	97.2	29.1
Averg.	6.25	243.8	232.7	381	3.7					25.7					19.6	97.5	27.2

Notes:
Diameter of Copper Cylinder = 50.1 mm
Cross-sectional Area of Copper Cylinder: A_{copper} = 0.001971357 m^2
Length of Copper Cylinder = 178 mm

Reservoir Dimensions:
Diameter: D = 405 mm
Height at overflow: H = 260 mm
Volume at overflow: V = 33.5 L = 33494.5 ml
Cross-sectional Area: A = 128824.9338 mm^2

Observations:
Bubble formation along the edge of the circular surface area at Max. Heat Flux.
Dryout in the center. (White Spots)
Very small (fine) droplet size. Nozzle TG 0.3 generates mist.
Note also the Full Cone Spray generated by Nozzle TG 0.3.

Nozzle TG 0.3			
psi	20	30	19.6
gpm	0.042	0.052	0.042
ml/sec	2.65	3.28	2.62

Estimated flow rate at 19.6 *psi* using Linear Interpolation technique.

1 Gal = 3785.411784 ml
Nozzle to Surface Distance = 30.1 mm

Note: Float point and pressure stable.

Experimental Data for Test 10

Date: 3-22-97 File Name: Test10.prn Nozzle: 1 TG 0.9
Time: 11:21 - 14:10 Case: Subcooled Water Spray Duration = 360 sec.
Test: Test 10

Run	Float Point	Water Level at Start	Water Level at End	Actual Run Time	Calculated Flow Rate	Voltage Range	Actual Voltage	Amps	Watts	Hot Resistance	Range KW/m^2	Actual KW/m^2	Proposed KW/m^2	Proposed Voltage	Pressure	T_{water}	T_{room}
		mm	mm	sec.	ml/sec.		V	A	W	Ohms					psig	Deg. C	Deg. C
1	20.0	250	226	381	8.1	70	70.2	2.76	193.8	25.4	97.7	98.3	100.0	70.8	21.0	24.7	24.1
2	20.0	252	230	381	7.4	85	85.5	3.36	287.3	25.4	144.0	145.7	150.0	86.7	21.0	24.7	23.9
3	20.0	252	228	381	8.1	100	100.4	3.94	395.6	25.5	199.1	200.7	200.0	100.2	22.0	24.6	22.3
4	20.0	251	229	381	7.4	120	121.2	4.74	574.5	25.6	285.7	291.4	300.0	123.0	21.5	24.4	24.2
5	20.0	251	228	381	7.8	135	134.8	5.26	709.0	25.6	360.7	359.7	360.0	134.9	21.0	22.7	23.1
6	20.0	252	230	381	7.4	145	144.9	5.65	818.7	25.6	415.9	415.3	420.0	145.7	21.0	22.2	24.4
7	20.0	248	225	381	7.8	155	155.6	6.04	939.8	25.8	473.1	476.7	475.0	155.3	22.0	21.9	22.7
8	20.0	252	230	381	7.4	170	170.7	6.6	1126.6	25.9	566.8	571.5	570.0	170.5	22.0	21.9	23.8
9	20.0	251	228	381	7.8	180	180.1	6.94	1249.9	26.0	633.3	634.0	635.0	180.2	22.0	21.4	23.1
10	20.0	251	229	381	7.4	190	190.4	7.33	1395.6	26.0	705.0	708.0	700.0	189.3	22.0	20.6	24.4
11	20.0	249	225	381	8.1	200	199.8	7.73	1544.5	25.8	785.0	783.4	785.0	200.0	22.0	20.5	25.1
12	20.0	252	228	381	8.1	210	210.4	8.18	1721.1	25.7	869.7	873.0	870.0	210.0	22.5	19.9	25.4
13	20.0	251	229	381	7.4	220	220.0	8.59	1889.8	25.6	958.6	958.6	960.0	220.2	22.5	20.2	24.7
14	20.0	251	226	381	8.5	225.0	225.8	8.83	1993.8	25.6	1004.2	1011.4	1000.0	224.5	23.5	19.9	24.8
15	20.0	252	230	381	7.4	230.0	231.5	9.06	2097.4	25.6	1050.2	1063.9	1050.0	230.0	22.5	20.4	22.6
Averg.	**20.0**	**251.0**	**228.1**	**381.0**	**7.8**					**25.7**					**21.9**	**22.0**	**23.9**

Notes:
Diameter of Copper Cylinder = 50.1 mm
Cross-sectional Area of Copper Cylinder: A_{copper} = 0.001971357 m^2
Length of Copper Cylinder = 178 mm

Reservoir Dimensions:
Diameter: D = 405 mm
Height at overflow: H = 260 mm
Volume at overflow: V = 33.5 L = 33494.5 ml
Cross-sectional Area: A = 128824.9338 mm^2

Observations:
No bubble formation at Max. Heat Flux and therefore no Nucleate Boiling.
Large evaporation at Max. Heat Flux.
Heavy splashing of droplets at Max. Heat Flux.

Nozzle TG 1.0			
psi	20	30	**21.9**
gpm	0.14	0.17	0.15
ml/sec	8.83	10.73	**9.31**

Estimated flow rate at *21.9 psi* using Linear Interpolation technique.

1 Gal = 3785.411784 ml
Nozzle to Surface Distance = 50.1 mm

Note: Float point and pressure very stable.

Experimental Data for Test 11

Date: 3-9-97 File Name: Test11.prn Nozzle 1 TG 0.9
Time: 16:15 - 18:00 Case: Subcooled Water Duration = 360 sec.
Test: Test 11

Run	Float Point	Water Level at Start mm	Water Level at End mm	Actual Run Time sec.	Calculated Flow Rate ml/sec.	Voltage Range	Actual Voltage V	Amps A	Watts W	Hot Resistance Ohms	Range KW/m^2	Actual KW/m^2	Proposed KW/m^2	Proposed Voltage	Pressure (+/- 0.5) psig	T_{water} Deg. C	T_{room} Deg. C
1	12.5	264	247	382	5.7	70	69.7	2.75	191.7	25.3	98.1	97.2	100.0	70.7	10.5	21.4	22.9
2	12.5	256	239	382	5.7	100	100.3	3.95	396.2	25.4	199.8	201.0	200.0	100.1	11.0	21.4	22.5
3	12.5	259	240	383	6.4	145	142.5	5.57	793.7	25.6	416.9	402.6	400.0	142.0	11.0	21.5	23.1
4	12.5	255	238	381	5.7	170	170.2	6.6	1123.3	25.8	568.5	569.8	560.0	168.7	11.0	21.4	22.4
5	12.5	242	225	381	5.7	185	185.2	7.12	1318.6	26.0	667.4	668.9	660.0	184.0	11.0	21.6	22.4
6	12.5	252	235	381	5.7	200	200.0	7.71	1542.0	25.9	782.2	782.2	800.0	202.3	11.0	21.5	21.5
7	12.5	250	234	381	5.4	210	210.0	8.12	1705.2	25.9	865.0	865.0	900.0	214.2	11.0	21.3	23.5
8	12.5	226	210	381	5.4	220	220.3	8.57	1888.0	25.7	955.1	957.7	1000.0	225.1	11.0	21.4	22.7
Averg.	**12.5**	**250.5**	**233.5**	**381.5**	**5.7**					**25.7**					**10.9**	**21.4**	**22.6**

Notes:
Diameter of Copper Cylinder = 50.1 mm
Cross-sectional Area of Copper Cylinder: A_{copper} = 0.001971357 m^2
Length of Copper Cylinder = 178 mm

Reservoir Dimensions:
Diameter: D = 405 mm
Hight at overflow: H = 260 mm
Volume at overflow: V = 33.5 L = 33494.5 ml
Cross-sectional Area: A = 128824.9338 mm^2

Observations:
No bubble formation at Max. Heat Flux, and therefore no Nucleate Boiling Regime.
The high Flow Rate is pushing bubbles of the surface.
No change in Spray Pattern, but heavy evaporation at Max. Heat Flux.

Nozzle TG 1.0			
psi	15	20	**10.9**
gpm	0.12	0.14	0.104
ml/sec	10.73	8.83	**6.54**

Estimated flow rate at 10.9 *psi* using Linear Interpolation technique.

1 Gal = 3785.411784 ml

Note: Float Point and Pressure stable.

Experimental Data for Test 12

Date: 3-9-97 File Name: Test12.prn Nozzle 1 TG 0.9
Time: 14:50 - 15:30 Case: Subcooled Water Spray Duration = 360 sec.
Test: Test 12

Run	Float Point	Water Level at Start mm	Water Level at End mm	Actual Run Time sec.	Calculated Flow Rate ml/sec.	Voltage Range	Actual Voltage V	Amps A	Watts W	Hot Resistance Ohms	Range KW/m^2	Actual KW/m^2	Proposed KW/m^2	Proposed Voltage	Pressure (+/- 0.5) psig	Twater Deg. C	Troom Deg. C
1	6.25	264	252	382	4.0	70	69.8	2.71	189.2	25.8	96.5	96.0	100.0	71.3	3.0	21.3	22.5
2	6.25	260	250	382	3.4	100	100.1	3.88	388.4	25.8	196.6	197.0	200.0	100.9	3.0	21.4	22.7
3	6.25	262	251	382	3.7	145	142.8	5.51	786.8	25.9	411.5	399.1	400.0	143.0	3.0	21.4	22.5
4	6.25	261	250	382	3.7	170	170.1	6.5	1105.7	26.2	560.2	560.9	560.0	170.0	3.0	21.4	23.4
5	6.25	260	250	381	3.4	185	185.2	7.06	1307.5	26.2	661.8	663.3	660.0	184.7	3.0	21.5	23.4
6	6.25	252	242	381	3.4	200	199.5	7.69	1534.2	25.9	782.1	778.2	800.0	202.3	3.0	21.6	24.3
7	6.25	264	254	381	3.4	210	209.8	8.12	1703.6	25.8	865.8	864.2	900.0	214.1	3.0	21.6	23.5
8	6.25	261	251	382	3.4	220	220.2	8.56	1884.9	25.7	954.4	956.1	1000.0	225.2	3.0	21.7	24.1
Averg.	**6.3**	**260.5**	**250.0**	**381.6**	**3.5**					**25.9**					**3.0**	**21.5**	**23.3**

Notes:
Diameter of Copper Cylinder = 50.1 mm
Cross-sectional Area of Copper Cylinder: A_{copper} = 0.001971357 m^2
Length of Copper Cylinder = 178 mm

Reservoir Dimensions:
Diameter: D = 405 mm
Height at overflow: H = 260 mm
Volume at overflow: V = 33.5 L = 33494.5 ml
Cross-sectional Area: A = 128824.9338 mm^2

Observations:
Bubble formation at Max. Heat Flux.
Nucleate Boiling along the circular edge of spray area.
Heavy Bubble formation in a nice circular pattern.
Slight discoloration of copper area during Max. Heat Flux.

Nozzle TG 1.0			
psi	15	20	**3**
gpm	0.12	0.14	0.072
ml/sec	10.73	8.83	**4.54**

Estimated flow rate at 3.0 *psi* using Linear Interpolation technique.

1 Gal = 3785.411784 ml

Note: Float Point and Pressure stable.

Experimental Data for Test 13

Date: 3-16-97 File Name: Test14.prn Nozzle: 2 TG 0.5
Time: 13:53 - 16:15 Case: Subcooled Water Duration = 360 sec.
Test: Test 13

Run	Float Point	Water Level at Start mm	Water Level at End mm	Actual Run Time sec.	Calculated Flow Rate ml/sec.	Voltage Range	Actual Voltage V	Amps A	Watts W	Hot Resistance Ohms	Range KW/m^2	Actual KW/m^2	Proposed KW/m^2	Proposed Voltage	Pressure psig	T_{water} Deg. C	T_{room} Deg. C
1	20.0	250	227	381	7.8	70	70.5	2.77	195.3	25.5	97.7	99.1	100.0	70.8	52.0	18.5	17.3
2	20.0	248	226	381	7.4	100	100.3	3.95	396.2	25.4	199.8	201.0	200.0	100.1	51.0	18.3	17.5
3	20.0	252	230	381	7.4	120	122.0	4.78	583.2	25.5	286.2	295.8	300.0	122.9	50.0	18.3	16.6
4	20.0	249	227	381	7.4	135	134.6	5.28	710.7	25.5	362.7	360.5	360.0	134.5	51.0	18.2	19.2
5	20.0	248	226	381	7.4	145	145.5	5.68	826.4	25.6	416.3	419.2	420.0	145.6	52.0	18.2	18.8
6	20.0	249	226	381	7.8	155	155.0	6.04	936.2	25.7	474.9	474.9	475.0	155.0	52.0	18.2	19.1
7	20.0	248	227	381	7.1	170	170.4	6.61	1126.3	25.8	568.7	571.4	570.0	170.2	51.5	18.3	18.1
8	20.0	246	224	381	7.4	180	180.3	6.96	1254.9	25.9	634.4	636.6	635.0	180.1	52.0	18.3	18.7
9	20.0	244	221	381	7.8	190	190.2	7.32	1392.3	26.0	704.8	706.2	700.0	189.4	52.0	18.3	19.5
10	20.0	248	224	381	8.1	200	199.8	7.71	1540.5	25.9	783.0	781.4	785.0	200.3	52.0	18.5	18.4
11	20.0	248	224	381	8.1	210	209.7	8.14	1707.0	25.8	868.4	865.9	870.0	210.2	52.0	18.7	20.0
12	20.0	252	230	381	7.4	220	220.4	8.58	1891.0	25.7	955.8	959.3	960.0	220.5	52.0	18.7	20.2
13	20.0	253	229	381	8.1	225	225.3	8.77	1975.9	25.7	999.6	1002.3	1000.0	225.0	52.0	18.8	20.7
14	20.0	244	221	381	7.8	230	230.2	8.97	2064.9	25.7	1045.6	1047.4	1050.0	230.5	51.0	18.8	20.8
Averg.	**20.0**	**248.8**	**226.2**	**381.0**	**7.6**					**25.7**					**51.7**	**18.4**	**18.8**

Notes:
Diameter of Copper Cylinder = 50.1 mm
Cross-sectional Area of Copper Cylinder: A_{copper} = 0.001971357 m^2
Length of Copper Cylinder = 178 mm

Reservoir Dimensions:
Diameter: D = 405 mm
Height at overflow: H = 260 mm
Volume at overflow: V = 33.5 L = 33494.5 ml
Cross-sectional Area: A = 128824.9338 mm^2

Observations:
No bubble formation at Max. Heat Flux and therefore no Nucleate Boiling.
Large evaporation at Max. Heat Flux.

Nozzle TG 0.5				
psi	20	30	25	50
gpm	0.071	0.087	0.079	0.11
ml/sec	4.48	5.49	4.99	6.94

Estimated flow rate at *50 psi* using Linear Interpolation technique.

1 Gal = 3785.411784 ml

Note: Float point and pressure stable.

Experimental Data for Test 14

Date: 3-10-97 File Name: Test15.prn Nozzle 2 TG 0.5
Time: 20:15 - 21:55 Case: Subcooled Water Spray Duration = 360 sec.
Test: Test 14

Run	Float Point (+/- .5)	Water Level at Start mm	Water Level at End mm	Actual Run Time sec.	Calculated Flow Rate ml/sec.	Voltage Range	Actual Voltage V	Amps A	Watts W	Hot Resistance Ohms	Range KW/m^2	Actual KW/m^2	Proposed KW/m^2	Proposed Voltage	Pressure (+/- 0.5) psig	T_{water} Deg. C	T_{room} Deg. C
1	6.25	252	241	381	3.7	70	70.3	2.78	195.4	25.3	98.3	99.1	100.0	70.6	13.0	21.4	22.6
2	6.25	228	217	381	3.7	100	100.3	3.96	397.2	25.3	200.3	201.5	200.0	99.9	13.0	21.4	22.4
3	6.25	251	238	382	4.4	145	142.7	5.59	797.7	25.5	417.8	404.6	400.0	141.9	13.0	21.3	22.5
4	6.25	251	240	381	3.7	170	169.5	6.58	1115.3	25.8	569.1	565.8	560.0	168.6	13.0	21.3	23.8
5	6.25	239	229	382	3.4	185	184.9	7.11	1314.6	26.0	667.6	666.9	660.0	183.9	13.0	21.2	22.9
6	6.25	249	238	381	3.7	200	200.8	7.76	1558.2	25.9	784.1	790.4	800.0	202.0	13.0	21.2	23.7
7	6.25	249	238	381	3.7	210	210.1	8.15	1712.3	25.8	867.8	868.6	900.0	213.9	13.0	21.1	23.8
8	6.25	229	218	381	3.7	220	220.3	8.56	1885.8	25.7	954.0	956.6	1000.0	225.2	13.0	21.1	23.4
Averg.	**6.3**	**243.5**	**232.4**	**381.3**	**3.8**					**25.7**					**13.0**	**21.3**	**23.1**

Notes:
Diameter of Copper Cylinder = 50.1 mm
Cross-sectional Area of Copper Cylinder: A_{copper} = 0.001971357 m^2
Length of Copper Cylinder = 178 mm

Reservoir Dimensions:
Diameter: D = 405 mm
Height at overflow: H = 260 mm
Volume at overflow: V = 33.5 L = 33494.5 ml
Cross-sectional Area: A = 128824.9338 mm^2

Observations:
High vapor concentration at Max. Heat Flux due to large evaporation rate.
Slight Nucleate Boiling along the edge.
Flow Rate too high, is pushing droplets of the heated surface.

Nozzle TG 0.5			
psi	20	30	**13**
gpm	0.071	0.087	0.057
ml/sec	4.48	5.49	**3.6**

Estimated flow rate at 13 *psi* using Linear Interpolation technique.

1 Gal = 3785.411784 ml

Note: Float Point and Pressure stable.

Experimental Data for Test 15

Date: 3-15-97 File Name: Test16.prn Nozzle: 2 TG 0.5
Time: 13:53 - 16:40 Case: Subcooled Water Spray Duration = 360 sec.
Test: Test 15

Run	Float Point	Water Level at Start mm	Water Level at End mm	Actual Run Time sec.	Calculated Flow Rate ml/sec.	Voltage Range	Actual Voltage V	Amps A	Watts W	Hot Resistance Ohms	Range KW/m^2	Actual KW/m^3	Proposed KW/m^2	Proposed Voltage	Pressure psig	T_{water} Deg. C	T_{room} Deg. C
1	12.5	250	234	381	5.4	70	70.1	2.77	194.2	25.3	98.2	98.5	100.0	70.6	25.0	19.7	19.0
2	13.0	248	231	381	5.7	100	100.5	3.96	398.0	25.4	199.9		200.0	100.0	26.0	19.6	19.2
3	12.5	248	232	381	5.4	120	120.4	4.74	570.7	25.4	287.6		300.0	122.6	25.0	19.6	19.6
4	12.5	246	230	381	5.4	135	135.3	5.31	718.4	25.5	362.8		360.0	134.5	25.0	19.6	20.3
5	12.5	245	229	381	5.4	145	145.0	5.68	823.6	25.5	417.8		420.0	145.4	26.0	19.8	20.6
6	12.5	251	235	381	5.4	155	155.0	6.05	937.8	25.6	475.7		475.0	154.9	26.0	19.8	18.9
7	12.5	252	236	381	5.4	170	169.5	6.58	1115.3	25.8	569.1		570.0	170.1	26.0	19.9	20.2
8	12.5	246	230	381	5.4	180	180.2	6.95	1252.4	25.9	633.9		635.0	180.2	26.0	20.1	20.5
9	12.5	250	235	381	5.1	190	190.5	7.32	1394.5	26.0	703.7		700.0	189.5	26.0	20.1	20.6
10	12.5	255	240	381	5.1	200	200.2	7.74	1549.5	25.9	784.5		785.0	200.1	26.0	20.2	19.6
11	12.5	252	237	381	5.1	210	210.2	8.16	1715.2	25.8	868.4		870.0	210.2	26.0	20.3	20.1
12	12.5	250	234	381	5.4	220	220.4	8.58	1891.0	25.7	955.8		960.0	220.5	26.0	20.2	19.1
13	12.5	243	227	381	5.4	225	225.4	8.78	1979.0	25.7	1000.3		1000.0	225.0	26.0	20.3	20.1
Averg.	**12.5**	**248.9**	**233.1**	**381.0**	**5.4**					**25.6**					**25.8**	**19.9**	**19.8**

Notes:
Diameter of Copper Cylinder = 50.1 mm
Cross-sectional Area of Copper Cylinder: A_{copper} = 0.001971357 m^2
Length of Copper Cylinder = 178 mm

Reservoir Dimensions:
Diameter: D = 405 mm
Height at overflow: H = 260 mm
Volume at overflow: V = 33.5 L = 33494.5 ml
Cross-sectional Area: A = 128824.9338 mm^2

Observations:
No bubble formation at Max. Heat Flux and therefore no Nucleate Boiling.
Large evaporation at Max. Heat Flux.

Nozzle TG 0.5			
psi	20	30	25
gpm	0.071	0.087	0.079
ml/sec	4.48	5.49	4.99

Estimated flow rate at 25 *psi* using Linear Interpolation technique.

1 Gal = 3785.411784 ml

Note: Float point and pressure stable.

Experimental Data for Test 17

Date: 3-22-97 File Name: Test18.prn Nozzle: 3 TG 0.3
Time: 15:50 - 18:35 Case: Subcooled Water Spray Duration = 360 sec.
Test: Test 17

Run	Float Point	Water Level at Start mm	Water Level at End mm	Actual Run Time sec.	Calculated Flow Rate ml/sec.	Voltage Range	Actual Voltage V	Amps A	Watts W	Hot Resistance Ohms	Range KW/m^2	Actual KW/m^2	Proposed KW/m^2	Proposed Voltage	Pressure psig	T_{water} Deg. C	T_{room} Deg. C
1	12.5	249	234	381	5.1	70	70.0	2.78	194.6	25.2	98.7	98.7	100.0	70.5	70.0	19.5	23.2
2	12.5	250	234	381	5.4	85	85.2	3.37	287.1	25.3	145.0	145.6	150.0	86.5	71.5	19.0	23.4
3	12.5	252	237	381	5.1	100	100.2	3.96	396.8	25.3	200.5	201.3	200.0	99.9	71.5	18.6	22.6
4	12.5	253	237	381	5.4	120	121.7	4.8	584.2	25.4	288.1	296.3	300.0	122.5	72.0	19.2	23.8
5	12.5	249	234	381	5.1	135	134.8	5.31	715.8	25.4	364.2	363.1	360.0	134.2	72.0	19.4	23.4
6	12.5	250	234	381	5.4	145	144.8	5.7	825.4	25.4	419.8	418.7	420.0	145.0	73.0	19.9	23.6
7	12.5	251	235	381	5.4	155	155.0	6.07	940.9	25.5	477.3	477.3	475.0	154.6	73.0	19.3	24.7
8	12.5	251	236	381	5.1	170	170.1	6.64	1129.5	25.6	572.3	572.9	570.0	169.7	73.0	20.1	22.1
9	12.5	251	236	381	5.1	180	180.2	6.99	1259.6	25.8	637.5	638.9	635.0	179.6	73.5	20.3	23.5
10	12.5	252	236	381	5.4	190	190.0	7.32	1390.8	26.0	705.5	705.5	700.0	189.3	73.5	20.2	24.9
11	12.5	251	235	381	5.4	200	200.1	7.72	1544.8	25.9	782.8	783.6	785.0	200.3	73.5	20.2	25.0
12	12.5	251	235	381	5.4	210	210.3	8.16	1716.0	25.8	868.0	870.5	870.0	210.2	74.0	20.5	25.6
13	12.5	251	235	381	5.4	220	220.2	8.58	1889.3	25.7	956.6	958.4	960.0	220.4	73.5	20.6	24.1
14	12.5	250	235	381	5.1	225	225.6	8.81	1987.5	25.6	1002.9	1008.2	1000.0	224.7	73.5	20.2	25.2
15	12.5	226	210	381	5.4	230	231.3	9.04	2091.0	25.6	1048.8	1060.7	1050.0	230.1	73.5	21.3	25.3
Averg.	**12.5**	**249.1**	**233.5**	**381.0**	**5.3**					**25.6**					**72.7**	**19.9**	**24.0**

Notes:
Diameter of Copper Cylinder = 50.1 mm
Cross-sectional Area of Copper Cylinder: A_{copper} = 0.001971357 m^2
Length of Copper Cylinder = 178 mm

Reservoir Dimensions:
Diameter: D = 405 mm
Height at overflow: H = 260 mm
Volume at overflow: V = 33.5 L = 33494.5 ml
Cross-sectional Area: A = 128824.9338 mm^2

Observations:
No bubble formation at Max. Heat Flux and therefore no Nucleate Boiling.
Large evaporation at Max. Heat Flux.

Nozzle TG 0.3			
psi	60	80	72.7
gpm	0.073	0.085	0.081
ml/sec	4.61	5.36	**5.09**

Estimated flow rate at 72.7 *psi* using Linear Interpolation technique.

1 Gal = 3785.411784 ml

Nozzle to Surface Distance = 30.1 mm

Note: Float point and pressure stable.

Experimental Data for Test 18

Date: 3-23-97 File Name: Test19a.prn Nozzle: 3 TG 0.3
Time: 10:00 - 13:25 Case: Subcooled Water Spray Duration = 360 sec.
Test: Test 18

Run	Float Point	Water Level at Start mm	Water Level at End mm	Actual Run Time sec.	Calculated Flow Rate ml/sec.	Voltage Range	Actual Voltage V	Amps A	Watts W	Hot Resistance Ohms	Range KW/m^2	Actual KW/m^2	Proposed KW/m^2	Proposed Voltage	Pressure psig	T_{water} Deg. C	T_{room} Deg. C
1	6.25	251	241	381	3.4	55	55.2	2.19	120.9	25.2	60.9	61.3	60.0	54.6	28.5	23.0	24.1
2	6.25	251	241	381	3.4	70	70.5	2.8	197.4	25.2	98.7	100.1	100.0	70.5	29.5	23.5	24.5
3	6.25	251	240	381	3.7	85	85.4	3.39	289.5	25.2	145.5	146.9	150.0	86.3	29.5	23.5	24.3
4	6.25	252	242	381	3.4	100	100.3	3.97	398.2	25.3	200.8	202.0	200.0	99.8	30.0	23.6	24.5
5	6.25	251	240	381	3.7	120	120.9	4.78	577.9	25.3	288.8	293.1	300.0	122.3	30.0	23.7	24.6
6	6.25	251	241	381	3.4	135	135.0	5.32	718.2	25.4	364.3	364.3	360.0	134.2	30.0	23.7	24.7
7	6.25	250	239	381	3.7	145	145.0	5.7	826.5	25.4	419.3	419.3	420.0	145.1	30.0	23.7	25.1
8	6.25	251	241	381	3.4	155	155.9	6.1	951.0	25.6	476.9	482.4	475.0	154.7	30.0	23.6	25.3
9	6.25	251	240	381	3.7	170	169.9	6.61	1123.0	25.7	570.3	569.7	570.0	169.9	30.0	22.8	24.8
10	6.25	250	240	381	3.4	180	179.9	6.95	1250.3	25.9	634.9	634.2	635.0	180.0	30.0	21.4	25.8
11	6.25	250	240	381	3.4	190	189.6	7.3	1384.1	26.0	705.1	702.1	700.0	189.3	29.5	21.3	26.2
12	6.25	250	240	381	3.4	200	199.8	7.72	1542.5	25.9	784.0	782.4	785.0	200.1	30.0	20.9	25.8
13	6.25	252	241	381	3.7	210	209.5	8.14	1705.3	25.7	869.2	865.1	870.0	210.1	31.0	20.1	26.1
14	6.25	250	239	381	3.7	215	215.3	8.38	1604.2	25.7	912.7	915.2	915.0	215.3	32.0	20.1	25.7
15	6.25	250	239	381	3.7	220	220.1	8.58	1888.5	25.7	957.1	957.9	950.0	219.2	33.0	19.8	25.6
16	6.25	250	239	381	3.7	225	225.3	6.79	1980.4	25.6	1001.9	1004.6	1000.0	224.8	32.5	19.7	26.1
17	6.25	249	239	361	3.4	230	230.4	9.00	2073.6	25.6	1048.2	1051.9	1050.0	230.2	31.0	19.8	26.8
18	6.25	250	239	381	3.7	235	235.3	9.19	2162.4	25.6	1094.1	1096.9	1100.0	235.6	31.0	19.8	25.9
Averg.	**6.25**	**250.6**	**240.1**	**381**	**3.6**					**25.5**					**30.4**	**21.9**	**25.3**

Notes:
Diameter of Copper Cylinder = 50.1 mm
Cross-sectional Area of Copper Cylinder: A_{copper} = 0.001971357 m^2
Length of Copper Cylinder = 176 mm

Reservoir Dimensions:
Diameter: D = 405 mm
Height at overflow: H = 260 mm
Volume at overflow: V = 33.5 L = 33494.5 ml
Cross-sectional Area: A = 128824.9338 mm^2

Observations:
No bubble formation at Max. Heat Flux and therefore no Nucleate Boiling.
Large evaporation at Max. Heat Flux.
Very small (fine) droplet size. Nozzle TG 0.3 generates mist.
Note also the Full Cone Spray generated by Nozzle TG 0.3.

Nozzle TG 0.3			
psi	20	30	**30.4**
gpm	0.042	0.052	0.0525
ml/sec	2.65	3.28	**3.31**

Estimated flow rate at 30.4 *psi* using Linear Interpolation technique.

1 Gal = 3785.411784 ml

Nozzle to Surface Distance = 30.1 mm

Note: Float point and pressure stable.

Appendix B

Heat Flux Analysis and Surface Temperature Data

Heat Flux Analysis

Nomenclature

a	slope obtained from linear regression analysis
b	intercept obtained from linear regression analysis
k_{Cu}	thermal conductivity of copper (W/m °C)
$q_w''_{(a)}$	test surface heat flux as a function of slope (kW/m^2)
$q_w''_{(x5)}$	test surface heat flux calculated at location of minimum heat loss (kW/m^2)
$T_{surface}$	extrapolated test surface temperature (°C)
x_5	thermocouple location at distance x_5 from test surface (58.5 mm)
x_0	location of test surface (0 mm)

The heat flux as a function of the slope was calculated using Equation 16.

$$q_w''_{(a)} = -k_{Cu} \times a \quad \text{(Eq. 16)}$$

The heat flux as a function of the distance x was calculated according to Equation 17.

$$q_w''_{(x)} = -k_{Cu} \frac{dT}{dx} \quad \text{(Eq. 17)}$$

The heat flux as a function of the distance x was evaluated at the location of minimum heat loss which was estimated at $x_5 = 58.5$ mm as shown in Equation 18.

$$q_w''_{(x=58.5)} = k_{Cu}\left(\frac{T_{Surface} - T_{(x)}}{x_0 - x}\right) \quad \text{(Eq. 18)}$$

Data Linear Regression Analysis

The linear regression calculates the slope (a) and intercept (b) from Equation 19.

$$T_{Surface} = (a \times x) + b \quad \text{..... (Eq. 19)}$$

where x is the independent variable and the Temperature $T_{(x)}$ is the dependent variable,

the slope (a) provides: $\dfrac{\Delta T}{\Delta x}$,

and the intercept (b) provides the surface temperature at $x = 0$ as shown in Figure 20. Figure 20 represents the linear temperature profile of the actual thermocouple readings to confirm the overall accuracy of the experiment.

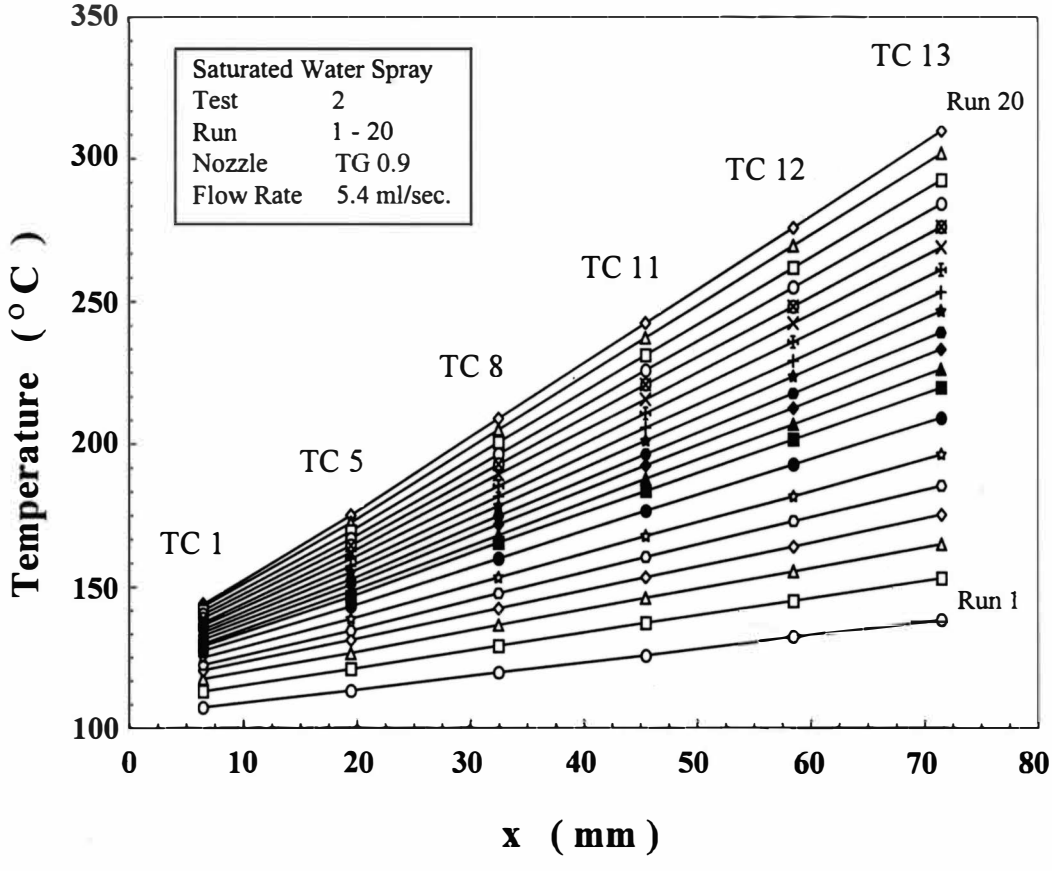

Figure 20. Surface Temperature as a Function of the Thermocouple Location for Test 2, Test Run 1 - 20.

KW Analysis for Test 1

k_{copper} = 390.3 [W / m K]

TC	X	Test1 1	Test1 2	Test1 3	Test1 4	Test1 5	Test1 6	Test1 7	Test1 8	Test1 9	Test1 10
1	6.5	103.0	104.8	107.1	111.7	114.8	118.0	121.1	123.3	124.3	125.5
5	19.5	110.0	113.1	117.7	123.1	127.7	132.8	137.4	140.7	142.7	144.9
8	32.5	118.4	123.2	129.1	135.7	142.6	149.3	155.3	160.2	163.1	166.4
11	45.5	126.6	132.4	140.3	148.8	157.2	165.8	174.1	179.8	184.0	188.2
12	58.5	135.2	142.2	151.6	160.9	171.3	181.9	192.1	199.4	204.0	209.6
13	71.5	143.3	151.8	162.5	173.7	185.5	197.9	210.2	218.6	224.5	231.3
Tsurface	0	98.3	99.5	101.3	104.9	107.1	109.3	111.2	112.7	113.3	113.8
a		0.627033	0.728571	0.856923	0.959341	1.096484	1.238022	1.381099	1.477363	1.551209	1.637143
Q" [KW/m^2]		Q1	Q2	Q3	Q4	Q5	Q6	Q7	Q8	Q9	Q10
Q" (a)		244.7	284.4	334.5	374.4	428.0	483.2	539.0	576.6	605.4	639.0
Q" (x5)		246.2	284.9	335.6	373.6	428.3	484.4	539.7	578.4	605.1	639.2

TC	X	Test1 11	Test1 12	Test1 13	Test1 14	Test1 15	Test1 16	Test1 17	Test1 18	Test1 19
1	6.5	126.6	128.3	129.5	130.7	131.9	133.2	133.9	135.5	137.0
5	19.5	147.2	149.3	151.7	154.0	156.5	159.2	161.2	164.1	166.8
8	32.5	169.8	173.3	176.8	180.8	184.3	188.2	191.7	196.1	200.0
11	45.5	192.7	197.5	202.2	207.2	212.2	217.4	222.1	228.5	233.4
12	58.5	215.4	221.4	227.0	233.3	239.8	246.2	252.3	260.3	266.8
13	71.5	238.3	245.2	252.4	259.8	267.9	276.0	282.8	292.4	300.5
Tsurface	0	114.3	115.1	115.7	116.3	116.7	117.3	117.5	118.1	118.8
a		1.727473	1.813187	1.902851	1.999560	2.105055	2.207033	2.303736	2.429670	2.529451
Q" [KW/m^2]		Q11	Q12	Q13	Q14	Q15	Q16	Q17	Q18	Q19
Q" (a)		674.2	707.7	742.7	780.4	821.6	861.4	899.1	948.3	987.2
Q" (x5)		674.5	709.2	742.6	780.6	821.3	860.0	899.4	948.7	987.4

KW Analysis for Test 2

k_{copper} = 390.3 [W / m K]

TC	X	Test2 1	Test2 2	Test2 3	Test2 4	Test2 5	Test2 6	Test2 7	Test2 8	Test2 9	Test2 10
1	6.5	107.1	112.9	117.3	120.3	122.3	124.9	127.2	128.9	129.8	131.3
5	19.5	113.2	120.8	126.4	131.1	134.4	138.7	143.1	146.5	148.4	150.7
8	32.5	119.6	129.1	136.4	142.3	147.6	153.3	159.9	165.3	168	171.8
11	45.5	125.7	137.2	146.1	153.4	160.4	167.7	176.5	183.4	187.7	192.4
12	58.5	132.3	145.1	155.5	164.1	172.9	181.6	192.9	201.6	206.9	212.6
13	71.5	138.5	153.1	165	175.2	185.4	196.3	209.3	219.8	226.3	233.3
Tsurface	0	103.8	108.9	112.4	114.8	115.8	117.6	118.7	119.6	119.8	120.6
a		0.484396	0.619780	0.737363	0.845275	0.975385	1.099121	1.267033	1.401978	1.489451	1.574286
Q" [KW/m^2]		Q1	Q2	Q3	Q4	Q5	Q6	Q7	Q8	Q9	Q10
Q" (a)		189.1	241.9	287.8	329.9	380.7	429.0	494.5	547.2	581.3	614.4
Q" (x5)		190.1	241.5	287.6	328.9	381.0	427.0	495.0	547.1	581.1	613.8

TC	X	Test2 11	Test2 12	Test2 13	Test2 14	Test2 15	Test2 16	Test2 17	Test2 18	Test2 19	Test2 20
1	6.5	132.5	133.7	134.9	136.2	137.3	138.8	140.2	141.5	143.1	143.9
5	19.5	152.6	155.1	157.3	159.8	162	164.4	166.8	169.4	172.4	175
8	32.5	174.7	178.2	181.5	185.2	189.3	192.8	196.4	200.5	205	208.8
11	45.5	196.4	201.1	205.6	210.7	215.6	220.8	225.8	231.1	237.2	242.4
12	58.5	217.7	223.7	229.2	235.8	242.4	248.3	254.9	261.7	269.4	275.7
13	71.5	239.2	246.7	253.3	261.1	268.9	276.1	284.1	292.5	301.8	309.6
Tsurface	0	121.2	121.7	122.3	122.9	123.3	124.0	124.5	125.0	125.8	126.1
a		1.649451	1.744396	1.828132	1.929670	2.034066	2.123516	2.226813	2.335165	2.454286	2.55868
Q" [KW/m^2]		Q11	Q12	Q13	Q14	Q15	Q16	Q17	Q18	Q19	Q20
Q" (a)		643.8	680.8	713.5	753.2	793.9	828.8	869.1	911.4	957.9	998.7
Q" (x5)		643.8	680.5	713.2	753.2	794.6	829.3	870.0	912.0	958.1	998.1

KW Analysis for Test 3

k_{copper} = 390.3 [W / m K]

TC	X	Test3 1	Test3 2	Test3 3	Test3 4	Test3 5	Test3 6	Test3 7	Test3 8	Test3 9	Test3 10	Test3 11
1	6.5	108.9	114.3	116.8	119.7	121.8	124.4	126.8	129.1	131.1	133.8	135.7
5	19.5	112.9	119.1	123.1	126.9	130.7	134.6	138.5	142.7	146.5	150.9	154.5
8	32.5	117.7	125.1	130.2	135.5	140.8	146.6	152.2	158.0	163.7	170.2	175.7
11	45.5	122.1	130.5	137.1	143.5	150.3	157.4	164.8	172.5	180.0	188.4	195.8
12	58.5	126.5	135.8	143.9	151.4	159.9	168.3	177.4	186.9	196.3	206.6	216.3
13	71.5	130.9	141.4	150.6	159.2	169.2	179.2	190.1	201.4	212.7	225.3	236.4
Tsurface	0	106.5	111.3	113.2	115.5	116.8	118.7	120.1	121.5	122.5	124.1	125.0
a		0.341099	0.419780	0.523736	0.613187	0.734286	0.848132	0.979780	1.117802	1.260879	1.412747	1.558242
Q" [KW/m^2]		Q1	Q2	Q3	Q4	Q5	Q6	Q7	Q8	Q9	Q10	Q11
Q" (a)		133.1	163.8	204.4	239.3	286.6	331.0	382.4	436.3	492.1	551.4	608.2
Q" (x5)		133.4	163.5	204.8	239.5	287.6	330.9	382.3	436.3	492.4	550.4	609.1

TC	X	Test3 12	Test3 13	Test3 14	Test3 15	Test3 16	Test3 17	Test3 18	Test3 19	Test3 20	Test3 21
1	6.5	137.7	139.5	142.1	143.3	145.1	145.9	148.5	150.0	151.9	153.4
5	19.5	158.4	161.6	166.0	168.7	171.5	173.0	177.2	180.2	183.0	186.4
8	32.5	181.5	186.4	192.4	195.6	199.8	201.9	208.3	212.3	216.9	221.2
11	45.5	204.0	210.5	217.9	222.5	227.7	230.7	239.1	244.4	250.4	256.1
12	58.5	226.1	234.5	243.2	249.2	255.5	259.5	269.8	276.6	283.8	290.7
13	71.5	248.4	258.2	269.1	276.0	283.8	288.4	300.7	308.7	317.4	325.6
Tsurface	0	125.9	126.8	128.7	129.3	130.5	130.8	132.3	133.1	134.2	135.3
a		1.712308	1.838022	1.960659	2.048132	2.139341	2.199560	2.350769	2.450110	2.556923	2.656703
Q" [KW/m^2]		Q12	Q13	Q14	Q15	Q16	Q17	Q18	Q19	Q20	Q21
Q" (a)		668.3	717.4	765.2	799.4	835.0	858.5	917.5	956.3	998.0	1036.9
Q" (x5)		668.5	718.6	763.9	799.9	834.0	858.7	917.4	957.4	998.1	1036.8

KW Analysis for Test 4

k_{copper} = 390.3 [W / m K]

TC	X	Test4 1	Test4 2	Test4 3	Test4 4	Test4 5	Test4 6	Test4 7	Test4 8	Test4 9	Test4 10	Test4 11
1	6.5	105.6	106.4	108.1	109.6	111.3	112.3	114.8	115.1	116.5	118.4	119.3
5	19.5	116.0	117.7	120.2	122.7	125.1	127.1	130.3	132.1	134.4	137.2	138.9
8	32.5	128.6	130.7	134.2	137.2	140.8	143.4	147.9	150.4	153.5	157.7	160.5
11	45.5	140.3	142.8	147.3	151.3	155.6	159.1	164.1	168.1	172.0	177.3	181.0
12	58.5	152.0	155.1	160.2	165.0	170.3	174.5	180.7	185.2	190.2	196.7	201.3
13	71.5	163.3	167.3	173.3	178.7	185.1	190.1	197.1	202.8	209.0	216.4	222.0
Tsurface	0	99.3	99.9	101.2	102.4	103.5	104.2	106.2	106.2	107.0	108.3	108.7
a		0.897143	0.942418	1.009011	1.069231	1.141538	1.201978	1.272308	1.352747	1.425055	1.512308	1.585055
Q" [KW/m^2]		Q1	Q2	Q3	Q4	Q5	Q6	Q7	Q8	Q9	Q10	Q11
Q" (a)		350.2	367.8	393.8	417.3	445.5	469.1	496.6	528.0	556.2	590.3	618.6
Q" (x5)		351.6	368.3	393.6	417.7	445.7	469.0	497.0	527.1	555.1	589.8	617.8

TC	X	Test4 12	Test4 13	Test4 14	Test4 15	Test4 16	Test4 17	Test4 18	Test4 19	Test4 20	Test4 21	Test4 22
1	6.5	120.6	122.3	123.6	125.1	126.7	128.2	129.4	130.4	131.5	134.1	135.4
5	19.5	141.1	143.9	146.6	149.1	151.9	154.4	157.0	159.4	162.2	166.0	168.1
8	32.5	163.5	167.6	171.3	175.1	179.3	182.7	187.1	192.0	196.1	200.7	204.4
11	45.5	185.3	190.2	195.2	200.2	205.6	210.7	215.7	221.4	227.5	234.6	239.4
12	58.5	206.6	212.9	218.9	225.3	231.9	238.5	244.9	251.8	259.6	268.6	274.8
13	71.5	228.1	235.7	243.1	250.8	258.5	266.9	274.3	284.0	291.8	302.8	310.6
Tsurface	0	109.4	110.5	111.3	112.0	113.0	113.4	114.2	114.4	115.0	116.2	116.6
a		1.661099	1.750769	1.842418	1.938901	2.033626	2.140220	2.234725	2.361758	2.472747	2.604835	2.705714
Q" [KW/m^2]		Q12	Q13	Q14	Q15	Q16	Q17	Q18	Q19	Q20	Q21	Q22
Q" (a)		648.3	683.3	719.1	756.8	793.7	835.3	872.2	921.8	965.1	1016.7	1056.0
Q" (x5)		648.5	683.2	717.9	755.9	793.3	834.6	872.0	916.7	964.7	1016.8	1055.5

KW Analysis for Test 5

k_{copper} = 390.3 [W / m K]

TC	X	Test5 1	Test5 2	Test5 3	Test5 4	Test5 5	Test5 6	Test5 7	Test5 8	Test5 9	Test5 10
1	6.5	108.4	112.8	116.8	120.4	124.7	127.5	129.9	132.1	134.8	137.1
5	19.5	115.6	122.6	128.1	133.6	140.4	144.6	148.9	153.9	158.5	163.1
8	32.5	125.0	134.1	141.3	148.6	157.9	164.2	171.1	178.1	185.0	192.4
11	45.5	134.4	145.3	154.5	163.4	175.3	183.9	192.8	202.4	211.7	221.8
12	58.5	143.4	156.6	167.0	178.0	192.6	203.1	214.4	226.4	238.2	251.0
13	71.5	152.2	167.7	179.9	192.6	210.0	222.6	236.1	250.6	265.0	280.5
Tsurface	0	103.1	106.6	109.8	112.5	115.3	116.8	118.0	119.1	120.3	121.1
a		0.685275	0.852088	0.978901	1.118681	1.319780	1.474066	1.646593	1.833626	2.014945	2.220000
Q" [KW/m^2]		Q1	Q2	Q3	Q4	Q5	Q6	Q7	Q8	Q9	Q10
Q" (a)		267.5	332.6	382.1	436.6	515.1	575.3	642.7	715.7	786.4	866.5
Q" (x5)		268.9	333.6	381.6	437.0	515.7	575.8	643.2	715.9	786.6	866.7

KW Analysis for Test 6

k_{copper} = 390.3 [W / m K]

TC	X	Test6 1	Test6 2	Test6 3	Test6 4	Test6 5	Test6 6	Test6 7	Test6 8	Test6 9	Test6 10	Test6 11
1	6.5	107.6	115.4	120.2	123.5	126.0	129.0	132.0	134.7	137.0	140.0	143.9
5	19.5	112.9	122.9	129.9	134.8	138.4	144.3	149.0	153.8	158.2	163.2	169.9
8	32.5	119.3	132.1	141.2	148.1	153.6	161.8	168.8	175.7	182.3	189.9	199.3
11	45.5	125.7	140.7	152.6	161.0	168.3	179.3	188.2	197.5	206.2	216.5	228.5
12	58.5	132.0	149.6	163.4	173.6	182.6	196.4	207.5	218.8	230.3	243.1	257.6
13	71.5	138.4	158.4	174.3	186.3	197.2	213.7	226.6	240.3	254.0	269.8	287.2
Tsurface	0	104.0	110.5	114.2	116.6	117.8	119.6	121.4	123.0	123.9	125.3	127.9
a		0.478462	0.667473	0.840440	0.974286	1.107538	1.312747	1.467912	1.636923	1.813626	2.011648	2.217143
Q" [KW/m^2]		Q1	Q2	Q3	Q4	Q5	Q6	Q7	Q8	Q9	Q10	Q11
Q" (a)		186.7	260.5	328.0	380.3	432.3	512.4	572.9	638.9	707.9	785.1	865.4
Q" (x5)		186.8	260.9	328.3	380.3	432.3	512.4	574.4	639.2	709.9	785.9	865.3

KW Analysis for Test 8

k_{copper} = 390.3 [W / m K]

TC	X	Test8 1	Test8 2	Test8 3	Test8 4	Test8 5	Test8 6	Test8 7	Test8 8
1	6.5	89.9	94.9	102.6	109.0	112.3	116.0	119.7	122.3
5	19.5	92.3	99.0	109.5	117.5	122.6	128.0	134.2	139.0
8	32.5	97.8	105.9	118.9	129.7	136.3	144.2	152.7	159.1
11	45.5	102.2	112.1	127.4	140.9	149.4	158.9	169.9	178.9
12	58.5	106.5	118.2	136.5	151.8	161.8	173.8	187.2	197.9
13	71.5	111.5	124.7	145.4	162.9	174.7	188.4	204.6	217.5
Tsurface	0	86.7	90.9	97.4	102.4	104.9	107.5	109.9	111.5
a		0.340659	0.467692	0.667033	0.843077	0.972967	1.129890	1.320220	1.478022
Q" [KW/m^2]		Q1	Q2	Q3	Q4	Q5	Q6	Q7	Q8
Q" (a)		133.0	182.5	260.3	329.1	379.7	441.0	515.3	576.9
Q" (x5)		132.1	182.1	260.9	329.6	379.6	442.3	515.7	576.4

TC	X	Test8 9	Test8 10	Test8 11	Test8 12	Test8 13	Test8 14	Test8 15
1	6.5	124.7	126.8	128.6	129.4	130.2	131.1	132.5
5	19.5	143.0	147.4	151.5	153.9	156.0	158.2	160.9
8	32.5	165.3	172.0	178.5	182.1	185.7	189.2	193.6
11	45.5	186.8	195.7	204.9	210.2	215.1	219.9	225.7
12	58.5	208.3	219.6	230.8	237.7	244.3	250.5	258.0
13	71.5	229.7	243.8	257.7	265.9	273.6	281.0	290.4
Tsurface	0	112.7	113.5	114.0	114.1	114.13	114.4	114.8
a		1.631648	1.813846	1.999560	2.114286	2.222637	2.323297	2.445934
Q" [KW/m^2]		Q9	Q10	Q11	Q12	Q13	Q14	Q15
Q" (a)		636.8	707.9	780.4	825.2	867.5	906.8	954.6
Q" (x5)		637.8	707.9	779.3	824.6	868.5	908.0	955.4

KW Analysis for Test 9

k_{copper} = 390.3 [W / m K]

TC	X	Test9 1	Test9 2	Test9 3	Test9 4	Test9 5	Test9 6	Test9 7	Test9 8
1	6.5	96.1	102.9	110.2	113.5	115.4	118.1	121.2	123.6
5	19.5	99.0	107.2	117.0	123.2	126.9	130.7	136.4	140.8
8	32.5	103.7	113.7	126.3	134.5	140.2	145.8	154.2	160.4
11	45.5	108.2	119.9	134.9	145.7	153.0	160.5	171.5	180.0
12	58.5	112.6	125.9	143.5	156.7	165.7	175.0	188.7	199.1
13	71.5	117.3	132.4	152.4	167.7	178.6	189.4	205.9	218.5
Tsurface	0	93.2	99.0	105.1	107.4	108.5	110.0	111.8	113.1
a		0.332527	0.461099	0.657363	0.841099	0.978462	1.107912	1.313626	1.470330
Q" [KW/m^2]		Q1	Q2	Q3	Q4	Q5	Q6	Q7	Q8
Q" (a)		129.8	180.0	256.6	328.3	381.9	432.4	512.7	573.9
Q" (x5)		129.4	179.5	256.2	328.9	381.6	433.7	513.1	573.8

TC	X	Test9 9	Test9 10	Test9 11	Test9 12	Test9 13	Test9 14	Test9 15	Test9 16
1	6.5	126.7	129.6	132.1	133.9	135.5	137.8	139.9	141.9
5	19.5	145.2	150.0	154.2	157.6	159.3	163.0	165.9	168.9
8	32.5	167.0	173.9	180.6	184.9	187.8	193.2	197.5	202.0
11	45.5	188.5	197.8	206.8	212.7	216.4	223.8	229.4	235.3
12	58.5	209.9	221.5	233.0	240.5	245.1	254.4	261.6	268.8
13	71.5	231.7	245.5	259.2	268.3	273.9	285.0	293.8	302.5
Tsurface	0	114.7	116.3	117.3	118.4	119.2	120.3	121.4	122.5
a		1.627692	1.797582	1.973846	2.084615	2.149451	2.287473	2.392308	2.496703
Q" [KW/m^2]		Q9	Q10	Q11	Q12	Q13	Q14	Q15	Q16
Q" (a)		635.3	701.6	770.4	813.6	838.9	892.8	933.7	974.5
Q" (x5)		635.2	701.9	771.9	814.6	840.0	894.7	935.4	976.1

KW Analysis for Test 10

k_{copper} = 393 [W / m K]

TC	X	Test10 1	Test10 2	Test10 3	Test10 4	Test10 5	Test10 6	Test10 7	Test10 8
1	6.5	38.3	43.3	48.6	57.6	64.4	69.0	75.4	84.6
5	19.5	39.6	46.0	53.3	65.1	74.1	80.4	88.9	100.6
8	32.5	43.7	51.3	59.9	74.9	86.5	94.2	104.8	119.8
11	45.5	46.4	55.5	66.2	83.8	98.0	107.9	120.4	137.5
12	58.5	49.3	59.9	72.3	92.7	109.4	120.8	135.5	155.4
13	71.5	52.4	64.7	78.6	102.3	120.9	134.3	150.5	172.5
Tsurface	0	36.2	40.3	44.9	52.4	57.9	61.6	67.1	75.1
a		0.224835	0.336044	0.468791	0.692747	0.878901	1.014066	1.166813	1.366154
Q" [KW/m^2]		Q1	Q2	Q3	Q4	Q5	Q6	Q7	Q8
Q" (a)		88.4	132.1	184.2	272.2	345.4	398.5	458.6	536.9
Q" (x5)		88.0	131.7	184.1	270.7	346.0	397.7	459.5	539.5

TC	X	Test10 9	Test10 10	Test10 11	Test10 12	Test10 13	Test10 14	Test10 15
1	6.5	92.2	98.7	105.4	113.6	120.6	123.1	126.6
5	19.5	109.8	118.6	127.4	137.5	147.0	151.1	155.8
8	32.5	131.1	141.0	152.4	165.3	176.4	182.5	188.4
11	45.5	150.9	163.2	176.2	191.8	205.7	213.1	221.1
12	58.5	170.3	184.6	199.8	218.0	234.6	243.8	253.1
13	71.5	189.7	206.2	223.7	244.7	263.9	274.7	285.7
Tsurface	0	81.6	87.1	92.8	99.3	104.9	106.6	109.1
a		1.513846	1.665275	1.829670	2.029670	2.216703	2.344396	2.461758
Q" [KW/m^2]		Q9	Q10	Q11	Q12	Q13	Q14	Q15
Q" (a)		594.9	654.5	719.1	797.7	871.2	921.3	967.5
Q" (x5)		595.9	655.0	718.8	797.4	871.3	921.7	967.4

KW Analysis for Test 11

k_{copper} = 393 [W / m K]

TC	X	Test11 1	Test11 2	Test11 3	Test11 4	Test11 5	Test11 6	Test11 7	Test11 8
1	6.5	36.5	48.4	70.9	89.2	100.1	111.1	119.6	128.1
5	19.5	39.3	54.6	84.0	108.6	122.1	136.8	147.0	157.5
8	32.5	42.4	60.9	97.2	127.1	143.3	161.0	173.6	186.8
11	45.5	42.3	61.0	97.0	127.2	143.8	161.5	174.2	187.4
12	58.5	48.3	73.5	122.5	162.1	184.4	208.9	226.5	245.7
13	71.5	51.7	79.6	135.0	179.7	204.7	232.7	253.0	275.2
Tsurface	0	34.9	45.3	64.8	81.2	90.5	99.9	106.8	113.4
a		0.233407	0.481538	0.985934	1.385934	1.606154	1.864835	2.049231	2.263516
Q" [KW/m^2]		Q1	Q2	Q3	Q4	Q5	Q6	Q7	Q8
Q" (a)		91.7	189.2	387.5	544.7	631.2	732.9	805.3	889.6
Q" (x5)		90.0	189.4	387.6	543.5	630.8	732.3	804.1	888.8

KW Analysis for Test 12

k_{copper} = 393 [W / m K]

TC	X	Test12 1	Test12 2	Test12 3	Test12 4	Test12 5	Test12 6	Test12 7	Test12 8
1	6.5	41.2	56.0	84.4	106.7	118.4	129.3	135.4	141.0
5	19.5	44.6	63.0	99.2	127.9	141.9	153.3	161.0	168.5
8	32.5	48.0	69.6	111.3	145.4	162.7	177.4	187.3	197.3
11	45.5	50.8	75.4	123.4	162.2	182.8	201.4	214.2	226.7
12	58.5	53.8	81.1	135.5	178.9	202.8	225.1	240.1	255.8
13	71.5	57.1	87.6	147.2	195.3	223.3	249.0	267.1	285.5
Tsurface	0	39.8	53.4	79.5	100.2	109.6	117.4	121.8	125.6
a		0.241538	0.479341	0.956044	1.346813	1.598462	1.841538	2.027912	2.228132
Q" [KW/m^2]		Q1	Q2	Q3	Q4	Q5	Q6	Q7	Q8
Q" (a)		94.9	188.4	375.7	529.3	628.2	723.7	797.0	875.7
Q" (x5)		94.1	186.1	376.2	528.7	626.1	723.5	794.7	874.7

KW Analysis for Test 13

k_{copper} = 393 [W / m K]

TC	X	Test13 1	Test13 2	Test13 3	Test13 4	Test13 5	Test13 6	Test13 7
1	6.5	37.0	48.4	60.8	68.8	75.4	81.5	90.7
5	19.5	38.3	52.8	68.1	78.2	86.3	94.3	106.3
8	32.5	42.0	59.3	77.2	89.9	100.2	109.7	124.9
11	45.5	44.4	64.8	86.5	101.3	113.3	124.9	142.5
12	58.5	47.5	71.1	95.7	112.8	126.6	140.0	160.1
13	71.5	50.8	77.3	105.0	124.5	140.0	154.8	177.5
Tsurface	0	34.8	44.7	55.4	62.2	67.8	73.1	81.1
a		0.217582	0.450330	0.688132	0.865275	1.004396	1.140220	1.347253
Q" [KW/m^2]		Q1	Q2	Q3	Q4	Q5	Q6	Q7
Q" (a)		85.5	177.0	270.4	340.1	394.7	448.1	529.5
Q" (x5)		85.3	177.4	270.7	339.9	395.0	449.4	530.7

TC	X	Test13 8	Test13 9	Test13 10	Test13 11	Test13 12	Test13 13	Test13 14
1	6.5	97.8	103.7	110.2	115.7	120.9	123.0	125.2
5	19.5	115.7	123.5	132.3	140.4	148.1	151.7	155.2
8	32.5	135.9	146.5	157.1	167.8	177.4	182.3	187.2
11	45.5	155.4	167.9	181.2	194.3	207.1	213.1	219.4
12	58.5	174.8	189.5	204.8	221.1	236.2	243.7	251.5
13	71.5	194.5	211.3	229.0	247.8	265.7	274.7	283.9
Tsurface	0	87.4	92.1	97.5	101.5	105.3	106.8	108.2
a		1.495165	1.664615	1.836484	2.041978	2.237363	2.341319	2.449670
Q" [KW/m^2]		Q8	Q9	Q10	Q11	Q12	Q13	Q14
Q" (a)		587.6	654.2	721.7	802.5	879.3	920.1	962.7
Q" (x5)		587.1	654.3	720.8	803.5	879.4	919.7	962.7

KW Analysis for Test 14

k_{copper} = 393 [W / m K]

TC	X	Test14 1	Test14 2	Test14 3	Test14 4	Test14 5	Test14 6	Test14 7	Test14 8
1	6.5	41.0	56.4	83.6	103.7	114.6	124.7	130.2	134.5
5	19.5	44.3	62.9	96.6	122.6	136.9	148.9	156.1	162.7
8	32.5	47.4	69.7	109.4	140.6	157.7	173.5	182.5	191.3
11	45.5	50.3	75.8	122.2	158.0	178.0	197.7	209.4	220.9
12	58.5	53.5	82.0	134.5	175.1	198.3	221.9	235.7	250.1
13	71.5	56.8	88.4	146.8	192.3	218.5	246.1	262.6	279.6
Tsurface	0	39.5	53.4	77.6	95.6	105.3	112.6	116.6	119.3
a		0.240659	0.490989	0.972527	1.358022	1.591209	1.868571	2.038901	2.235824
Q" [KW/m^2]		Q1	Q2	Q3	Q4	Q5	Q6	Q7	Q8
Q" (a)		94.6	193.0	382.2	533.7	625.3	734.3	801.3	878.7
Q" (x5)		94.1	192.1	382.3	534.1	624.8	734.3	800.1	878.7

KW Analysis for Test 15

k_{copper} = 393 [W / m K]

TC	X	Test15 1	Test15 2	Test15 3	Test15 4	Test15 5	Test15 6	Test15 7
1	6.5	37.1	50.5	61.1	70.0	76.9	83.8	94.4
5	19.5	39.0	55.7	68.8	79.7	88.6	97.4	110.5
8	32.5	42.1	62.0	77.6	91.3	102.0	112.4	127.8
11	45.5	44.9	67.9	86.7	102.6	115.1	127.6	145.4
12	58.5	48.0	74.5	95.8	114.1	128.5	142.7	162.8
13	71.5	50.9	80.9	105.0	125.7	141.5	157.2	179.9
Tsurface	0	35.2	46.9	56.0	63.5	69.7	75.8	85.2
a		0.217143	0.470989	0.680440	0.863736	1.001758	1.138681	1.323077
Q" [KW/m^2]		Q1	Q2	Q3	Q4	Q5	Q6	Q7
Q" (a)		85.3	185.1	267.4	339.4	393.7	447.5	520.0
Q" (x5)		86.0	185.4	267.4	339.9	395.0	449.4	521.3

TC	X	Test15 8	Test15 9	Test15 10	Test15 11	Test15 12	Test15 13
1	6.5	102.1	109.8	117.1	123.3	129.0	131.5
5	19.5	120.4	129.9	138.9	147.8	156.0	159.5
8	32.5	140.0	151.7	163.0	174.0	184.9	189.7
11	45.5	159.9	173.7	187.1	200.7	214.3	220.8
12	58.5	179.2	195.1	211.1	227.1	243.8	251.6
13	71.5	198.5	216.7	235.1	254.0	273.6	282.4
Tsurface	0	91.9	98.4	104.2	109.1	113.2	114.9
a		1.490769	1.652967	1.825714	2.017802	2.232527	2.333846
Q" [KW/m^2]		Q8	Q9	Q10	Q11	Q12	Q13
Q" (a)		585.9	649.6	717.5	793.0	877.4	917.2
Q" (x5)		586.5	649.6	718.1	792.7	877.4	918.3

KW Analysis for Test 17

k_{copper} = 393 [W / m K]

TC	X	Test17 1	Test17 2	Test17 3	Test17 4	Test17 5	Test17 6	Test17 7	Test17 8
1	6.5	36.6	43.3	50.0	62.2	71.9	78.9	85.0	94.9
5	19.5	38.3	46.2	54.4	69.2	80.7	89.3	97.5	105.1
8	32.5	41.6	50.9	60.8	78.8	92.2	102.9	112.7	128.0
11	45.5	44.7	55.7	67.0	87.8	104.1	116.2	127.8	145.8
12	58.5	47.3	60.1	73.3	97.0	115.6	129.2	142.5	163.2
13	71.5	50.4	64.6	79.5	106.4	127.1	142.7	157.3	180.4
Tsurface	0	34.7	40.4	46.1	56.7	65.0	71.2	76.6	83.2
a		0.217358	0.335600	0.461507	0.687417	0.861153	0.991420	1.122163	1.359083
Q" [KW/m^2]		Q1	Q2	Q3	Q4	Q5	Q6	Q7	Q8
Q" (a)		85.4	131.9	181.4	270.2	338.4	389.6	441.0	534.1
Q" (x5)		84.6	132.3	182.7	270.7	339.9	389.6	442.7	537.4

TC	X	Test17 9	Test17 10	Test17 11	Test17 12	Test17 13	Test17 14	Test17 15
1	6.5	101.8	107.7	112.7	118.2	122.5	124.4	126.4
5	19.5	118.6	126.3	133.8	141.8	148.8	152.6	155.7
8	32.5	138.9	148.5	158.3	168.8	178.3	183.5	188.2
11	45.5	158.8	170.1	182.6	195.3	207.7	214.2	220.8
12	58.5	178.1	191.6	206.0	221.7	236.7	244.9	252.8
13	71.5	197.5	213.1	230.1	248.2	266.0	275.8	285.4
Tsurface	0	91.0	95.8	99.7	103.9	106.8	108.0	109.0
a		1.484738	1.633013	1.815923	2.009619	2.216672	2.335115	2.454210
Q" [KW/m^2]		Q9	Q10	Q11	Q12	Q13	Q14	Q15
Q" (a)		583.5	641.8	713.7	789.8	871.2	917.7	964.5
Q" (x5)		585.1	643.6	714.1	791.4	872.7	919.7	966.0

KW Analysis for Test 18

k_{copper} = 393 [W / m K]

TC	X	Test18 1	Test18 2	Test18 3	Test18 4	Test18 5	Test18 6	Test18 7	Test18 8	Test18 9
1	6.5	35.3	41.4	49.5	57.8	71.2	82.1	90.0	97.9	107.4
5	19.5	36.3	43.7	52.5	62.4	78.5	91.3	101.0	111.1	123.3
8	32.5	38.2	46.9	57.1	68.9	87.5	103.2	114.8	126.8	141.3
11	45.5	39.7	49.5	61.3	74.8	96.4	114.4	127.7	141.5	159.2
12	58.5	41.5	52.6	65.8	81.0	105.2	125.8	140.6	156.2	176.2
13	71.5	43.4	55.7	70.4	87.4	114.4	137.0	154.1	171.0	193.6
Tsurface	0	34.1	39.7	46.7	54.1	66.1	75.6	82.6	89.9	98.1
a		0.126593	0.221538	0.326593	0.460879	0.670330	0.855385	0.993846	1.132967	1.335385
Q" [KW/m^2]		Q1	Q2	Q3	Q4	Q5	Q6	Q7	Q8	Q9
Q" (a)		49.8	87.1	128.4	181.1	263.4	336.2	390.6	445.3	524.8
Q" (x5)		49.7	86.7	128.3	180.7	262.7	337.2	389.6	445.4	524.7

TC	X	Test18 10	Test18 11	Test18 12	Test18 13	Test18 14	Test18 15	Test18 16	Test18 17	Test18 18
1	6.5	114.0	118.7	122.6	125.6	126.6	127.7	129.4	131.5	133.5
5	19.5	131.8	138.6	145.2	149.7	153.1	155.4	158.0	161.2	164.6
8	32.5	152.2	160.7	169.6	177.4	181.2	184.7	188.8	193.5	197.9
11	45.5	172.1	182.4	193.7	204.0	209.4	214.2	219.7	225.6	231.7
12	58.5	191.3	203.7	217.1	230.4	237.2	243.3	250.5	257.8	265.1
13	71.5	210.8	225.2	241.2	257.3	265.4	272.8	281.4	290.1	298.8
Tsurface	0	103.5	107.3	110.2	111.3	112.0	112.4	113.1	114.4	115.7
a		1.499780	1.647253	1.830330	2.037802	2.141758	2.238901	2.348132	2.450330	2.553407
Q" [KW/m^2]		Q10	Q11	Q12	Q13	Q14	Q15	Q16	Q17	Q18
Q" (a)		589.4	647.4	719.3	800.9	841.7	879.9	922.8	963.0	1003.5
Q" (x5)		589.8	647.6	718.1	800.1	841.1	879.4	923.0	963.4	1003.7

Appendix C

Heat Loss Analysis

Heat Loss Analysis

The heat loss in radial direction was calculated according to the following example for Test 9 at the maximum voltage, and Test 11 at the minimum voltage. The heat loss, q, in radial direction was calculated from Equation 20 as follows:

$$q_{(T,r)} = \frac{2 \times \pi \times k \times L \times \Delta T}{\ln\left(\frac{r_2}{r_1}\right)} \quad \text{..... (Eq. 20)}$$

where: $q_{(T, r)}$ is the heat loss to the ambient, k is the thermal conductivity of the fiberglass insulation, k = 0.05 W/m K, L is the length of the test object, L = 178 mm, ΔT is the temperature gradient in radial direction, where some representative values have been chosen for T_1, and T_2, r_1 is the distance of the thermocouple located at the outer surface of the copper cylinder, r_1 = 25.05 mm, and r_2 is the distance of the thermocouple embedded inside the fiberglass insulation, r_2 = 37.05 mm. Substituting the above values in Equation 20, we have:

$$q_{(T,r)} = \frac{2 \times \pi \times 0.05 \times 0.178 \times (302.5 - 196.3)}{\ln\left(\frac{37.05}{25.05}\right)} \quad \text{..... (Eq. 21)}$$

$$= 15.2 \text{ W}$$

The above heat loss value of 15.2 W was calculated for Test 9 at maximum power supply. Substituting representative values for Test 11 at minimum power supply, we have:

$$q_{(r,r)} = \frac{2 \times \pi \times 0.05 \times 0.178 \times (51.7 - 50.0)}{\ln\left(\frac{37.05}{25.05}\right)} \quad \text{(Eq. 22)}$$

$= 0.2$ W

The above results for the heat loss are reasonable low. Therefore, the final heat flux analysis, and procedure for test surface temperature extrapolation stand validated.

Data for the Heat Loss in Radial Direction

Calculating the Heat Loss: q
q = 2*PI*k*L*(T1-T2)/ln(r2/r1) T2 = TC 15
k(Fiberglas) = 0.05 W/m*K T1= TC 13

Test at Max. Voltage	T1 Deg. C	T2 Deg. C	r1 mm	r2 mm	L m	q Watts
8Test1	276.2	174.8	25.05	37.05	0.178	14.5
7Test2	262.0	164.9	25.05	37.05	0.178	13.9
7Test3	270.8	167.1	25.05	37.05	0.178	14.8
11Test4	282.8	182.9	25.05	37.05	0.178	14.3
10Test5	280.5	179.3	25.05	37.05	0.178	14.5
11Test6	287.2	180.9	25.05	37.05	0.178	15.2
15Test8	290.4	188.0	25.05	37.05	0.178	14.6
16Test9	302.5	196.3	25.05	37.05	0.178	15.2
15Test10	285.7	183.5	25.05	37.05	0.178	14.6
8Test11	275.2	171.4	25.05	37.05	0.178	14.8

Test at Min. Voltage	T1 Deg. C	T2 Deg. C	r1 mm	r2 mm	L m	q Watts
1Test1	102.7	64.2	25.05	37.05	0.178	5.5
1Test2	106.6	62.3	25.05	37.05	0.178	6.3
1Test3	106.5	61.5	25.05	37.05	0.178	6.4
1Test4	146.1	82.8	25.05	37.05	0.178	9.0
1Test5	152.2	88.5	25.05	37.05	0.178	9.1
1Test6	138.4	83.7	25.05	37.05	0.178	7.8
1Test8	111.5	68.8	25.05	37.05	0.178	6.1
1Test9	117.3	73.4	25.05	37.05	0.178	6.3
1Test10	52.4	38.3	25.05	37.05	0.178	2.0
1Test11	51.7	50.0	25.05	37.05	0.178	0.2

Appendix D

Error Analysis

Error Analysis

All measurements conducted during the experimental investigation of the present study contain errors which are the difference between the true and the measurement value. In the present error analysis only the maximum random error is used to report the uncertainty in the final correlation equations for saturated and subcooled water spray. The random error, $\varepsilon_{Meas.}$, for each parameter is presented in the table below as follows:

Description	$\varepsilon_{Meas.}$	**Reading Value**	$\varepsilon_{Meas.}$ **(%)**
Q (ml/sec.)	0.5	3.7	13.51
A (mm)	0.8	50.0	1.6
d_0 (mm)	0.015	0.760	1.97
Prandtl Number	0.03	5.2	0.58
$\nu \times 10^6$ (Ns/m^2)	0.005	0.82	0.61
c_f (kJ/kg K)	8.4×10^{-3}	4.218	0.19
ΔT (°C)	0.2	24.7	0.81
h_{fg} (kJ/kg)	0.67	2257	0.03
Δp (psig)	3.7	72.7	5.09
σ (N/m)	1.6×10^{-4}	0.05891	0.27
ρ_f (kg/m^3)	0.2	958.3	0.02
d_{32} (μm)	0	0	25

The maximum error that might reasonably be expected is called uncertainty. In the present error analysis the uncertainty parameter, $U_{Meas.}$, is estimated using the following relationship:

$$U_{Meas.} = \pm \left(2 \times \mathcal{E}_{Meas.}\right) \quad \text{..... (Eq. 23)}$$

where:

$$\mathcal{E}_{Meas.}(\%) = \frac{\mathcal{E}_{Meas.}}{Reading\ Value} \times 100\% \quad \text{..... (Eq. 24)}$$

The random errors can be obtained from the differential form of the correlation. Equation 7 presented the correlation for spray cooling with saturated water spray.

$$\frac{q'' x}{\mu_f h_{fg}} = 93.8 \left(We_{d_{32}}\right)^{0.43} \left(\frac{c_f \Delta T}{h_{fg}}\right)^{0.98} \quad \text{..... (Eq. 7)}$$

The correlation can be written as:

$$A = 93.8\ We^{0.43} B^{0.98} \quad \text{..... (Eq. 25)}$$

The random error of this correlation is:

$$\mathcal{E}_{(A)} = \frac{\partial (A)}{\partial (We)} \mathcal{E}_{(We)} + \frac{\partial (A)}{\partial (B)} \mathcal{E}_{(B)} \quad \text{..... (Eq. 26)}$$

Now, the percentile random error can be written as follows:

$$\frac{\varepsilon_{(A)}}{A} \times 100 = \left[0.43 \frac{\varepsilon_{(We)}}{We} + 0.98 \frac{\varepsilon_{(B)}}{(B)} \right] \times 100 \quad \text{..... (Eq. 27)}$$

$$= \left[0.43 \left(\frac{\varepsilon_{(\rho_f)}}{\rho_f} + 2\frac{\varepsilon_{(v)}}{v} + \frac{\varepsilon_{(d_{32})}}{d_{32}} + \frac{\varepsilon_{(\sigma)}}{\sigma} \right) + 0.98 \left(\frac{\varepsilon_{(c_f)}}{c_f} + \frac{\varepsilon_{(\Delta T)}}{\Delta T} + \frac{\varepsilon_{(h_{fg})}}{h_{fg}} \right) \right] \times 100$$

$$= \left[0.43 \times (0.02 + 2 \times 5.11 + 25 + 0.27) + 0.98 \times (0.19 + 0.81 + 0.03) \right]$$

$$= 16.28\ \%$$

where: $We_{d_{32}} = \dfrac{\rho_f v^2 d_{32}}{\sigma}$ and $v^2 = \dfrac{2\Delta p}{\rho_f}$

$$\frac{\varepsilon_{(v^2)}}{v^2} \times 100 = \left[\frac{\varepsilon_{(\Delta p)}}{\Delta p} + \frac{\varepsilon_{(\rho_f)}}{\rho_f} \right] \times 100$$

Therefore, the uncertainty of the correlation for saturated water spray is:

$$U_{\left(\frac{q''x}{\mu_f h_{fg}}\right)} = \pm (2 \times 16.28) = 32.56\ \%$$

The correlation for spray cooling with subcooled water spray was presented in Equation 11.

$$Nu = 2.53\ \mathrm{Re}^{0.67}\ \mathrm{Pr}^{0.31} \quad \text{(Eq. 11)}$$

The percentile random error of this correlation is:

$$\frac{\varepsilon_{(Nu)}}{Nu} \times 100 = \left[0.67 \frac{\varepsilon_{(\mathrm{Re})}}{\mathrm{Re}} + 0.31 \frac{\varepsilon_{(\mathrm{Pr})}}{\mathrm{Pr}} \right] \times 100 \quad \text{(Eq. 28)}$$

$$= \left[0.67 \times (17.69) + 0.31 \times (0.58) \right] \times 100$$

$$= 12.03\ \%$$

where: $\mathrm{Re} = \dfrac{Q'' d_o}{\nu}$ and $Q'' = \dfrac{Q}{A}$

$$\frac{\varepsilon\ (Q'')}{Q''} = \frac{\varepsilon\ (Q)}{Q} + \frac{\varepsilon\ (A)}{A} \quad \text{and} \quad \frac{\varepsilon\ (\mathrm{Re})}{\mathrm{Re}} = \frac{\varepsilon\ (Q'')}{Q''} + \frac{\varepsilon\ (d_o)}{d_o} + \frac{\varepsilon\ (\nu)}{\nu}$$

Therefore, the uncertainty of the correlation for subcooled water spray is:

$$U_{(Nu)} = \pm (2 \times 12.03) = 24.06\ \%$$

Appendix E

Flow Rate Calibration Data

Water Flow Rate Calibration

Test	Nozzle	Float Point	Water Temp. Deg. C	Pressure psig	Flow Rate Calc. ml/sec.	Flow Rate Nozzle ml/sec.	Flow Rate Nozzle GPM
Test 1	TG 0.9	20	97.0	18.1	8.7	8.35	0.1324
Test 2	TG 0.9	12.5	97.6	5.3	5.4	5.12	0.0812
Test 3	TG 0.9	6.25	98.0	1.7	4.7	4.21	0.0668
Test 4	TG 0.5	20	95.8	42.6	8.7	6.47	0.1026
Test 5	TG 0.5	12.5	96.0	15.2	5.4	3.87	0.0614
Test 6	TG 0.5	6.25	96.5	6.6	3.7	2.79	0.0442
Test 7	TG 0.3	20					
Test 8	TG 0.3	12.5	97.4	49.2	5.5	4.16	0.06598
Test 9	TG 0.3	6.25	97.5	19.6	3.7	2.62	0.0416
Test 10	TG 0.9	20	22.0	21.9	7.8	9.31	0.1476
Test 11	TG 0.9	12.5	21.4	10.9	5.7	6.54	0.1036
Test 12	TG 0.9	6.25	21.5	3.0	3.5	4.54	0.072
Test 13	TG 0.5	20	18.4	51.7	7.6	7.05	0.1117
Test 14	TG 0.5	12.5	19.9	25.8	5.4	5.06	0.08028
Test 15	TG 0.5	6.25	21.3	13.0	3.8	3.60	0.057
Test 16	TG 0.3	20					
Test 17	TG 0.3	12.5	19.9	72.7	5.3	5.09	0.08062
Test 18	TG 0.3	6.25	21.9	30.4	3.6	3.31	0.0524

Note 1: Nozzle Flow Rates for Nozzle TG 0.9 compared to Fullcone Spray Nozzle Data Type TG 1.

Note 2: Test 7 & Test 16 void. Float Point at 20 is too high for Nozzle TG 0.3.

Note 3: Flow Rate Nozzle interpolated from data supplied by manufacturer.

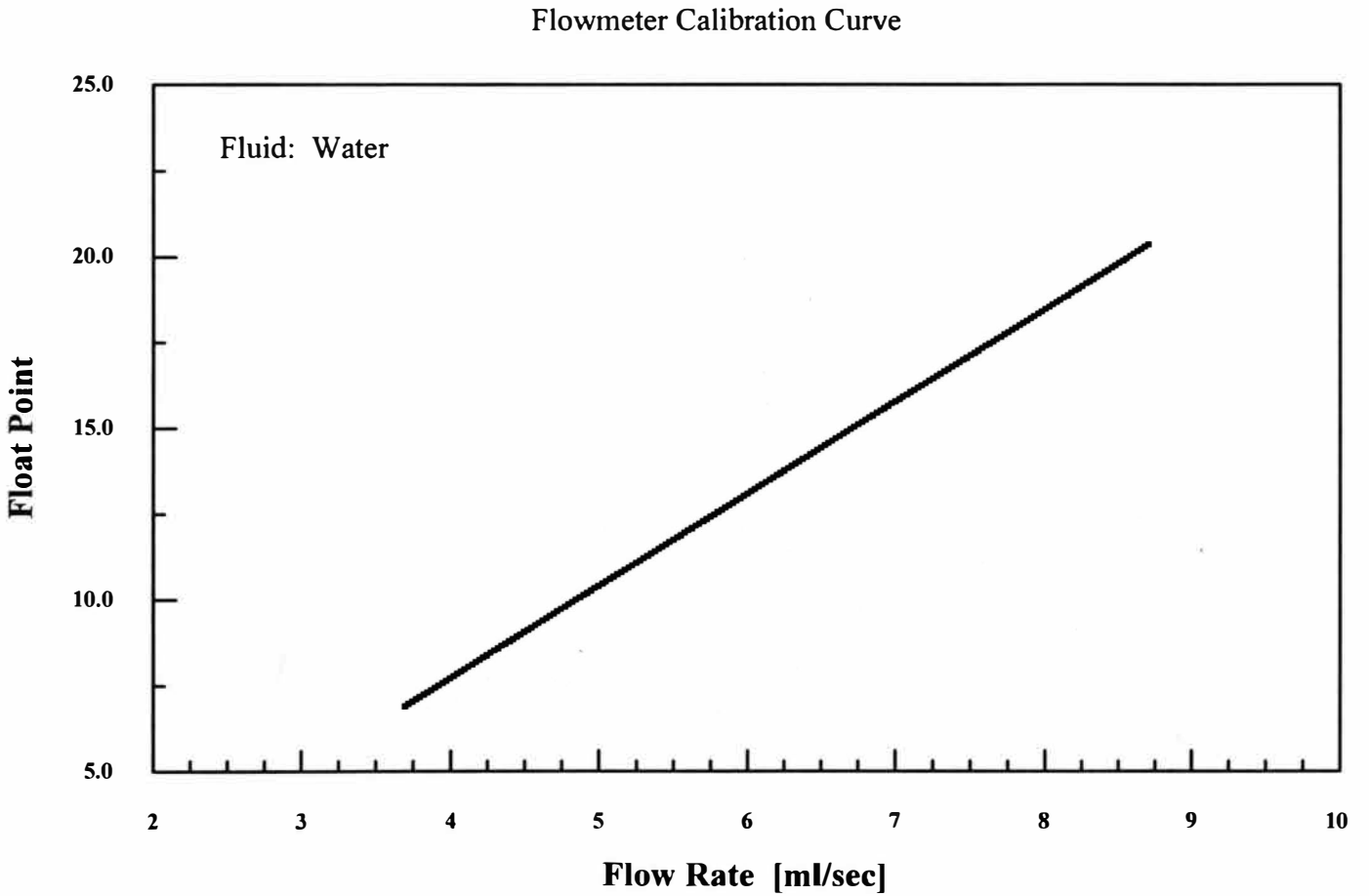
Flowmeter Calibration Curve
Fluid: Water
Float Point
25.0
20.0
15.0
10.0
5.0
2
3
4
5
6
7
8
9
10
Flow Rate [ml/sec]

Appendix F

Thermocouple Calibration Data

Thermocouple Calibration Data

Troom = 24.0 Deg. C
Tcopper = 24.7 Deg. C
Duration = 360 sec.

TC1	TC2	TC3	TC4	TC5	TC6	TC7	TC8	TC9	TC10	TC11	TC12	TC13	Thermocouple
24.9	24.1	25.8	24.3	24.1	25.0	25.1	24.5	23.3	24.9	25.0	24.1	24.0	Sample 1
24.9	25.3	24.6	24.3	24.1	25.0	26.3	23.3	24.5	26.1	25.0	25.3	25.2	Sample 2
24.9	24.1	24.6	25.5	25.3	23.6	26.3	25.7	24.5	24.9	25.0	24.1	25.2	Sample 3
24.9	25.3	25.8	24.3	24.1	25.0	24.0	24.5	24.5	24.9	25.0	24.1	25.2	Sample 4
23.7	25.3	24.6	24.3	24.1	25.0	24.0	24.5	24.5	26.1	25.0	25.3	25.2	Sample 5
24.9	25.3	24.6	24.3	24.1	26.1	26.3	24.5	25.6	24.9	25.0	25.3	24.0	Sample 6
24.9	25.3	24.6	24.3	25.3	25.0	26.3	25.7	24.5	24.9	23.8	25.3	24.0	Sample 7
24.9	24.1	24.6	24.3	24.1	25.0	22.8	25.7	24.5	24.9	25.0	24.1	24.0	Sample 8
24.9	24.1	24.6	25.5	25.3	23.8	24.0	24.5	23.3	23.7	25.0	24.1	24.0	Sample 9
24.9	24.1	24.6	25.5	24.1	26.1	26.3	24.5	24.5	24.9	25.0	25.3	24.0	Sample 10
24.9	24.1	24.6	24.3	23.9	25.0	25.1	24.3	24.5	24.9	23.8	22.9	25.2	Sample 11
24.9	25.3	24.6	24.3	24.1	25.0	24.0	24.5	24.5	24.9	23.6	25.3	25.2	Sample 12
24.7	24.1	24.6	24.1	24.1	23.6	26.1	24.5	24.5	24.7	25.0	25.1	24.0	Sample 13
24.7	24.1	24.6	24.3	25.1	26.1	23.8	25.7	25.6	23.5	23.8	25.3	24.0	Sample 14
24.9	25.3	24.6	24.3	24.1	24.8	24.0	24.5	24.5	23.5	23.6	25.3	25.2	Sample 15
24.7	24.1	24.6	25.5	25.1	24.8	23.8	24.5	24.5	24.9	25.0	25.3	24.0	Sample 16
24.9	25.3	24.4	24.3	25.3	23.8	26.1	24.3	23.3	24.9	24.8	23.9	25.2	Sample 17
24.9	24.1	24.6	25.5	25.3	24.8	24.0	25.7	24.5	24.9	25.0	25.3	25.2	Sample 18
24.7	24.1	24.6	25.5	25.3	25.0	25.1	24.5	24.5	23.7	24.8	24.1	25.2	Sample 19
24.9	25.3	24.6	25.5	24.1	25.0	24.0	25.7	24.5	24.9	23.8	25.3	25.2	Sample 20
24.7	24.1	24.6	25.5	25.3	22.4	25.1	25.7	24.5	24.9	23.6	24.1	25.2	Sample 21
24.7	24.1	24.4	24.1	24.1	23.8	24.0	25.5	24.5	24.9	25.0	22.9	24.0	Sample 22
24.9	25.3	24.6	24.3	25.3	25.0	24.0	24.3	24.5	23.5	24.8	25.3	24.0	Sample 23
24.9	25.3	24.6	24.1	22.9	25.0	26.3	24.5	25.4	22.5	24.8	24.1	25.2	Sample 24
24.9	25.3	24.6	25.5	24.1	24.8	24.0	24.5	25.6	24.9	25.0	22.9	25.2	Sample 25
24.9	24.1	25.8	24.3	25.3	25.0	25.1	25.7	24.5	24.9	24.8	24.1	24.0	Sample 26
24.9	25.1	24.4	24.3	24.1	24.8	25.1	23.3	24.3	24.9	24.8	23.9	24.0	Sample 27
24.9	25.3	24.6	25.5	24.1	24.8	24.9	25.5	24.5	24.7	23.8	25.3	24.0	Sample 28
24.7	24.1	24.4	24.3	23.9	25.0	24.0	24.3	24.5	24.9	25.0	25.1	25.2	Sample 29
24.9	25.3	25.6	24.3	24.1	25.0	23.8	24.5	24.3	24.9	23.8	24.1	23.8	Sample 30
24.9	25.3	24.6	24.1	25.3	24.8	24.0	24.3	24.5	24.9	25.0	25.3	25.2	Sample 31
24.7	25.3	24.6	25.3	26.4	24.8	23.8	24.3	24.3	24.7	23.6	24.1	24.0	Sample 32
24.7	25.1	24.4	24.1	25.1	24.8	23.8	25.5	25.4	23.5	24.8	25.1	25.0	Sample 33
24.7	23.9	24.6	24.3	23.9	23.6	26.3	24.3	24.3	24.7	24.8	25.1	23.8	Sample 34
24.9	25.3	25.6	24.1	22.7	24.8	25.1	24.5	24.5	24.7	23.6	22.9	25.2	Sample 35
24.9	23.9	24.4	24.3	25.3	23.6	25.1	24.5	24.3	24.9	24.8	23.9	25.2	Sample 36
24.9	23.9	25.8	25.3	23.9	23.6	26.1	25.7	24.3	24.9	25.0	25.1	25.2	Sample 37
24.8	24.7	24.8	24.6	24.5	24.7	24.8	24.8	24.5	24.7	24.6	24.5	24.6	Sample Average
24.7	24.7	24.7	24.7	24.7	24.7	24.7	24.7	24.7	24.7	24.7	24.7	24.7	$T_{copper\ per\ Calibrator}$
2.67	3.07	3.53	3.23	3.03	2.73	1.73	2.27	2.23	2.67	2.73	3.03	3.00	Final Offset

Labtech Block Data

Block No.	Block Name	Dev	Ch	Block Function	Scale Factor	Offset	Iter	Stg	Duration	Rate	Start State	Trigger Block	File Name (first)
1	TC1	1	17	Thermocouple	1	2.67	1	1	360	0.1	ON		
2	TC2	1	18	Thermocouple	1	3.07	1	1	360	0.1	ON		
3	TC3	1	19	Thermocouple	1	3.53	1	1	360	0.1	ON		
4	TC4	1	20	Thermocouple	1	3.23	1	1	360	0.1	ON		
5	TC5	1	21	Thermocouple	1	3.03	1	1	360	0.1	ON		
6	TC6	1	22	Thermocouple	1	2.73	1	1	360	0.1	ON		
7	TC7	1	23	Thermocouple	1	1.73	1	1	360	0.1	ON		
8	TC8	1	24	Thermocouple	1	2.27	1	1	360	0.1	ON		
9	TC9	1	25	Thermocouple	1	2.23	1	1	360	0.1	ON		
10	TC10	1	26	Thermocouple	1	2.67	1	1	360	0.1	ON		
11	TC11	1	27	Thermocouple	1	2.73	1	1	360	0.1	ON		
12	TC12	1	28	Thermocouple	1	3.03	1	1	360	0.1	ON		
13	TC13	1	29	Thermocouple	1	3	1	1	360	0.1	ON		
14	av1			Block Av(1)	1	0	1	1	360	0.1	ON		C:\TestData\Test1\1Test1.prn
15	av2			Block Av(2)	1	0	1	1	360	0.1	ON		C:\TestData\Test1\1Test1.prn
16	av3			Block Av(3)	1	0	1	1	360	0.1	ON		C:\TestData\Test1\1Test1.prn
17	av4			Block Av(4)	1	0	1	1	360	0.1	ON		C:\TestData\Test1\1Test1.prn
18	av5			Block Av(5)	1	0	1	1	360	0.1	ON		C:\TestData\Test1\1Test1.prn
19	av6			Block Av(6)	1	0	1	1	360	0.1	ON		C:\TestData\Test1\1Test1.prn
20	av7			Block Av(7)	1	0	1	1	360	0.1	ON		C:\TestData\Test1\1Test1.prn
21	av8			Block Av(8)	1	0	1	1	360	0.1	ON		C:\TestData\Test1\1Test1.prn
22	av9			Block Av(9)	1	0	1	1	360	0.1	ON		C:\TestData\Test1\1Test1.prn
23	av10			Block Av(10)	1	0	1	1	360	0.1	ON		C:\TestData\Test1\1Test1.prn
24	av11			Block Av(11)	1	0	1	1	360	0.1	ON		C:\TestData\Test1\1Test1.prn
25	av12			Block Av(12)	1	0	1	1	360	0.1	ON		C:\TestData\Test1\1Test1.prn
26	av13			Block Av(13)	1	0	1	1	360	0.1	ON		C:\TestData\Test1\1Test1.prn
27	av14			Block Av(28)	1	0	1	1	360	0.1	ON		C:\TestData\Test1\1Test1.prn
28	TC14 Nozzle	1	30	Thermocouple	1	3.3	1	1	360	0.1	ON		
29	av15			Block Av(30)	1	0	1	1	360	0.1	ON		C:\TestData\Test1\1Test1.prn
30	TC15 Insul.	1	31	Thermocouple	1	2.8	1	1	360	0.1	ON		

Appendix G

Thermophysical Properties

Variation of the Thermal Conductivity of Copper with Temperature

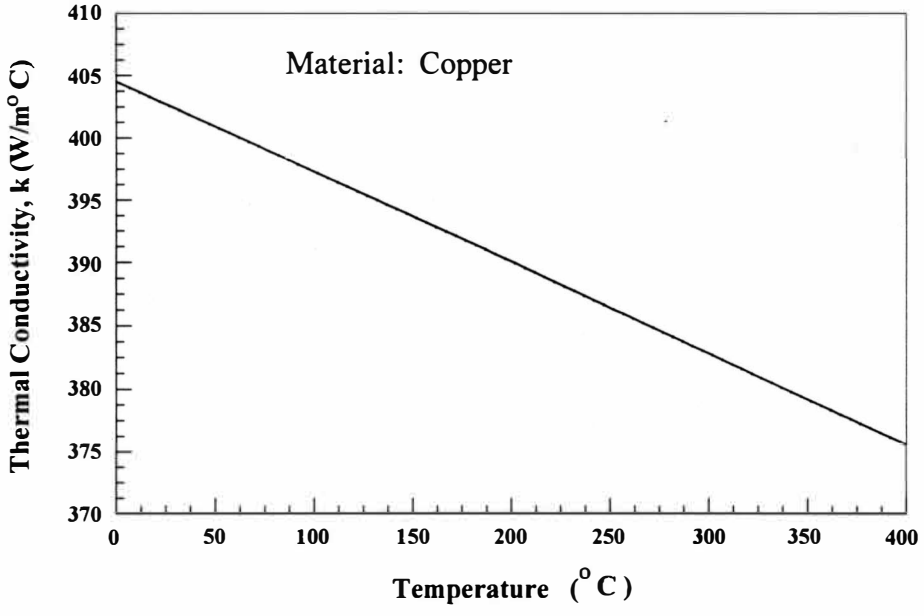

Variation of the Thermal Conductivity of Water with Temperature

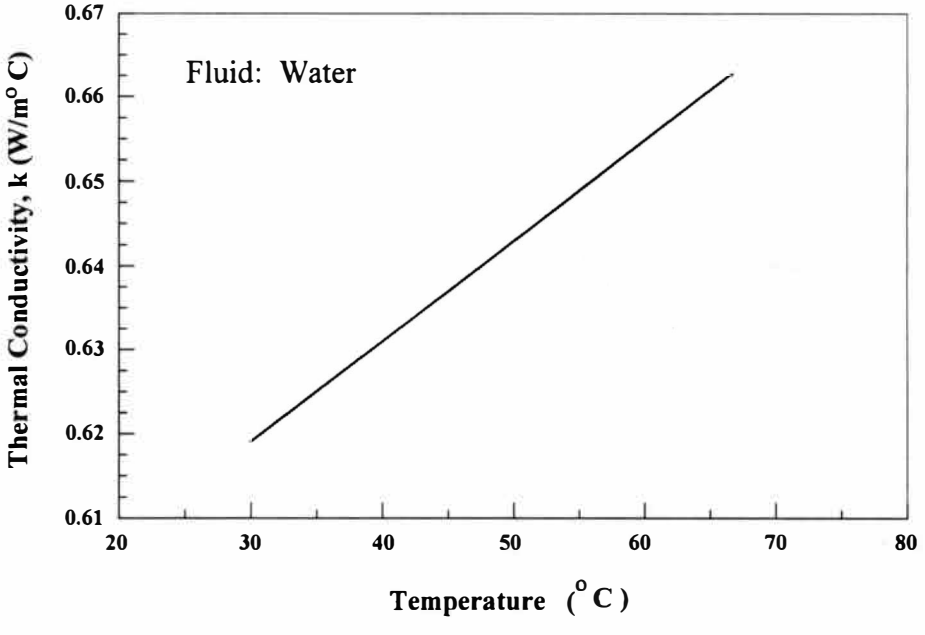

Variation of the Prandtl Number of Water with Temperature

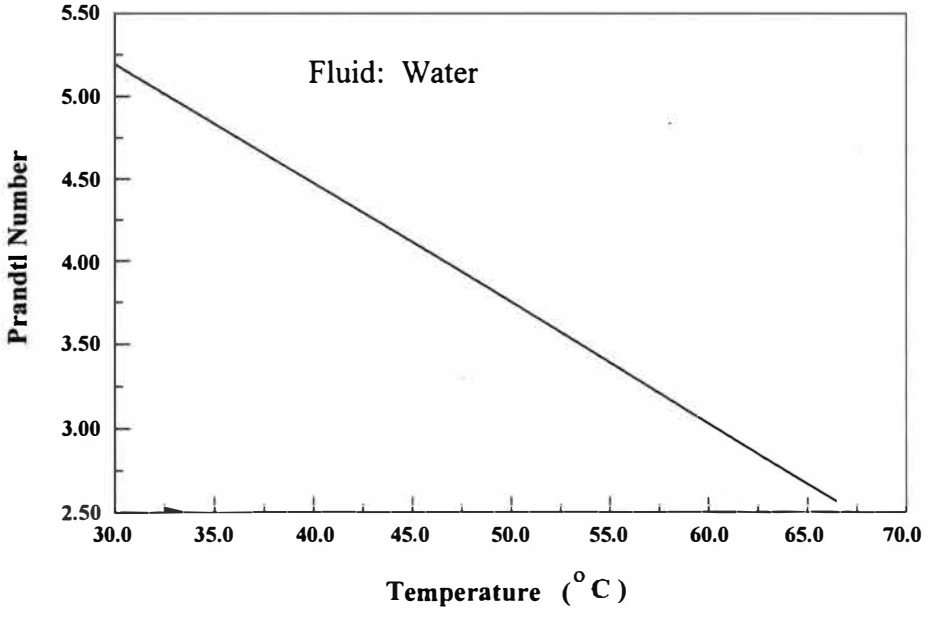

Summary of Fluid Properties

specific heat of the fluid:	$c_f = 4.218$ kJ/kg K
latent heat of vaporization:	$h_{fg} = 2257$ kJ/kg
dynamic viscosity:	$\mu_{100\,°C} = 278.99 \times 10^{-6}$ Ns/m^2
surface tension:	$\sigma_{100\,°C} = 0.05891$ N/m
density of fluid:	$\rho_{100\,°C} = 958.3$ kg/m^3
density of air:	$\rho_{25.9\,°C} = 1.184$ kg/m^3
kinematic viscosity:	$\nu \times 10^6$ Ns/m^2

Note: The value of the kinematic viscosity, Prandtl number and thermal conductivity were evaluated at the film temperature.
The value of the specific heat and the latent heat of vaporization were evaluated at the saturation temperature.

Appendix H

Photographs

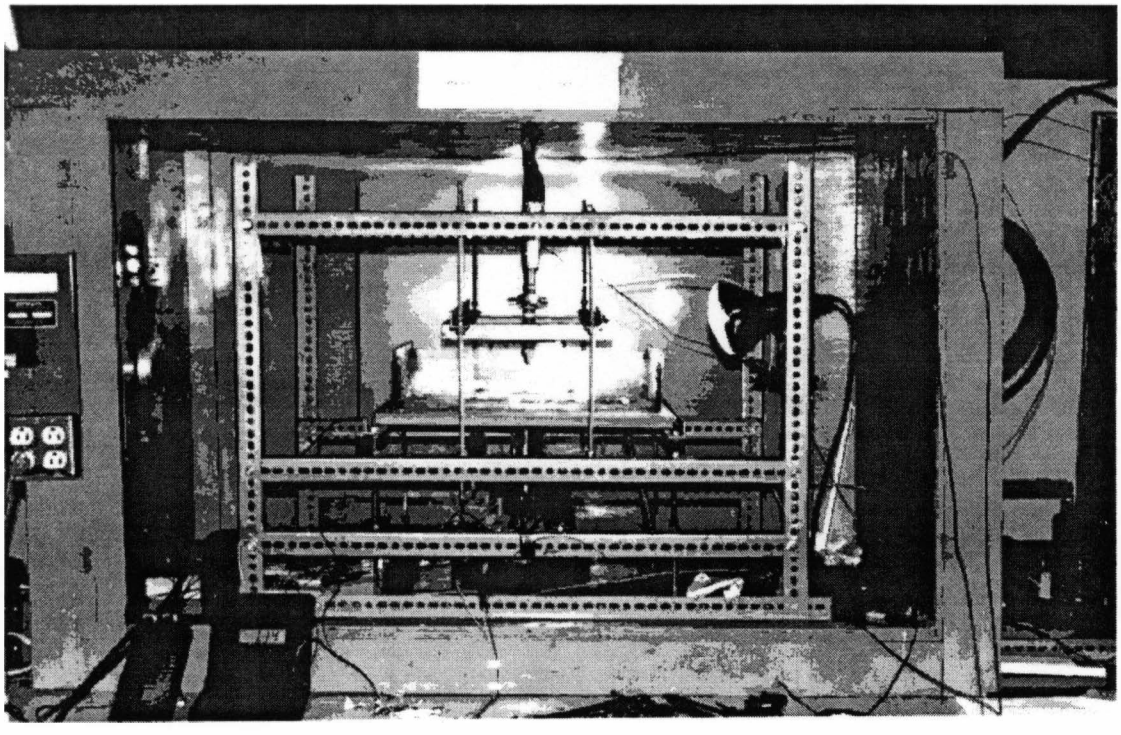

Figure 22. Spray Cooling Test Chamber.

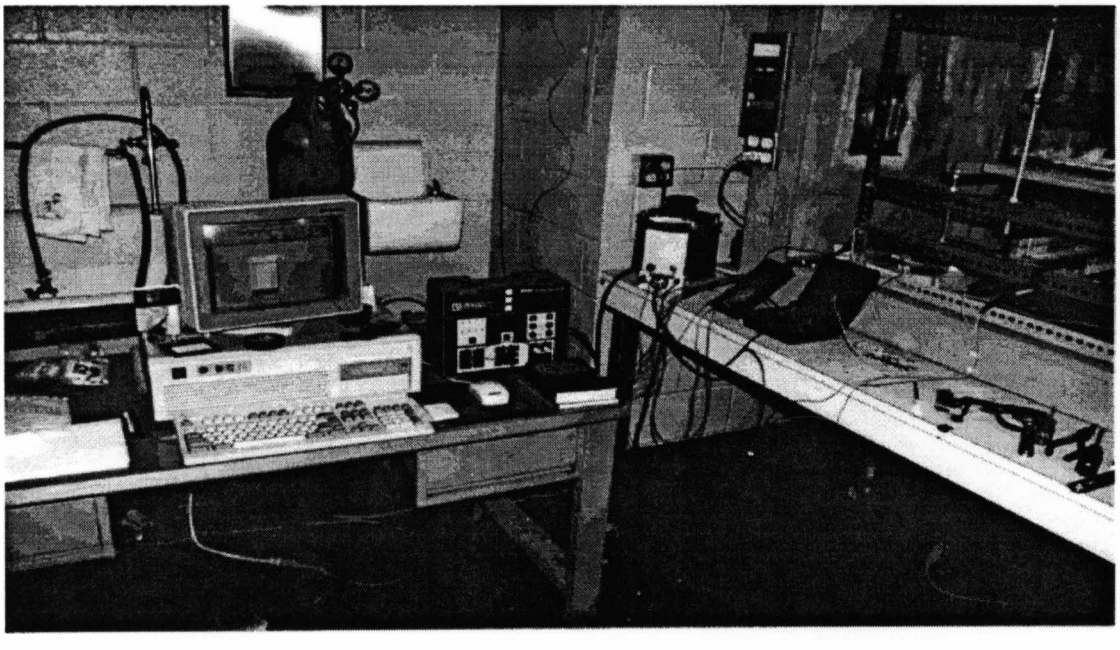

Figure 23. Data Acquisition System.

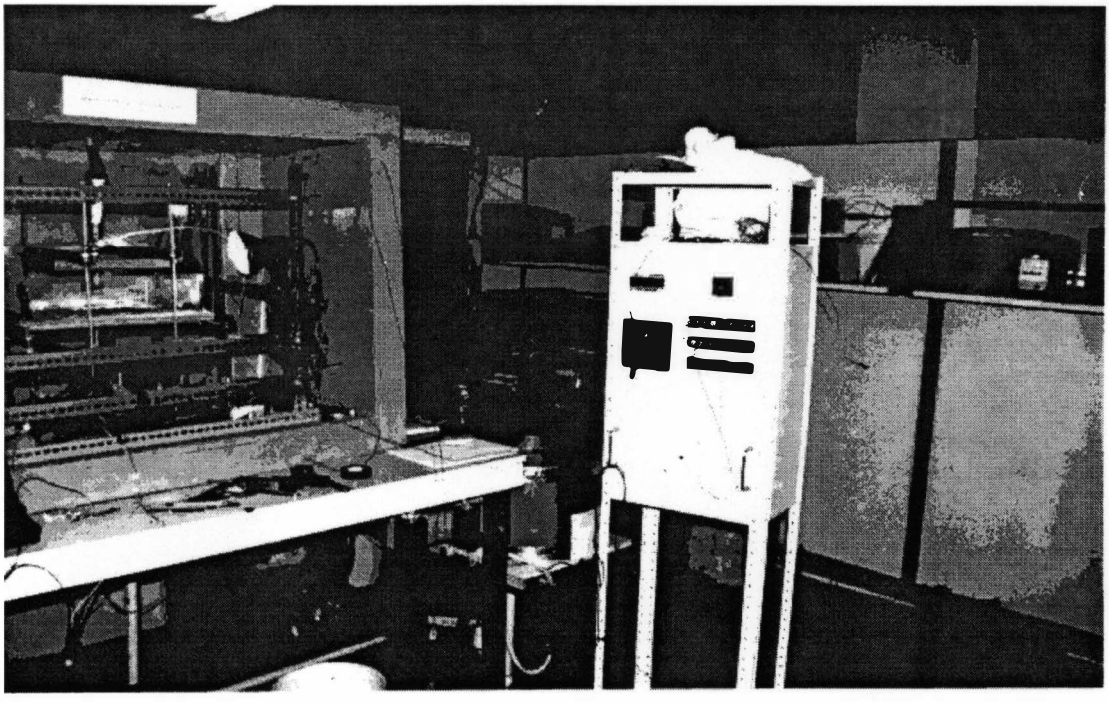

Figure 24. Temperature Control Panel.

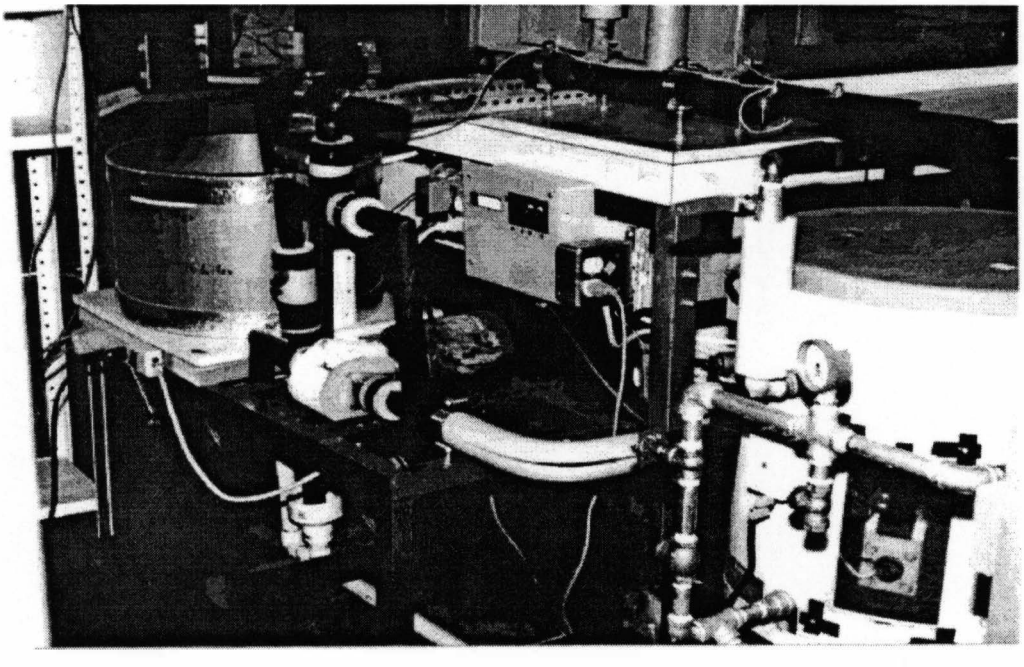

Figure 25. Test Loop with Reservoir and Boiler.

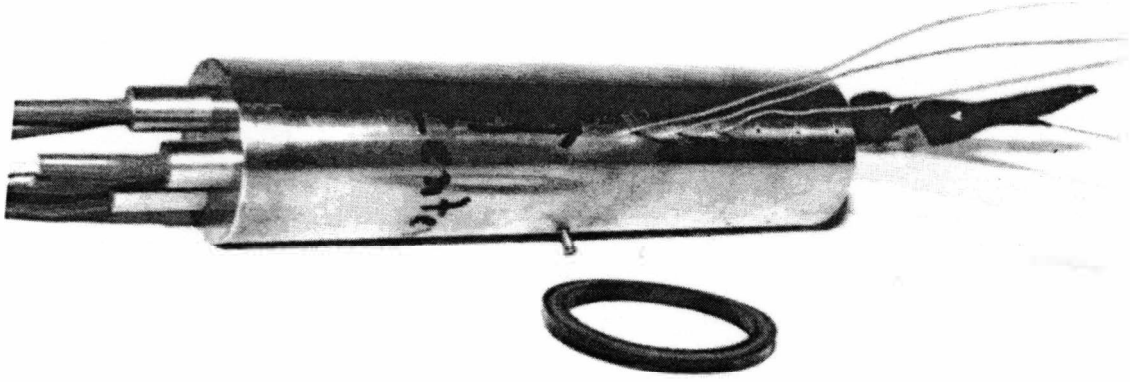

Figure 26. Copper Cylinder with Thermocouples along the Axis.

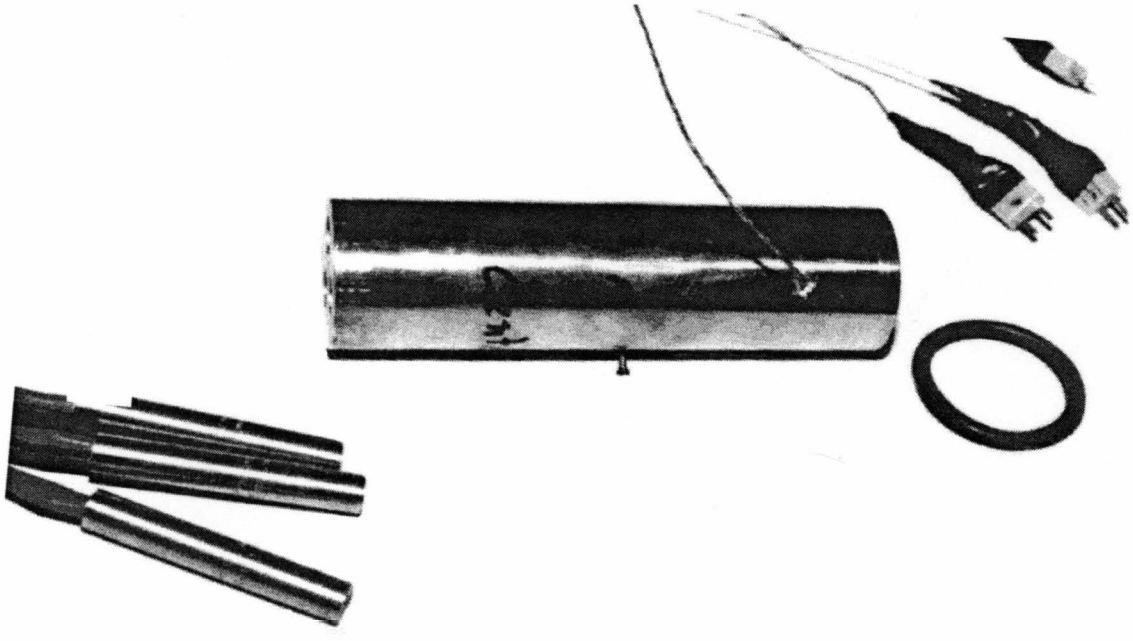

Figure 27. Copper Cylinder with Cartridge Heaters and Seal.

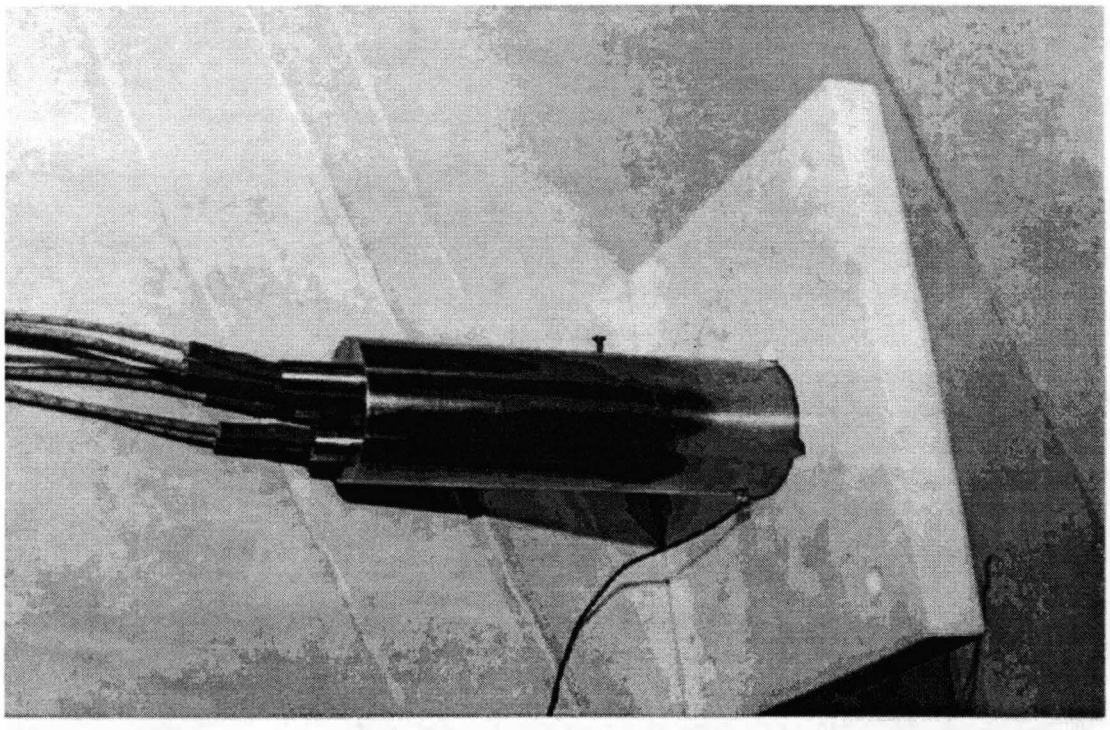

Figure 28. Copper Cylinder inserted into Teflon Plate.

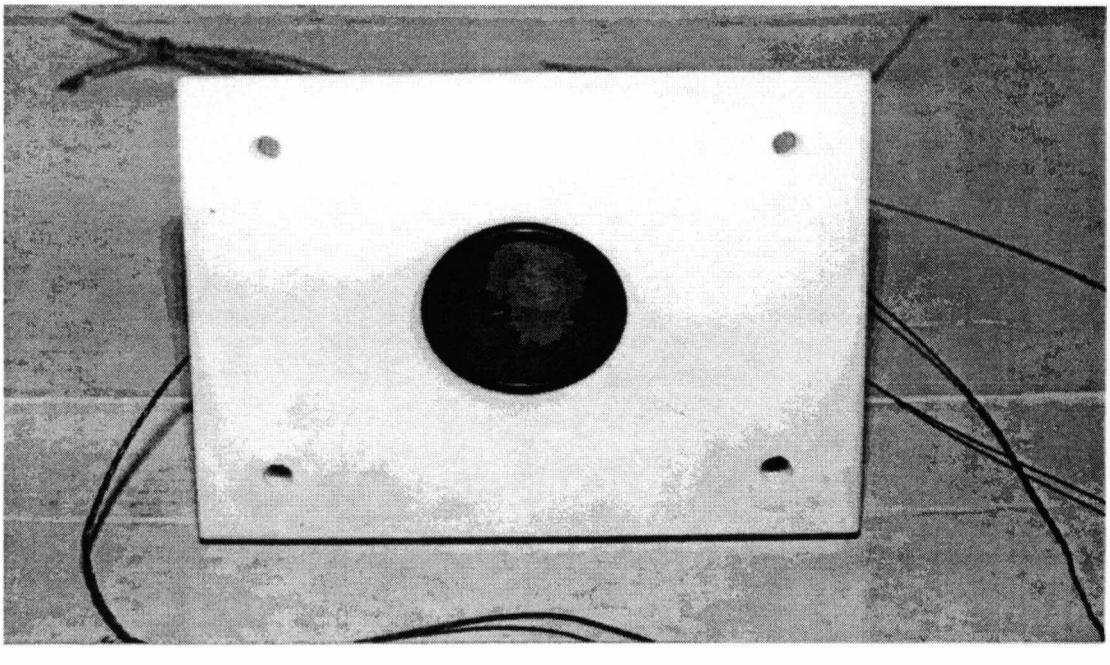

Figure 29. Top View of Test Surface.

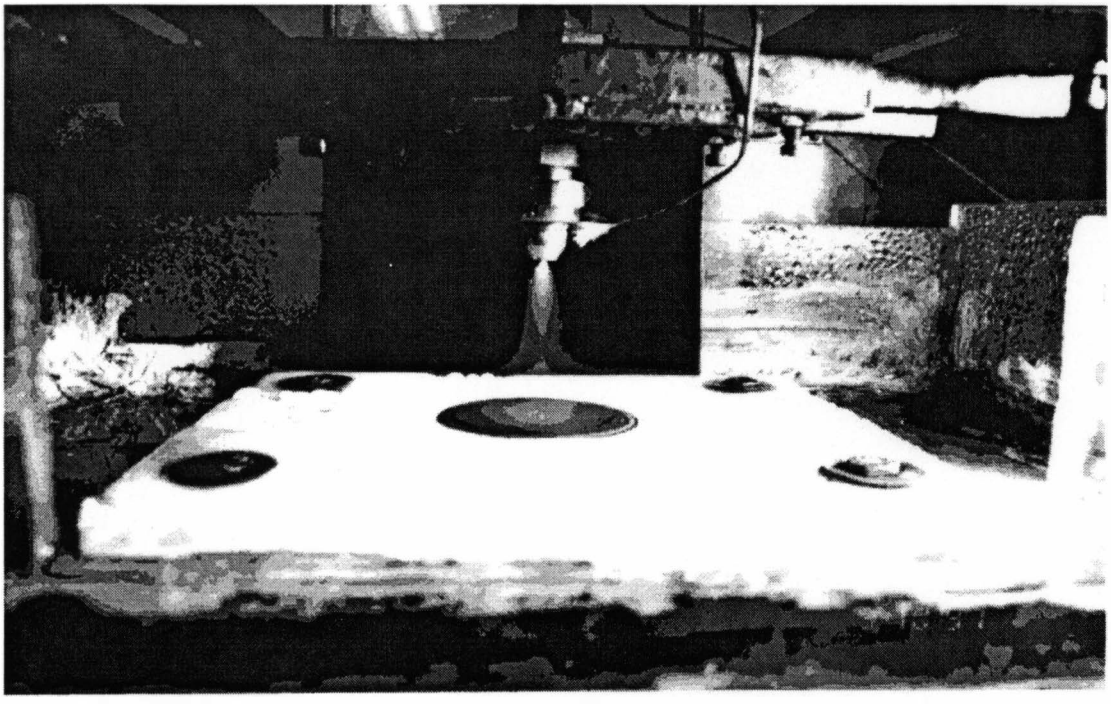

Figure 30. Spray Cooling at Low Heat Flux.

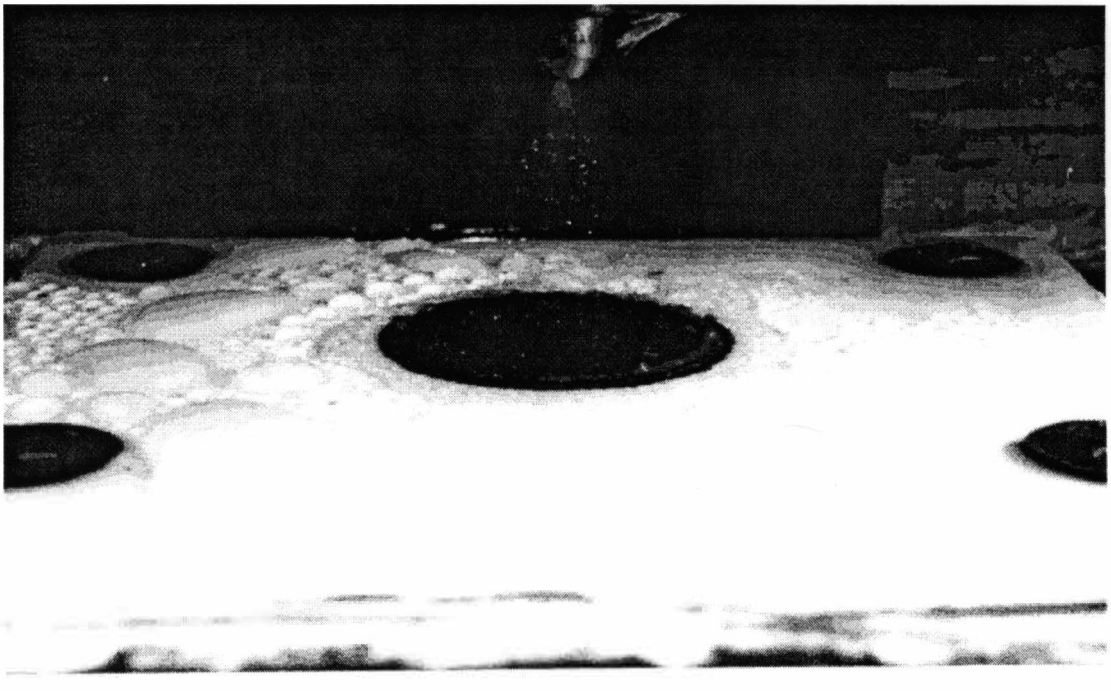

Figure 31. Spray Cooling with Nucleate Boiling Site.

BIBLIOGRAPHY

Bonacia, C., Del Giudice, S., & Comini, G. (1979). Dropwise Evaporation. ASME Journal of Heat Transfer. 101, 441-446.

Brimacombe, J. K., Agarwal, P. K., Baptista, L.A., Hibbins, S. & Prabhakar, B. (1980). Spray Cooling in the Continuous Casting of Steel. Proceedings of the 63rd National Open Hearth and Basic Oxygen Steel Conference, Washington, D.C., 235-252.

Cho, C. S. K., & Sharma, J. (1987). Burnout in a High Heat Flux Element with Subcooled Freon. Temperature/Fluid Measurement in Electronic Equipment. ASME HTD, 89, 37-43.

Cho, C. S. K., & Wu, K. (1988). Comparison of burnout characteristics in jet impingement cooling and spray cooling. National Heat Transfer Conference Proceedings, Houston, TX. ASME HTD, 96, 561-567.

Estes, K., & Mudawar, I. (1995). Correlation of Sauter Mean Diameter and Critical Heat Flux for Spray Cooling of Small Surfaces. International Journal of Heat and Mass Transfer. 38(16), 2985-2996.

Ghodbane, M., & Holman, J. P. (1991). Experimental Study of Spray Cooling with Freon-113. International Journal of Heat and Mass Transfer. 34(4/5), 1163-1174.

Goodling, J. S., & Jaeger, R. C. (1987, December 13-18). Wafer Scale Cooling using Jet Impingement Boiling Heat Transfer. ASME Winter Annual Meeting, Boston, MA, (87-WA/EEP-2).

Grissom, W. M., & Wierum, F. A. (1981). Liquid Spray Cooling of a Heated Surface. International Journal of Heat and Mass Transfer. 24, 261-271.

Haji, M., & Chow, L. C. (1988). Experimental Measurement of Water Evaporation Rate into Air and Superheated Steam. ASME Journal of Heat Transfer. 110, 237-242.

Hodgson, J. W., & Sutherland, J. E. (1968). Heat Transfer from a Spray Cooled Isothermal Cylinder. Ind. Engng. Chem. Fundam. 7, 567-571.

Liu, X., & Lienhard, V. J. H. (1991). Convective Heat Transfer by Impingement of Circular Liquid Jets. ASME Journal of Heat Transfer. 113, 571-581.

Ma, C. F., & Bergles, A. E. (1983). Boiling Jet Impingement Cooling of Simulated Microelectronic Chips. Heat Transfer in Electronic Equipment. HTD, 28, ASME Winter Annual Meeting, 5-12.

Mahefkey, T., Sehmbey, M. S., Chow, L. C., & Pais, M. R. (1994). A Review of High Heat Flux Spray Cooling. Heat Transfer in High Heat Flux Systems. HTD, 301, ASME, 39-46.

Martin, H. (1977). Heat and Mass Transfer Between Impinging Jets and Solid Surfaces. Advances in Heat Transfer, Academic Press. 13, 1-60.

Monde, M., & Katto, Y. (1978). Burnout in a High Heat-Flux Boiling System with an Impinging Jet. International Journal of Heat and Mass Transfer. 21, 295-305.

Mudawar, I., & Valentine, W. S. (1989). Determination of the local quench curve for spray cooled metallic surfaces. ASME Journal Heat Treating. 7, 107-121.

Park, K. A., & Bergles, A. E. (1986). Effect of Size of Simulated Microelectronic Chips on Boiling and Critical Heat Flux. Heat Transfer in Electronic Equipment. HTD 28, ASME Winter Annual Meeting, 5-12.

Reiners, U., Jeschar, R., Scholz, R., Zebrowski, D., & Reichelt, W. (1985). A measuring method for quick determination of local heat transfer coefficients in spray cooling within the range of stable film boiling. Steel Research. 56, 239-246.

Rohsenow, W. M. (1985). Boiling. Handbook of Heat Transfer Fundamentals. (Ch. 12). New York: McGraw Hill, Inc.

Ruch, M. A., & Holman, J. P. (1978). Boiling Heat Transfer to a Freon-113 Jet Impinging Upward onto a Flat Heat Surface. International Journal of Heat and Mass Transfer. 21, 295-305.

Sehmbey, M. S., Pais, M. R., & Chow, L. C. (1992a). Effect of surface material properties and surface characteristics in evaporative spray cooling. Journal of Thermophysics and Heat Transfer. 6(3), 505-512.

Toda, S. (1974). A study of Mist Cooling. Heat Transfer-Japanese Research. 3, 1-44.

Trabold, T. A., & Obot, N. T. (1991). Evaporation of Water with Single and Multiple Impinging Air Jets. ASME Journal of Heat Transfer. 113, 669-704.

Ubanowich, L., Goryanionov, V., Sevost'yanov, V., Boev, Y., Niskovskikh, V., Grachev, A., Sevost'yanov, A., & Gur'ev, V. (1981). Spray Cooling of High-Temperature Metal Surfaces with High Water Pressures. Steel in USSR. 11, 184-186.

Xiong, T.Y., & Yuen, M.C. (1991). Evaporation of a Liquid Droplet on a Hot Plate. International Journal of Heat and Mass Transfer. 34(7), 1881-1894.

Yanosy, J. L. (1985). Water Spray Cooling in a Vacuum. Ph.D. Dissertation, University of Connecticut, Storrs, Connecticut.